May 2014

Mercury Transport and Fluxes in the Lake Ontario Basin

Joseph Steven Denkenberger
Syracuse University

Abstract

In this dissertation I assess mercury dynamics in the Lake Ontario Basin. In four interrelated phases, ecosystem mercury concentrations and fluxes were analyzed at increasing scales. Each phase is presented in order of increasing scale, starting with a reach-by-reach analysis in the Seneca River in New York, then moving up to an analysis of the Lake Ontario watershed, followed by an assessment of Lake Ontario, and culminating with an estimate of atmospheric mercury exchange for the entire Great Lakes Basin.

Phase 1 of my research is a multi-year study exploring mercury (Hg) dynamics in the Three Rivers system, with particular emphasis on the Seneca River in Central New York. In addition to bi-weekly water sampling, additional field investigations were conducted to estimate elemental Hg (Hg^0) volatilization rates from the river, and to assess the impacts of zebra mussel metabolism on Hg^0 volatilization. Elemental Hg volatilization was estimated at 1.3 ng m^{-2} hr^{-1} for the field season, and was positively correlated to incident solar radiation. It appears that the clearing of the water column caused by zebra mussels may increase Hg^0 volatilization rates due to subsequent increased penetration of incident solar radiation, though additional limiting factors are apparent. Reach-by-reach Hg mass balances were developed for three river reaches to assess the effects of an intervening hypereutrophic lake, a zone of intense zebra mussel infestation, and contributions from Onondaga Lake which is contaminated with elevated levels of Hg. It was determined that particulate Hg (THg_P) is the dominant form of Hg in the Seneca River, and Hg flux in the ecosystem is governed by flow characteristics. Intervening Cross Lake serves an important role for Hg transport in the Seneca River, reducing total Hg (THg) flux in the river by over 65% due to deposition of THg_P. Methylmercury (MeHg) concentration increased over the

reach of intense zebra mussel infestation, possibly due to support of anaerobic respiration as a result of the zebra mussel oxygen demand. The river reach receiving input from Onondaga Lake shows a 15% increase in THg flux. Net atmospheric Hg exchange is in the direction of deposition. However, direct atmospheric Hg deposition to the water surface plays a minimal role in Seneca River reaches, representing less than 1% of the fluvial Hg flux of the river. Overall, the Seneca River watershed is a sink for inputs of atmospheric Hg at a rate of 42 kg yr^{-1}, and the watershed efficiently retains >85% of this Hg, exporting approximately 5 kg yr^{-1} to the Three Rivers confluence.

For Phase 2, Hg speciation and concentrations were measured near the mouths of nine tributaries to Lake Ontario during two independent field-sampling programs. Among the study tributaries, mean THg ranged from 0.9 to 2.6 ng L^{-1}; mean dissolved Hg (THg_D) ranged from 0.5 to 1.5 ng L^{-1}; mean THg_P ranged from 0.3 to 2.0 ng L^{-1}; and mean MeHg ranged from 0.05 to 0.14 ng L^{-1}. Watershed land-cover, total suspended solids (TSS), and dissolved organic carbon (DOC) were evaluated as potential controls of Hg. Significant relationships between THg_D and DOC were limited, whereas significant relationships between THg_P and TSS were common. Methylmercury was largely associated with the aqueous phase, and MeHg as a fraction of THg was positively correlated to open water land-cover. Wetland cover was positively correlated to THg and MeHg particle associations. A relation was evident between dense urban land-cover and higher THg_P fractions.

Phase 3 utilized the results of Phase 2 to estimate Hg flux for ten inflowing tributaries and the outlet for Lake Ontario. Total Hg flux for nine study watersheds that directly drain into the lake ranged from 0.2 kg yr^{-1} to 13 kg yr^{-1}, with the dominant fluvial THg load from the Niagara River

at 154 kg yr^{-1}. Total Hg loss at the outlet (St. Lawrence River) was 68 kg yr^{-1}. Fluvial Hg inputs largely (62%) occur in the dissolved fraction and are similar to estimates of atmospheric Hg inputs. Fluvial mass balances suggest strong in-lake retention of THg_P inputs (99%), compared to THg_D (45%) and MeHg (22%) fractions. Wetland land-cover is a good predictor of MeHg yield for Lake Ontario watersheds. Sediment deposition studies and coupled atmospheric and fluvial Hg fluxes indicate that Lake Ontario is a net sink of Hg inputs and not at steady-state likely due to recent decreases in point source inputs and atmospheric Hg deposition.

In Phase 4, rates of surface-air Hg^0 fluxes in the literature were synthesized for the Great Lakes Basin (GLB). For the majority of surfaces, fluxes were net positive (evasion). Annual Hg^0 evasion for the GLB was estimated at 7.7 Mg yr^{-1}, whereas Hg deposition to the area is estimated at 15.9 Mg yr^{-1}. This analysis therefore suggests the GLB is a net sink for atmospheric Hg. Land-cover types that contributed most to the annual Hg^0 evasion for the GLB are agriculture (~55%) and forest (~25%), and the open water of the Great Lakes (~15%). Most land-cover types displayed similar areal evasion rates, with a range of 7.0 to 21.0 μg m^{-2} yr^{-1}. The highest rates were associated with urban (12.6 μg m^{-2} yr^{-1}) and agricultural (21.0 μg m^{-2} yr^{-1}) lands. Considerable uncertainty was noted in estimates of Hg^0 evasion. Methods used to estimate Hg^0 evasion vary, and results are affected based on the methods applied. A unified methodological approach could partially remedy uncertainty in estimating Hg^0 fluxes.

Mercury Transport and Fluxes

in the Lake Ontario Basin

By

Joseph S. Denkenberger

B.S. Chemistry, Le Moyne College, 2000

M.S. Environmental Engineering Science, Syracuse University, 2005

DISSERTATION

Submitted in partial fulfillment of the requirements for the degree of Doctor of Philosophy in Civil Engineering in the Graduate School of Syracuse University

May 2014

Acknowledgements

This research was supported by the US Environmental Protection Agency, the Ontario Ministry of the Environment, the New York Energy Research and Development Authority, and the Syracuse Center of Excellence through the Collaborative Activities for Research and Technology Innovation (CARTI) program. Partial funding for this work was also provided by the Wen-Hsiung and Kuan-Ming Li Graduate Fellowship.

In the US, field and laboratory support was provided by Mario Montesdeoca and Edward Mason at Syracuse University and Adam J.P. Effler, Bruce A. Wagner, David M. O'Donnell, Michael Spada, Tony R. Prestigiacomo, and many others at Upstate Freshwater Institute. Extra thanks go to Adam who provided technical and moral support on the river and throughout my research activities; Mario who fielded calls in the middle of the night regarding malfunctioning equipment, and also provided more than a fair share of technical and moral support; and Ed who did all the leg work for the US portion of the Lake Ontario tributary sampling, and made sure to get me outside when I needed it.

In Canada, field and laboratory support was provided by Ashley Warnock, Tracie Greenberg, Tom Ulanowski, Britney Meyers, and Geoff Stupple at the University of Toronto. Extra special thanks go to Ashley for graciously fielding all my questions and data requests regarding the Canada portion of the Lake Ontario tributary sampling, for very insightful editing efforts, and for support of publication development for the Lake Ontario work. Ram Yerubandi at Environment Canada and Tony Zhang at the University of Toronto increased the accuracy and precision of this work by aiding in development of discharge estimates for the Trent River.

Brad Blackwell and Colin Fuss donated significant time and effort to support the Seneca River evasion work, staying awake through the middle of the night to monitor sampling equipment so that I could sleep. A special mention and heartfelt thanks also go to AnneMarie Glose, who spent multiple sleepless nights sitting in a lawn chair, surrounded by poison ivy and biting insects, watching sampling equipment occasionally work and occasionally malfunction. AnneMarie also provided laboratory support.

Chris S. Eckley, Mark Cohen, and Pranesh Selvendiran provided significant support as coauthors of a publication generated from the Great Lakes Basin evasion synthesis work. Marty Risch, David Gay, Tom Holsen and Kim Driscoll also provided considerable aid with the analysis of Great Lakes Basin evasion estimates.

Mark Gravelding and Alain Hebert, of ARCADIS U.S., Inc., provided additional support during my dissertation development. Completion of this work may not have been possible without their aid, and my thanks go out to them for that.

I thank all my Syracuse University graduate student confederates that have yet to be mentioned: Afshin Pourmokhtarian, Amy Sauer, Dimitar and Svetla Todorova, Sam Werner, Jason Townsend, Rouzbeh Berton, Habib Fakhraei, Sam Fashu-Kanu, Qingtao Zhou. Special thanks go to Afshin, Amy, and Sam W. for being some of the more supportive friends I've had in the past several years at Syracuse University. Special thanks also go out to my good friends Jason Dittman (who secured a very nice desk for me before leaving the department, and made sure it was fully stocked with the necessities of research) and Richard Warby (who served as a ceaseless source of encouragement during my undertaking of this degree).

My family deserves special thanks for their support and understanding over the last several years. My mother, Denise Elliott, has been particularly instrumental in my success, always believing in me and encouraging me, and providing a constant source of support.

I would also like to give special thanks to the members of my committee: Drs. Steve Effler, Chris Johnson, Philippe Vidon, Andria Costello Staniec, Tara Kahan, Brian Branfireun, and Charley Driscoll. Very special thanks go to Dr. Kahan, who graciously accepted the task of chairing this committee at the last minute; Dr. Effler, who several years ago fueled my interest in limnology; and Dr. Branfireun, who directed the Canada portion of the Lake Ontario sampling and has provided considerable input as a coauthor on manuscripts developed or under development from this research.

I dedicate this work especially to my wife, Jen Bryz-Gornia, and also to my advisor, Dr. Charley Driscoll. I stood on their shoulders to get here, and they are the foundation for my achievements.

Table of Contents

List of Tables

List of Figures

1. Introduction

Mercury (Hg) occurs naturally in the environment, but industrial activities, mining, and electrical generation have greatly increased Hg emissions to the atmosphere that are subject to long-distance transport. The result has been widespread Hg contamination of aquatic environments and dangerously high concentrations in biota. Urban aquatic ecosystems are typically highly disturbed due to the number and intensity of stressors, such as domestic waste effluent, runoff from impervious surfaces, industrial contaminants, and exotic invasive species. Effective management can be confounded by the complexity of these ecosystems, their responses to stressors, temporal and spatial manifestations of the impacts of stressors, and multiple use goals. Mercury is of particular concern to environmental managers, especially in zones that are conducive to the efficient production of methylmercury (MeHg), and consequent bioaccumulation in higher organisms. The risks to society from Hg are reflected in long-standing government-issued advisories to reduce human exposure by limiting fish consumption.

My dissertation research focuses on the Hg dynamics of three linked systems: the Seneca/Oswego River, Lake Ontario, and the Great Lakes Basin (GLB). Although efforts have been made to assess the impacts of Hg on some of the Great Lakes (Mason and Sullivan 1997; Hurley et al. 1998a; Hurley et al. 2003; Rolfhus et al. 2003; Back et al. 2003), little information is available on the inputs of Hg to Lake Ontario.

2. Literature Review

2.1 Mercury Sources and Human Health Concerns

Elevated emissions Hg occur in the United States (US) and globally, in the form of primary anthropogenic emissions such as waste incineration, industrial processes, mining, and the burning of fossil fuels (Seigneur et al. 2003; Driscoll et al. 2007b; Driscoll et al. 2013). The increased global Hg pool that results from current and legacy anthropogenic emissions is chiefly responsible for elevated Hg levels in surface waters (Fitzgerald et al. 1991; Fitzgerald et al. 1998). The extent of this contamination is highly variable in time and space due to watershed processes which influence transformations and ultimately the supply of Hg to surface waters. In addition to atmospheric Hg deposition, industrial processes and wastes, non-point runoff, and wastewater treatment plants (WWTPs) can contribute to local Hg problems, particularly in urban areas. An example of local Hg contamination is evident in Onondaga Lake in Central New York, due to waste from a former chlor-alkali facility that historically operated on the shore of the lake.

It is difficult to characterize and predict the effects of Hg contamination on humans and wildlife due to the complexity of Hg associated with transport, transformations/conversions, and bioaccumulation along food webs in the environment. Of particular interest is the conversion of divalent Hg (Hg[II]) to MeHg, which largely occurs in wetlands, surface water sediments, and other reducing environments (Selvendiran et al. 2008a). Methylmercury efficiently bioaccumulates and is biomagnified (by a factor of a million to 10 million) along food chains (Kamman et al. 2005a; Driscoll et al. 2007b). This results in potentially dangerous levels of exposure of humans and wildlife to MeHg from consumption of fish, the extent and impact of

which is well documented in the literature (Mahaffey 1999; Mahaffey 2004; Evers et al. 2008; Sandheinrich and Wiener 2011). In the US, fish consumption advisories have been established in all 50 states in an attempt to limit human Hg exposure (Schmeltz et al. 2011). Similarly, Canada has fish consumption advisories in place for waterways in all the Provinces and Territories (except Nunavut) due to Hg contamination (Government of Canada 2007). The prevalence of these advisories underscores the need for a quantitative understanding of Hg fate and transport in ecosystems. This information will help environmental managers and stakeholders to characterize and quantify the effects of elevated Hg levels, and to anticipate ecosystem responses to controls and mitigation measures.

2.2 Watershed Effects on Mercury

Watershed characteristics, including topography and land-use patterns, have the potential to regulate the supply and bioavailability of Hg in receiving waters (Shanley et al. 2005; Riscassi et al. 2011). Soils with poor drainage, either as a result of chemical/physical characteristics, steep slopes, or paving, support increased flow of water over the surface, and therefore increased flushing of Hg into receiving waters (Dennis et al. 2005; Shanley et al. 2005). In watersheds dominated by urban, agriculture, or forest lands, Hg(II) is the dominant fraction and is most commonly associated with particulate or dissolved organic matter (Hurley et al. 1998b). In urbanized and industrialized watersheds Hg contamination is associated with elevated particulate Hg (THg_P) loads (Hurley et al. 1995; Mason and Sullivan 1998; Lyons et al. 2006). Lyons and others (2006) suggest that urbanization has a greater effect on THg_P loads than agricultural activities, though agricultural land-use is frequently linked to increased THg_P concentrations and loading (Hurley et al. 1995; Babiarz et al. 1998; Wang et al. 2004). As a result of the particulate-

association, high discharge events that mobilize particulate matter in such watersheds can serve as an important transport mechanism for Hg.

Forested catchments serve as sinks for Hg (St. Louis et al. 1996; Driscoll et al. 2007b). Grigal (2002) suggests that Hg coming into temperate and boreal watersheds is dominated by throughfall and litterfall (approximately 38 $\mu g\ m^{-2}\ yr^{-1}$), with precipitation providing a smaller contribution (approximately 10 $\mu g\ m^{-2}\ yr^{-1}$). He further suggests that only a small amount of deposited Hg is exported from watersheds via streamflow (approximately 2 $\mu g\ m^{-2}\ yr^{-1}$), though the characteristics of this small relative amount of Hg are very important to its fate and potential bioavailability. Strong associations with the dissolved phase (i.e., higher fractions of THg_D) were noted by Hurley et al. (1998b) in heavily forested watersheds. Additionally, associations between THg_D and DOC are frequently reported in the literature (Driscoll et al. 1995; Hurley et al. 1998b; Selvendiran et al. 2009; Dittman et al. 2010). Elevated DOC concentrations are typical of catchments with significant contributions of forest and wetland land-cover. Some have suggested that a MeHg pulse occurs from litterfall inputs in forested catchments (St. Louis et al. 2001; Balogh et al. 2003).

Relationships between wetlands and MeHg are noted frequently throughout the literature (Hurley et al. 1995; St. Louis et al. 1996; Driscoll et al. 1998; Grigal 2002; Warner et al. 2005). In watersheds that contain wetlands, Hg methylation is supported via anaerobic pathways (Selvendiran et al. 2008a). As a result, streamflow with higher MeHg:THg ratios is commonly observed from watersheds with significant wetland coverage. The positive correlation noted in the literature between watershed wetland area and MeHg flux has led one researcher to note the irony that wetlands are often targeted for protection via regulation and legislation, and yet are the

"single most identifiable source of MeHg in terrestrial systems," and that an "obvious method to reduce MeHg flux…would be to reduce the area of wetlands in watersheds" (Grigal 2002).

2.3 Riverine Mercury Transport

A number of studies have focused on Hg cycling in rivers (e.g., Babiarz et al. 1998; Balogh et al. 1998; Dalziel et al. 1998; Hurley et al. 1998b; Lawson et al. 2001; Balogh et al. 2005; Lyons et al. 2006; Bradley et al. 2011; Burns et al. 2012; Bradley et al. 2013). Most researchers compare and contrast Hg fate and transport among different watersheds, using factors such as watershed land-cover, geology, flow regimes, and particle-Hg relationships to explain trends in Hg observations (e.g., Babiarz et al. 1998; Balogh et al. 1998; Babiarz et al. 2012). Many also combine discharge data with Hg concentrations to estimate Hg flux rates from rivers to receiving waters (e.g., Hurley et al. 1998b; Lawson et al. 2001; Balogh et al. 2005; Westenbroek 2010).

The transport characteristics of Hg in rivers are often governed by the dominant phase associations of Hg, which in turn are largely a product of watershed characteristics. Hurley and others (1998b) note strong relative particulate-phase associations for Hg ($\%THg_P$) as well as particle-enrichment in rivers with industrialized watersheds. They also report a pattern of greater dissolved-phase associations ($\%THg_D$) in rivers draining more forested watersheds. This pattern is a common, recurring theme throughout the literature; that is, rivers draining urbanized watersheds tend to have greater $\%THg_P$, and rivers draining forested watersheds often have greater $\%THg_D$. This generalization can be further expanded: Hg in rivers draining watersheds with significant amounts of agriculture typically have higher $\%THg_P$, whereas Hg in rivers draining watersheds with significant wetland coverage more commonly have higher $\%THg_D$ (Hurley et al. 1995; Babiarz et al. 1998; Balogh et al. 1998; Hurley et al. 1998b; Balogh et al.

2003; Babiarz et al. 2012). Rivers with strong particle-Hg relationships typically exhibit elevated Hg transport during periods of high discharge (e.g., during rain events or spring melt) due to overland runoff and resuspension of sediments. Conversely, rivers with weak particle-Hg relationships and higher $\%THg_D$ will often exhibit a dilution effect during periods of elevated discharge (Babiarz et al. 1998; Hurley et al. 1998b).

Though efforts have been made to estimate tributary Hg loading based on land-cover analysis (Babiarz et al. 2012), these generalizations should be used with caution in estimating Hg dynamics in rivers. For example, the bulk of a single watershed may consist of forested land. Hypothetically, such a watershed might be expected to have high $\%THg_D$. However, the river may pass through a relatively small, though densely urbanized area prior to reaching its outlet, which would have the potential to greatly increase the THg_P load in the river due to runoff during precipitation events or point source discharges (Lawson and Mason 2001; Lyons et al. 2006). Similarly, physical alterations such as dams and impoundments, often located in urbanized rivers to support flood control and navigation, have been noted to decrease THg_P concentrations due to reductions in water velocity and subsequent deposition of THg_P to sediments (Lawson et al. 2001). Such characteristics of a river would not be ascertainable by land-cover analysis alone. Due to the strong potential for particle-Hg associations in rivers, the various watershed factors that can influence these associations, and the potential effects of in-river physical alterations, aquatic field sampling (in particular discharge event sampling) is a vital component in determining fluvial Hg transport in rivers (Shanley et al. 2008).

2.4 Mercury Mass Balances in the Great Lakes

The Great Lakes are collectively one of the world's largest sources of freshwater. As such, they provide drinking water, food, recreation, employment, and transportation to a considerable number of stakeholders (Evers et al. 2011). The region itself is characterized by elevated emissions and deposition of Hg (Pirrone et al. 1998; Miller et al. 2005; USEPA 2005; NESCAUM 2005; Choi et al. 2008; Denkenberger et al. 2012). A review of Hg studies for the Great Lakes shows an intense research focus on certain lakes (e.g., Lake Michigan) alongside a striking dearth of studies on others (e.g., Lake Huron, Lake Erie).

Lake Superior is the largest of the Great Lakes both in terms of water area (82,100 km^2) and total volume (12,100 km^3) (Government of Canada and United States Environmental Protection Agency 1995). However, the ratio of drainage area (127,700 km^2) to water area for Lake Superior is the lowest of all the Great Lakes, and the approximate population living within the Lake Superior watershed (i.e., 0.61 million) is less than 25% of the next smallest population of the Great Lakes watersheds (Lake Huron; 2.7 million) (Government of Canada and United States Environmental Protection Agency 1995). Despite the size of Lake Superior, relatively few studies have been conducted to assess Hg dynamics in the lake, perhaps due to the relatively low human population living adjacent to the lake. Some investigations have focused on Hg bioavailability (e.g., Kozie and Anderson 1991; Back et al. 2002; Back et al. 2003) and sediment Hg content (e.g., Kerfoot et al. 1999; Rossmann 1999). Major studies addressing tributary Hg contributions and open water Hg processes have been limited to tributary sampling conducted in the 1990s (Babiarz et al. 2012) and research cruises conducted in April and August of 2000 (Rolfhus et al. 2003) and May and July 2006 (Jeremiason et al. 2009). Rolfhus and others (2003) synthesized results from the literature to develop a preliminary mass balance for Lake Superior,

where the dominant component of the Hg budget was found to be atmospheric exchange. However, the researchers noted that estimates of Hg evasion from the lake (720 kg yr^{-1}) nearly balance estimates of atmospheric Hg deposition (740 kg yr^{-1}). With respect to net fluvial and atmospheric Hg, the researchers suggest that Lake Superior is a net Hg sink at a rate of approximately 270 kg yr^{-1} (Rolfhus et al. 2003). Jeremiason et al. (2009) utilized most of the estimates of Rolfhus et al. (2003) in development of a mass balance model for Lake Superior, but substituted their own range of estimates of Hg evasion (160-310 kg yr^{-1}) generated from research cruises conducted in 2006. From these estimates, the researchers propose the dominant loss mechanisms of Hg from Lake Superior are sedimentation and volatilization. The general lack of data for Lake Superior was noted as a source of uncertainty for the model (Jeremiason et al. 2009). An additional modeling attempt based off of the results reported by Rolfhus et al. (2003) has also proposed sedimentation and volatilization as the dominant loss mechanisms of Hg from Lake Superior (Qureshi et al. 2009).

Lake Superior drains directly to Lake Huron through the St. Mary's River. Lake Huron and Lake Michigan are hydrologically the same lake, being joined by the Straits of Mackinac and having the same water elevation. Viewed separately, Lake Huron is the second-largest of the Great Lakes by surface area (59,600 km^2) and the third-largest by volume (3,540 km^3); Lake Michigan is the third-largest of the Great Lakes by surface area (57,800 km^2) and the second-largest by volume (4,920 km^3) (Government of Canada and United States Environmental Protection Agency 1995). There is a general paucity of recent Hg data and research on Lake Huron. Most of the literature that does address Lake Huron is four decades old (pre-dating clean sampling techniques; USEPA 1996), and does not address the lake from a mass balance perspective, but is instead limited to analysis of sediments (Thomas 1973; Kemp and Thomas

1976) or biota (Weseloh et al. 1983). Conversely, Lake Michigan may be described as the most extensively monitored and studied of all the Great Lakes. Most notably, a large-scale effort known as the Lake Michigan Mass Balance Study (LMMBS) was initiated by the US Environmental Protection Agency (USEPA) Great Lakes National Program Office (GLNPO) to gather information regarding persistent environmental pollutants in Lake Michigan. The LMMBS supported several investigations regarding Hg in the water column (Mason and Sullivan 1997; Sullivan and Mason 1998), atmospheric Hg deposition (Landis and Keeler 2002), and Hg in tributaries to Lake Michigan (Hurley et al. 1998b). These studies have, in turn, supported numerous consequential efforts in development of Hg cycling models for Lake Michigan (Qureshi et al. 2009; Jeremiason et al. 2009); these more recent works largely reference the Hg loading rates developed in the earlier LMMBS studies. From the LMMBS effort, tributary Hg input to Lake Michigan was estimated at 230 kg yr^{-1} (Hurley et al. 1998b), fluvial Hg export was estimated to be 20 kg yr^{-1} (Mason and Sullivan 1997), atmospheric Hg deposition was estimated at 1,173 kg yr^{-1}, and Hg evasion was estimated at 453 kg yr^{-1} (Landis and Keeler 2002). These components suggest that Lake Michigan was a net sink for fluvial and atmospheric Hg at a rate of 930 kg yr^{-1}. A more recent USGS study revisited 5 of the original 11 tributaries sampled as part of the LMMBS, sampling for Hg, nutrients, and polychlorinated biphenyls (PCBs) (Westenbroek 2010). The USGS study described decreases in tributary Hg loading rates of approximately 50%, and attributed these observations to reduced sampling effort, different flow regimes during sampling periods, and overall net reductions in environmental Hg levels (Westenbroek 2010). As noted for Lake Superior, evasion and sedimentation are considered the dominant mechanisms of Hg loss from Lake Michigan (Qureshi et al. 2009; Jeremiason et al. 2009).

Lake Huron's outlet is the St. Clair River, which in turn drains into Lake St. Clair. With a surface area of 1,100 km^2, Lake St. Clair is significantly smaller than any of the Great Lakes. As such, it is not considered a Great Lake and therefore will not be addressed here. Lake St. Clair is drained via the Detroit River, which empties into Lake Erie. Of the five Great Lakes, Lake Erie is the fourth largest by surface area (25,700 km^2) and the fifth largest by volume (484 km^3) (Government of Canada and United States Environmental Protection Agency 1995). Similar to Lake Huron, very little research has been published regarding Hg in Lake Erie. What does exist is outdated or focused on sediments (Thomas and Jaquet 1976), biota (Kelso and Frank 1974; Hogan et al. 2007), or atmospheric deposition (Pirrone et al. 1995). Estimates of Hg concentrations in Lake Erie are provided in a study by Dove and others (2012), which indicated that the western basin of the lake had THg concentrations of approximately 12 ng L^{-1}, at least an order of magnitude higher than those observed in any of the other Great Lakes. However, this study did not address tributary inputs of Hg. Based on the Hg concentrations noted in the open water of the lake, it is apparent that additional research would be beneficial regarding Hg cycling and tributary Hg inputs to Lake Erie.

The Niagara River drains Lake Erie from the eastern end of the lake into the southwestern end of Lake Ontario. Lake Ontario is the fifth largest of the Great Lakes by surface area (18,960 km^2) and the fourth largest by volume (1,640 km^3). Although efforts have been made to assess the impacts of Hg on some of the Great Lakes (e.g., Mason and Sullivan 1997; Hurley et al. 1998b; Hurley et al. 2003; Rolfhus et al. 2003; Back et al. 2003), little information is available on the inputs of Hg to Lake Ontario. Lai et al. (2007) estimated net deposition of Hg to Lake Ontario, including wet deposition, net exchange of Hg^0 with the atmosphere, and dry deposition of reactive gaseous Hg and particulate Hg to the lake surface. However, the fluvial component of

Hg transport was not included in their study. In addition, Ethier et al. (2012) developed a model depicting transport and transformations of Hg within the lake, with the concentration of Hg in inflow water noted as having one of the largest impacts on model predictions of Hg. Despite this noted importance, fluvial inputs and export of Hg from the lake have not been characterized. French et al. (2006) suggested that while slight declines were occurring in fish tissue Hg concentrations, overall Hg levels remain high, and it is not clear what factors are responsible for these patterns. Information that would provide for a quantitative understanding of Hg transport and cycling has been largely lacking for Lake Ontario. A recent review of the literature found record of only three dated sediment cores from Lake Ontario that include Hg analysis, two of which were collected in 1981 and the other in 2008 (Drevnick et al. 2012). Evidence of Hg deposition derived from these cores indicates that in recent years, Hg sedimentation has decreased up to 80% from peak levels. However, flux ratios are still three- to seven-fold higher in Lake Ontario relative to what is expected in lakes without point sources (Drevnick et al. 2012). Further, though sedimentation may act as a sink for Hg, enriched sediments may also represent an important internal source of Hg to a lake (Todorova et al. 2009).

2.5 Hg Emissions and Atmospheric Deposition in the Great Lakes Basin

[Note: Section 2.5 includes material published in the journal *Environmental Pollution* by myself and the following coauthors: Charles T. Driscoll, Brian A. Branfireun, Chris S. Eckley, Mark Cohen, and Pranesh Selvendiran (Denkenberger et al. 2012). The original material has been edited to comply with the dissertation format. As such, the introduction of the publication is largely included here, the body of the work is included in Chapter 6, and the conclusions are presented in Chapter 8.4. Reuse of the published material in this dissertation complies with the

The entire global Hg pool includes inputs from both natural processes and anthropogenic activities. Important natural Hg emissions include processes such as volcanic eruptions, soil mineral weathering, and forest fires (Rasmussen 1994). Industrial emissions, mainly from coal combustion, waste incineration, mining, and industrial processes, add significantly to the global pool and are the primary sources of Hg to the atmosphere (Seigneur et al. 2003; Driscoll et al. 2007b; Pirrone et al. 2010). Human-related contributions are particularly important in urban areas, where potential Hg sources are often more densely located. These additional anthropogenic atmospheric emissions and subsequent deposition are largely responsible for Hg contamination in aquatic ecosystems (Fitzgerald et al. 1991; Fitzgerald et al. 1998). Likewise, it has been previously discussed that atmospheric Hg exchange represents the largest component where Hg mass balances have been developed for the Great Lakes (Mason and Sullivan 1997; Landis and Keeler 2002; Rolfhus et al. 2003).

The global biogeochemical cycle of Hg is characterized by numerous oxidation/reduction reactions, where Hg^0 is oxidized through different mechanisms to Hg(II), and Hg(II) is in turn reduced through various pathways to Hg^0. In aquatic and terrestrial ecosystems, the majority of Hg is Hg(II) (typically bound to particulate matter or other complexing ligands) with lesser amounts occurring as Hg^0 and MeHg. There is a critical interplay of processes for Hg(II), where Hg(II) can be either methylated to MeHg or reduced to Hg^0. Evasion of Hg^0 from lands and waters is a significant input to the atmosphere, and at the same time is an output of Hg from the terrestrial environment.

Terrestrial and aquatic processes can result in the chemical reduction of oxidized Hg species to Hg^0, resulting in volatilization of Hg^0. Loss of Hg^0 to the atmosphere can occur from water, vegetation, and soil surfaces (Amyot et al. 1994; Ericksen and Gustin 2004; Ericksen et al. 2006). For soils, Hg volatilization has been shown to vary spatially, as a function of surface characteristics such as Hg concentration, moisture content, and grain size distribution; and temporally as a function of changing meteorological conditions such as solar radiation, temperature, and soil moisture (Ericksen et al. 2006; Selvendiran et al. 2009; Choi and Holsen 2009a; Eckley et al. 2011). In lakes, photo-reduction of Hg(II) appears to be the primary process driving the production of dissolved gaseous Hg (DGM) and its subsequent loss to the atmosphere (e.g., Amyot et al. 1994; Lindberg et al. 2000b; O'Driscoll et al. 2003b). Several proposed mechanisms include direct photolysis of Hg(II) to Hg^0 (Munthe and McElroy 1992; Amyot et al. 1994) including photosensitizing of Fe^{3+} complexes (Zhang and Lindberg 2001; Ababneh et al. 2006), sulfite complexes (Munthe et al. 1991; Van Loon et al. 2000), DOC and humic substances (Xiao et al. 1991; Nriagu 1994; Xiao et al. 1995), and reduction of Hg(II) involving oxygen radicals such as $O_2^{\bullet-}$, $HO^{\bullet}$, and H_2O_2 (Schroeder et al. 1992; Dommergue et al. 2003). Photodecomposition of MeHg directly to Hg^0 has also been suggested (Tossell 1998). Because photo-reduction of Hg(II) is an important driving mechanism in the volatilization of Hg^0, studies are characterized by marked diel changes in evasion rates.

Recent estimates have suggested that Hg^0 evasion may account for a substantial fraction of Hg loss from ecosystems. For example, Quémerais et al. (1999) estimated that the fluvial loss of Hg from Lake Ontario to its only outlet, the St. Lawrence River, is approximately 5.9 $\mu g\ m^{-2}\ yr^{-1}$. The volatilization rate of Hg^0 from Lake Ontario was estimated by Lai et al. (2007) to be approximately 5.8 $\mu g\ m^{-2}\ yr^{-1}$. Likewise, in a Hg mass balance for Arbutus Lake in the

Adirondack Mountains, New York, Selvendiran et al. (2009) estimated fluvial Hg loss to be 1.2 $\mu g\ m^{-2}\ yr^{-1}$ and Hg^0 volatilization to be 7.8 $\mu g\ m^{-2}\ yr^{-1}$.

Published measurements of Hg^0 volatilization rates include both aquatic and land surfaces. The rates of Hg volatilization reported in the literature range from < 5 $ng\ m^{-2}\ hr^{-1}$ from pristine lakes and forest soils to >10,000 $ng\ m^{-2}\ hr^{-1}$ from contaminated soils (Gustin et al. 2003; Amyot et al. 2004). Gaseous Hg^0 has an atmospheric residence time of around 1 year (Fitzgerald and Mason 1997; Smith-Downey et al. 2010). As a result, Hg^0 may be transported globally prior to being deposited back to the Earth's surface following volatilization. Deposition occurs following oxidation of Hg^0 to Hg(II), and subsequent complexation of Hg(II) with airborne particulates or dissolution in water. In forest systems Hg^0 can also enter the stomata of leaves which can be deposited to the forest floor during litter fall (Driscoll et al. 2007a). Divalent Hg returns to the Earth's surface as wet (i.e., rain), dry (i.e., particulate, gaseous), or litter fall deposition.

2.6 Dissertation Objectives and Approach

The objectives of my research are: 1) to perform a large river reach analysis by characterizing and quantifying the transport, transformations, and fate of Hg in the Seneca River; 2) to perform a sub-watershed analysis for major tributaries to Lake Ontario with respect to land-cover and Hg dynamics; 3) to collect and analyze tributary samples for Lake Ontario and develop a preliminary mass balance of Hg for the lake; and 4) to perform a literature review and synthesis of Hg emissions estimates and examine these in the context of atmospheric emissions, deposition, and fluvial losses of Hg for the GLB.

Three interrelated field efforts in conjunction with laboratory and data analyses have been carried out to meet these goals, and the research has been divided into the following four phases in order to address the proposed objectives:

Phase 1: In order to improve understanding of Hg fate and transport in the Seneca River, water samples were collected every two weeks from multiple locations along an approximate 38 kilometer reach beginning immediately upstream of Cross Lake (navigation buoy 430) to just upstream of the Oneida River/Seneca River juncture (navigation buoy 224). Sample collection occurred during the summer field seasons (approximately June through September) of 2007, 2008, and 2009, and these samples have been analyzed for both whole-water (i.e., THg) and filtered (i.e., THg_D) forms of THg, and whole-water MeHg. Methylmercury analysis was initially performed on filtered samples as well, but it was determined that all detectable MeHg in samples collected from the Seneca River was associated with the particulate form, and therefore MeHg analysis of filtered samples was abandoned. Additional detailed field sampling, involving novel Hg evasion equipment, was conducted over a diurnal period at points directly above and below the reach of intense zebra mussel infestation. During the diurnal experiments evasion measurements were made hourly over 24 hour periods. Additional water quality parameters (i.e., dissolved oxygen [DO], chlorophyll-a [Chl_a], turbidity [T_n], pH, temperature, and specific conductance) were routinely recorded at each sampling station throughout the field seasons using computer controlled robotic profiling platforms (Effler et al. 2002) and field-deployed Yellow Springs Instruments (YSI) DataSonde 6600 units configured with probes for each parameter (O'Donnell 2001). These measurements, coupled with flow data available from US Geological Survey (USGS) gauging stations, have supported fate determination of mass fluxes of Hg species on a reach-by-reach basis. By coupling discharge with river concentrations, the mass fluxes of

Hg species were calculated. The details and results of Phase 1 of my research are presented in Chapter 3.

Phase 2: The Lake Ontario tributary sampling involved the collection of samples twice per month from nine rivers within the lake's immediate watershed (i.e., not connected via Lake Erie and the Niagara River). Sample analysis included supplementary chemistry (e.g., TSS, cations, anions, particulate organic carbon [POC], DOC, pH) in addition to THg and MeHg. Four of the study rivers are located in the US (Genesee, Oswego, Salmon, and Black) and were sampled between June 2009 and May 2010. The remaining five study rivers are located in Canada (Twenty Mile, Credit, Humber, Ganaraska, and Trent) and were sampled between June 2008 and December 2009. Results from the sample analysis have been used in conjunction with a geographic information system (GIS) approach to assess the effects of watershed characteristics on Hg speciation and fluxes. The details and results of Phase 2 of my research are presented in Chapter 4.

Phase 3: In addition to the rivers discussed for Phase 2, the Niagara and St. Lawrence rivers were also sampled twice per month between June 2008 and December 2009 (Niagara) and from June 2009 to May 2010 (St. Lawrence). The mass transport of Hg species for all sampled tributaries has been estimated by coupling fluvial concentration measurements with discharge data available from USGS and Environment Canada stations. An overall Hg budget was developed for the lake based on fluvial inputs and losses. The results of this exercise have been used in conjunction with independent estimates of atmospheric Hg exchange and in-lake sedimentation to develop a Hg mass balance for Lake Ontario, and are presented and discussed in Chapter 5.

Phase 4: In order to better place results of the Lake Ontario mass balance within the context of the GLB, part of my research also included a literature review and synthesis of atmospheric Hg evasion for the GLB. Atmospheric Hg evasion fluxes were estimated for land-cover classes within the GLB based on published data, and scaled in conjunction with digital land-cover data to estimate annual Hg^0 evasion for the entire basin. This flux was put in context by comparison with estimates of direct anthropogenic Hg emissions, atmospheric Hg deposition, and riverine Hg loss. The details of the literature review and synthesis conducted for Phase 4 of my research are provided in Chapter 6.

3. Seneca River Analysis

3.1 Introduction

Considerable research has been conducted on the Seneca River. However, despite elevated Hg inputs resulting from Onondaga Lake, there is no information on Hg transport and transformations in the river. Likewise, there is no information on the effects on Hg cycling of the dense population of zebra mussels that have infested the river. The formation of MeHg is favored under reducing conditions, as this process is largely mediated by sulfate reducing bacteria, which are strict anaerobes (Benoit et al. 2001). The dense population of zebra mussels documented in the Seneca River Barge Canal Cut results in a significant oxygen demand across this reach as a result of both zebra mussel respiration and the decomposition of zebra mussel pseudofeces (Effler et al. 1996). As a result, zebra mussel metabolism may facilitate the formation of MeHg by supporting the potential for anaerobic conditions in the river. In addition, zebra mussels are nondiscriminatory filter feeders and as such, they will take in and process any particulate matter possible. This may result in dissociation and mobilization of Hg from particulate matter following egestion. The documented clearing of the water column by the zebra mussels (Denkenberger et al. 2007) allows additional penetration of solar radiation. Reduction of Hg(II) to volatile Hg^0 has been identified to occur largely via sunlight-induced reactions (Xiao et al. 1995; O'Driscoll et al. 2003a). Increases in light penetration as a result of zebra mussel metabolism may therefore increase volatilization (i.e., loss) of Hg from the Seneca River. The effects of zebra mussels on Hg cycling are therefore expected to be complex and variable.

The results of a multi-year study have been combined to explore Hg dynamics in the Three Rivers system, with particular emphasis on the Seneca River. Results from these sampling efforts are presented here in the context of a reach-by-reach Hg mass balance analysis for the Seneca River. Relationships between ancillary chemistry and Hg speciation and transport are also explored. It is hypothesized that Hg in the Seneca River is largely in a particulate form and transport is therefore governed by flow. This largely unavailable form of Hg can be altered in space and time due to shifts in redox conditions associated with the stratification of adjacent lakes (Onondaga Lake, Cross Lake) and zebra mussel metabolism.

3.2 Study System

The Seneca River is a river system located in Central New York that drains the Finger Lakes region and is influenced by diverse land-cover and associated human activities (i.e., urban, forest, agricultural lands; Figure 3.1, p. 21). The Seneca River flows eastward through Cross Lake towards the outlet of Onondaga Lake, and turns northward to join the Oneida River. At this confluence, both rivers form the Oswego River. The Oswego River flows northward, draining into Lake Ontario. Collectively, these rivers are known as the Three Rivers system. The Three Rivers support multiple uses including navigation, power generation, and waste discharge. All three rivers are channelized, with a minimum maintained depth of 4.5 meters, and all support a series of locks and impoundments due to inclusion in the NYS Barge Canal System. As a result of this channelization, natural reaeration has been greatly reduced (Canale et al. 1995). Also, a 1.7 km reach of the Seneca River supports a considerable infestation of invasive zebra mussels (*Dreissena polymorpha*) (Effler et al. 2004). Numerous water quality impacts have been documented over this reach resulting from zebra mussel metabolism, including depletion of DO and increased water clarity (Effler et al. 2004; Denkenberger et al. 2007; Effler

et al. 2010). Onondaga Lake is an important site of local Hg contamination from the former chlor-alkali facility and urban runoff from the city of Syracuse. Indeed, the sediments of Onondaga Lake are on the National Priority List. Fluvial Hg inputs from Onondaga Lake are transported downstream to the Seneca/Oswego River system and ultimately Lake Ontario.

Samples were collected at four navigational buoys along the Seneca River (Figure 3.1, p. 21). Navigational buoy 430 (B430) is located approximately 1.5 km upstream of the Seneca River's entrance into the southern end of hypereutrophic Cross Lake (Effler and Carter 1987). Cross Lake is approximately 1.5 km wide between the points where the Seneca River enters and exits. Navigational buoy 409 (B409) is located approximately 1.5 km downstream of Cross Lake, at the beginning of the NYS Barge Canal Cut. Immediately downstream of B409, the Seneca River flow follows the NYS Barge Canal Cut, which is characterized by a significant infestation of zebra mussels. The water quality signatures of this invasive species have been recorded by routine monitoring at Navigational Buoy 317 (B317), and are described elsewhere (Effler and Siegfried 1998; Effler et al. 2004; Denkenberger et al. 2007; Glaser et al. 2009). Specific effects of the zebra mussels include reductions in T_n, Chl_a, and DO, as well as increases in water clarity. Below the Cut, the Seneca River has no significant point-source inputs or notable physical characteristics until it reaches Lock 24 in Baldwinsville, NY. The river is slow-moving through this reach and often exhibits evidence of stratification, with minimal reaeration potential as a result of channelization (Glaser et al. 2009; Effler et al. 2010).

The downstream boundary of the study system is marked by Navigational Buoy 224 (B224), which is located just upstream of the confluence of the Seneca River and the Oneida River, and the beginning of the Oswego River (Figure 3.1, p. 21). The Seneca River travels approximately

19 km between B317 and B224. The single most notable characteristic of this reach occurs approximately 7 km downstream of B317, where the only outlet of Onondaga Lake discharges into the river. In the past, Onondaga Lake has been characterized as one of the most contaminated lakes in the country (Hennigan 1990). This distinction came as a result of the lake receiving significant industrial and domestic waste inputs during the settling and industrialization of the area, and failure to meet a number of water quality standards. Most notably, approximately 75,000 kg of Hg were disposed of in the lake as a by-product of a chlor-alkali facility situated near the lake's southwestern shore between the 1940s and mid-1980s (Effler and Bloom 1990). As a result of this severe Hg contamination, Onondaga Lake has been the focus of significant remediation efforts since the latter part of the 20th century; dredging activities began in 2012 as part of the selected remedy to address this Hg contamination (Honeywell 2013). However, the period of this study (i.e., 2007-2009) was prior to in-lake remediation activities.

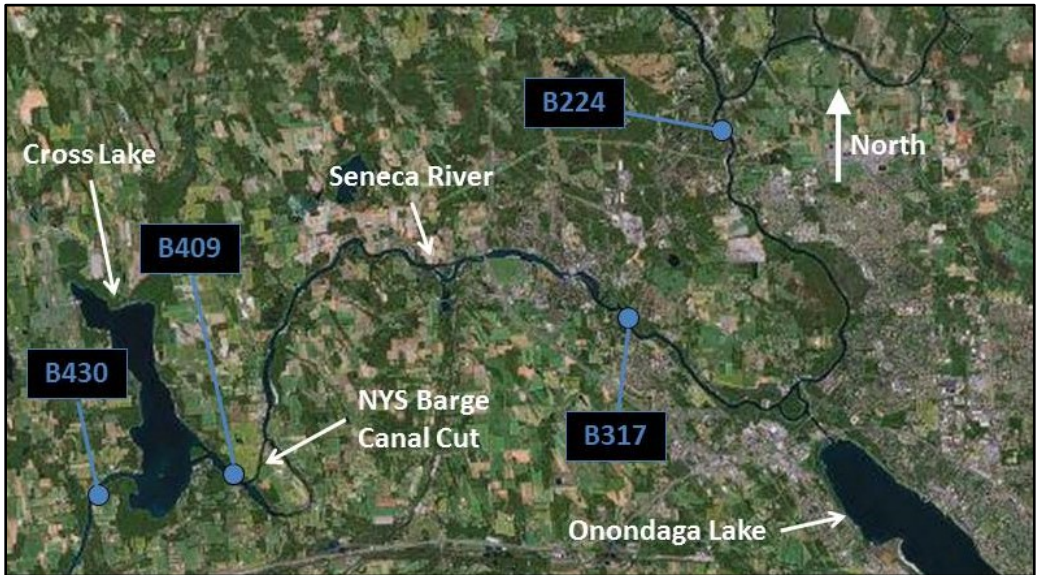

Figure 3.1 Study system and sample locations (B430, B409, B317, and B224). Aerial image from Google Earth.

3.3 Methods

In order to improve understanding of Hg fate and transport in the Seneca River, water samples were routinely collected every two weeks from four locations (Figure 3.1, p. 21) along an approximate 38 kilometer reach beginning immediately upstream of Cross Lake (B430) to just upstream of the Oneida River/Seneca River confluence (B224). Sample collection occurred during the summer field seasons (approximately June through September) of 2007, 2008, and 2009. Samples were collected from a depth of 3-m at all locations; additional samples were collected from a depth of 1-m at B409 and B224. Samples collected from the Seneca River were analyzed for both THg_P and THg_D, and whole-water MeHg.

Sample collection was performed using trace metal clean protocols as described in Method 1669 (USEPA 1996). Upon arrival at the laboratory, 250-500 mL water sample aliquots were filtered through pre-cleaned 0.45-µm filters. Whole and filtered water samples were then preserved using 4 mL L^{-1} 11.6 M trace metal grade hydrochloric acid. Total Hg analysis was conducted using cold vapor atomic fluorescence spectrometry (CVAFS; Bloom 1989; USEPA 2002). Methylmercury determination was performed via aqueous phase ethylation with sodium tetraethylborate ($NaB[C_2H_5]_4$), purge and trap separation and detection by CVAFS (Horvat et al. 1993a; Horvat et al. 1993b; Liang et al. 1994). Total particulate Hg was calculated as the difference between whole- and filtered-sample results; consequently, some reported THg_P concentrations are below THg and MeHg detection limits (0.20 and 0.02 ng L^{-1}, respectively). Supplementary water quality measures included DO, Chl_a, T_n, pH, temperature, and specific conductance. The supplementary measures were collected as discussed earlier using computer controlled robotic profiling platforms (Effler et al. 2002) and field-deployed YSI DataSonde

6600 units configured with probes for each parameter (O'Donnell 2001). Collection of supplemental measures did not extend beyond the Seneca River.

Additional detailed field sampling, involving novel Hg evasion equipment, was conducted over a diurnal period at points immediately upstream and downstream of the reach of intense zebra mussel infestation (i.e., the NYS Barge Canal Cut; Figure 3.1, p. 21). The upstream site was forested to the river bank, while the downstream site was a privately-owned lawn with some trees nearby. Three field sampling events were conducted over the summer of 2010 (July 13-15, July 26-28, and August 24-26). During each event, the sampling equipment was initially deployed in the late afternoon at the upstream site and allowed to run for nearly 24 hr. In the mid-afternoon of the following day, the instrumentation was disassembled, moved, and redeployed at the downstream site, where it was again allowed to run for nearly 24 hr.

The Cut is particularly well-suited for analysis of the water quality signatures of zebra mussels, as there are no point-source loadings or noteworthy tributary inflows along this 1.7 km reach. It can therefore be viewed as an input-output system. Gaseous Hg^0 flux (i.e., Hg^0 volatilization) from the Seneca River was estimated using a variation of the method detailed by O'Driscoll et al. (2003b). A 1.5 L volumetric glass sparger in series with a Hydrolab Minisonde 4a and Tekran 2537A elemental Hg analyzer was used to measure dissolved gaseous Hg (DGM) in river water every 5 minutes. A 0.64-cm diameter Teflon sample inlet tube was installed as far from the river bank as possible without impeding the navigational channel (approximately 50 feet from shore at the upstream site and 20 feet from shore at the downstream site). The sample inlet was suspended approximately 15 cm below the river surface. River water was continuously pumped at a rate of 50 mL min^{-1} using a Cole Parmer 7524-40 peristaltic pump. The sample water first

passed through the Hydrolab flow cell for measurement of temperature, pH, redox potential, conductivity, and DO. The river water was then pumped into the bottom of the 1.5-L glass sparger, where a glass frit bubbled 1.0 L min^{-1} of Hg-free air as provided by a Tekran Model 1110 zero-air generator. Sample water exited the sparger at the 1.0 L mark, and sample air was flushed through Teflon tubing to the Tekran 2537A, where it was analyzed for gaseous Hg concentration. Weather conditions (i.e., temperature [°C], humidity, wind speed [km h^{-1}], barometric pressure [Pa], solar radiation [W m^{-2}]) were continually recorded by a Vantage Pro 2 Plus weather station. Electricity was provided by both a gasoline-powered generator and deep-cycle batteries.

Elemental Hg volatilization was calculated as outlined by Selvendiran et al. (2009). Specifically, the following mass transfer model (Liss and Slater 1974) was used to estimate gaseous Hg^0 flux from DGM measurements:

$$F = \frac{(C_a - HC_w)}{{}^{1}/_{K_a} + {}^{H}/_{K_w}} \qquad \text{(Eq. 3.1)}$$

where F = Hg^0 volatilization, reported as a flux (ng m^{-2} hr^{-1}); C_a = concentration of Hg^0 in air (ng m^{-3}); H = dimensionless Henry's Law constant; C_w = concentration of DGM in water (ng m^{-3}); K_a = air mass transfer coefficient of Hg^0 (9 m hr^{-1}); and K_w = water mass transfer coefficient of Hg^0 (0.09 m hr^{-1}). A value of 1.5 ng m^{-3} was used for C_a (Selvendiran et al. 2009). Values for K_a and K_w were estimated by Schroeder et al. (1992). The Henry's Law constant was calculated using a temperature-variable model developed by Sanemasa (1975):

$$H = 0.0074T + 0.1551 \qquad \text{(Eq. 3.2)}$$

where H = Henry's Law constant (dimensionless) and T = water temperature (°C).

Statistical analysis was performed using SigmaPlot 11.0 (Systat Software, Inc. 2008). For tests of significance, α was set to 0.05 unless otherwise noted. Student's t-tests were used to test for sample differences unless normality tests failed, in which case Mann-Whitney rank sum tests were applied. For calculation of means, medians, and standard deviations, non-detect samples were assigned a value of one-half the detection limit of 0.20 ng L^{-1} for THg and 0.02 ng L^{-1} for MeHg. This approach was used to fill data gaps for less than 4% of all Hg analyses (15 of 473 samples), though the majority of non-detects occurred for MeHg analyses (10 of 108 samples).

The mass transport of Hg species was estimated by coupling fluvial concentration measurements with discharge data available from the USGS station in Baldwinsville, New York (USGS Station 04237500). Calculations were performed using $FLUX_{32}$ software, version 3.03 (Walker 1987). The $FLUX_{32}$ model utilizes daily discharge rates (where available) in conjunction with analyte concentrations to estimate material fluxes. Multiple calculation methods are provided in the software package, allowing the user to choose the one that best suits the flow and concentration characteristics of each tributary. Continuous flow data are available for the Seneca River, and sample data are available for most Hg species on a biweekly basis for the field seasons (i.e., June through September) of 2007, 2008, and 2009. Estimates of fluxes for Hg species in this study generally displayed small relative variations among most calculation methods. However, the smallest coefficients of variation were typically noted for Calculation Method 2 (which bases flux estimates on flow-weighted concentrations), and as a result this method was selected for generation of the reported flux rates.

The Community Multi-scale and Air Quality (CMAQ; http://www.epa.gov/asmdnerl/EcoExposure/deposition Mapping.html; Bullock and Brehme 2002) model was used to support development of mass balances for the river reaches based on the Hg emission inventory for 2005. This model has been used to develop estimates of particulate and ionic atmospheric Hg deposition on a 12 km grid. A GIS approach was used to analyze depositional rates for each of the 12 km squares over the Three Rivers watershed.

A simple input/output model was used to assess Hg fate and transport through the river reaches. Key elements included estimates of fluvial Hg flux at each bounding station. Flux estimates at upstream buoys were considered as inputs to the reach whereas estimates at downstream buoys where expressed as outputs. Atmospheric exchange was held constant across all river reaches as the net sum of evasion and deposition estimates. Net gains or losses across reaches are explored relative to reach characteristics.

3.4 Results and Discussion

3.4.1 Physical Controls on Mercury Volatilization in the Seneca River

In situ measurements of DGM resulted in detailed time series records over the study periods. The complete records of DGM, modeled Hg^0 volatilization flux, solar radiation, and water temperature for the bounding sites are illustrated as time-series in Figures 3.2.1, 3.2.2, and 3.2.3 (pp. 28-30). The DGM concentration and Hg^0 volatilization flux were low during the evening and night, and increased markedly during the day with increases in solar radiation and temperature. Air temperature and river discharge varied during the study periods as outlined in Table 3.1 (p.27).

Table 3.1 Summary of Seneca River discharge and air temperature during the 2010 Hg^0 volatilization field sampling events. Air temperature recorded in the field using Vantage Pro 2 Plus weather station. Daily river discharge recorded at the USGS station in Baldwinsville, New York (USGS Station 04237500).

Event		Date Range	Air Temperature (°C)		Daily River Discharge (m^3 s^{-1})	
			Min	Max	Min	Max
1	Upstream	July 13-14	21.1	28.8	52.7	78.2
	Downstream	July 14-15	19.3	32.4	52.7	78.7
2	Upstream	July 26-27	17.6	27.8	135.9	176.4
	Downstream	July 27-28	17.5	29.9	62.9	135.9
3	Upstream	August 24-25	17.3	22.3	100.2	104.5
	Downstream	August 25-26	15.8	23.0	92.6	100.2

Preliminary studies in 2008 and 2009 suggested a relationship of increasing Hg evasion from the water column with increases in incident solar radiation. Regression analysis of data collected in 2010 supported these observations. Daytime (i.e., sunrise to approximately 15:00 hours) Hg^0 volatilization as a function of solar radiation is shown in Figure 3.3 (p. 33). Note that each event at the upstream site appears to follow a distinct relationship between Hg^0 volatilization and solar radiation. Data from the downstream site may also exhibit different Hg^0 volatilization – solar radiation relationships for each event, though the differences are not as evident and all three sampling events seem to blend together due to considerable scatter in the data with increasing solar radiation. At the upstream site, maximum observed Hg^0 volatilization values varied by nearly an order of magnitude between events, from approximately 0.7 ng m^{-2} hr^{-1} during Event 3 to approximately 5.5 ng m^{-2} hr^{-1} during Event 1. A lesser degree of variability was noted between events at the downstream site, where maximum observed Hg^0 volatilization values varied twofold between events, from approximately 2.9 ng m^{-2} hr^{-1} during Event 3 to

approximately 5.8 ng m^{-2} hr^{-1} during Event 2. Based on these results, it is likely that an additional factor is limiting Hg^0 volatilization.

In addition to solar radiation, Hg^0 volatilization has been linked to water temperature (Xiao et al. 1991; Schroeder et al. 1992; Amyot et al. 1994; Gårdfeldt et al. 2001). The observations in my study suggest both physical factors may limit volatilization in the Seneca River. Linear regression suggested that solar radiation could explain 29% of daytime Hg^0 volatilization in the study system, whereas water temperature appeared to be a much stronger predictor of Hg^0 volatilization ($r^2 = 0.77$). However, regardless of water temperature, overnight Hg^0 volatilization values are largely zero or slightly negative (i.e., suggesting deposition; Figures 3.2.1, 3.2.2, and 3.2.3; pp. 29-31). Though the lower overall water temperatures recorded during Event 3 (Figure 3.2.3, p. 31) appear to have decreased the response of Hg^0 volatilization to solar radiation (Figure 3.3, p. 33), net volatilization does not generally occur without solar radiation.

The scatter plot presented in Figure 3.4 (p. 34) provides a closer look at the relationship between water temperature and Hg^0 volatilization. The figure presents Hg^0 volatilization at the upstream site during the 13-15 July 2010 event (Event 1) as a function of water temperature, with separate symbols used to identify (1) the first day and night of sampling ("Day 1 and Night;" open triangle), and then (2) the second day of sampling ("Day 2;" closed circle). Nonlinear relationships appear evident; however, as water temperature continued to increase on Day 2, Hg^0 volatilization values appeared to peak and then decrease. This observation indicates that Hg^0 volatilization is not primarily driven by water temperature. Instead, solar radiation, which is related ($r^2 = 0.26$) to water temperature (Figure 3.5, p. 35), appears to be the strongest primary factor influencing Hg^0 volatilization. As solar radiation decreases, Hg^0 volatilization values

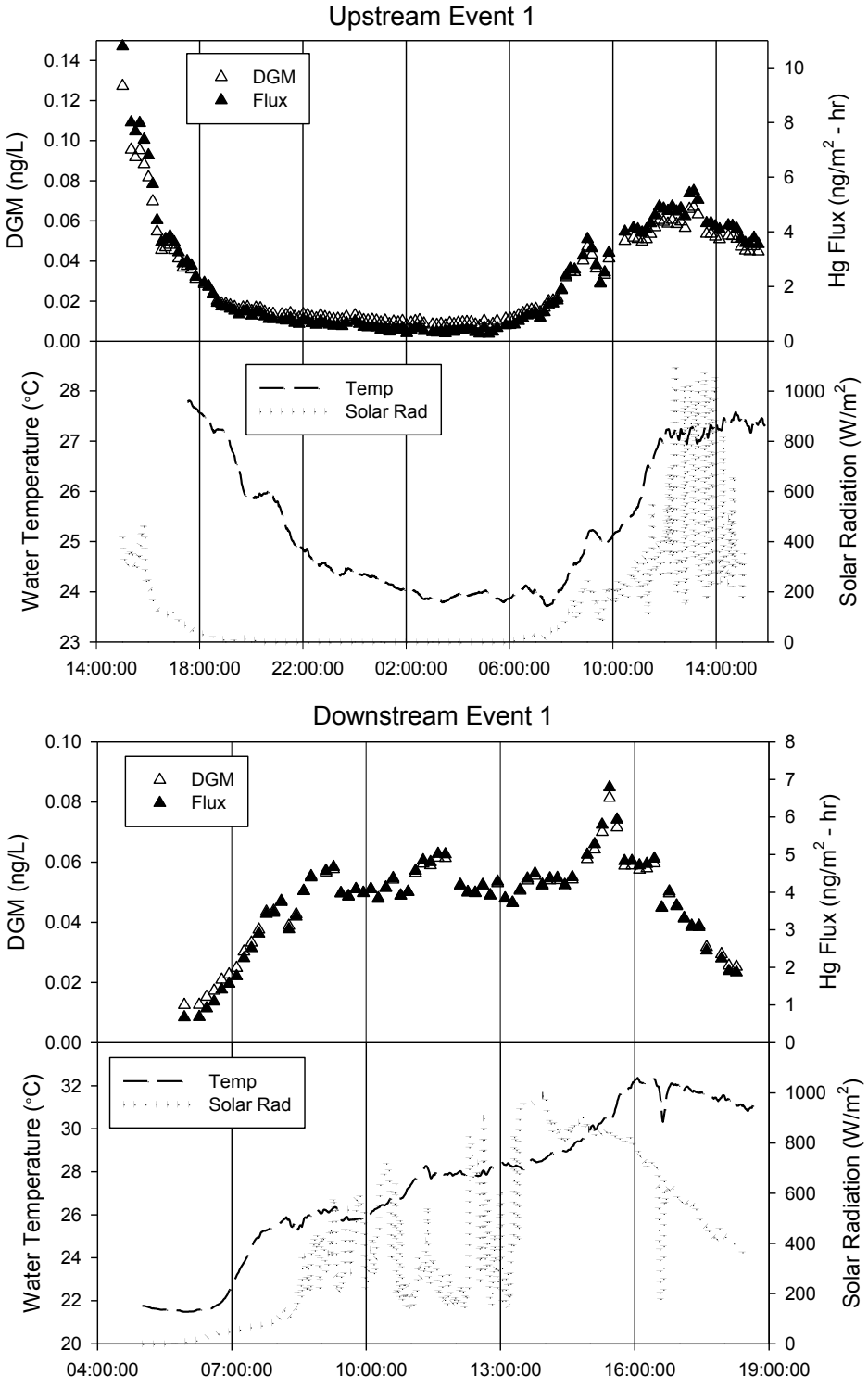

Figure 3.2.1 Event 1. Time series of DGM concentration and Hg^0 volatilization (reported as flux) and supporting values of water temperature and solar radiation for a sampling event July 13-15, 2010 upstream and downstream of the Cut in the Seneca River.

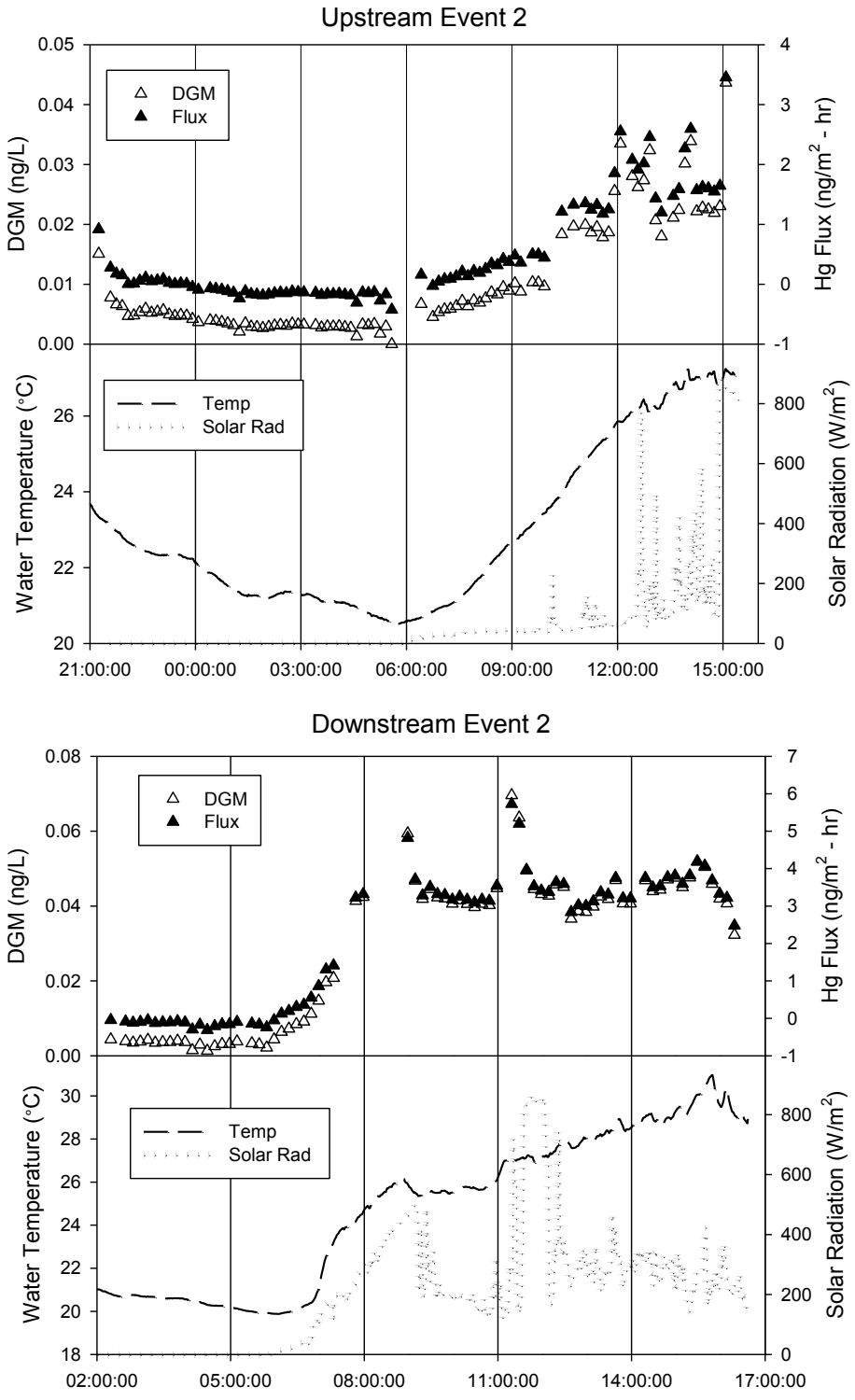

Figure 3.2.2 Event 2. Time series of DGM concentration and Hg^0 volatilization (reported as flux) and supporting values of water temperature and solar radiation for a sampling event July 26-28, 2010 upstream and downstream of the Cut in the Seneca River.

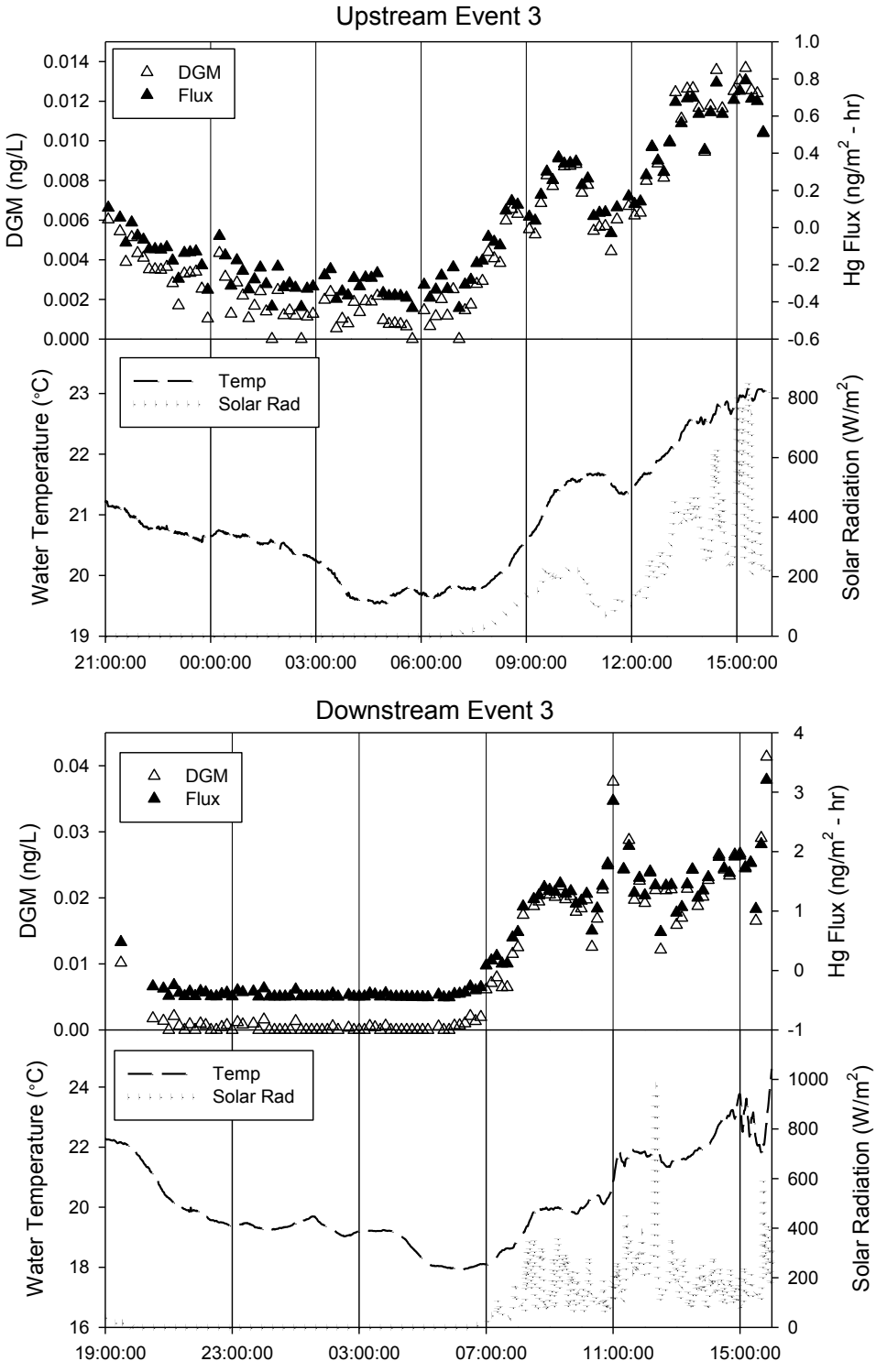

Figure 3.2.3 Event 3. Time series of DGM concentration and Hg^0 volatilization (reported as flux) and supporting values of water temperature and solar radiation for a sampling event August 24-26, 2010 upstream and downstream of the Cut in the Seneca River.

almost immediately decrease (Figures 3.2.1, 3.2.2, and 3.2.3; pp. 29-31). On the other hand, water retains heat from solar radiation for a short period, and therefore water temperature is not as responsive to changes in solar radiation as Hg^0 volatilization. Note the different values of Hg^0 volatilization at equivalent temperatures between the "Day 1 and Night" and "Day 2" periods on Figure 3.4 (p. 34). At equal water temperatures "Day 2" Hg^0 volatilization values are as much as threefold higher than "Day 1 and Night" Hg^0 volatilization values. The "Day 1 and Night" data in the temperature range of 24- to 27 °C were collected overnight, between 19:00 and sunrise of the following day (Figure 3.2.1, p. 29). The "Day 2" data in the same temperature range were collected after sunrise on the following day (Figure 3.2.1, p. 29). This observation underscores the direct dependence of Hg^0 volatilization on solar radiation.The data recorded in my study suggest that solar radiation predicts 33% and 42% of Hg^0 volatilization at the upstream and downstream sites, respectively, and that water temperature predicts 69% and 80% of the variation in Hg^0 volatilization at the upstream and downstream sites, respectively. In addition, solar radiation is less strongly correlated to water temperature at the upstream site ($r^2 = 0.19$) than at the downstream site ($r^2 = 0.40$). Although best efforts were made to collect comparable field data at both sites, sun exposure was more limited at the upstream site due to adjacent forest cover. The decoupling of solar radiation and Hg^0 volatilization, particularly at the upstream site, may therefore be partly attributable to experimental conditions. In addition, the photoreduction of Hg(II) is more efficient when caused by light with shorter wavelengths (i.e., ultraviolet, < 400 nm) (Costa and Liss 2000). The solar radiation sensor included with the Vantage Pro 2 Plus weather station used for my study detects wavelengths in the range of 400 – 1,100 nm. As a result, variations in ultraviolet radiation were not recorded, though these variations may be partly

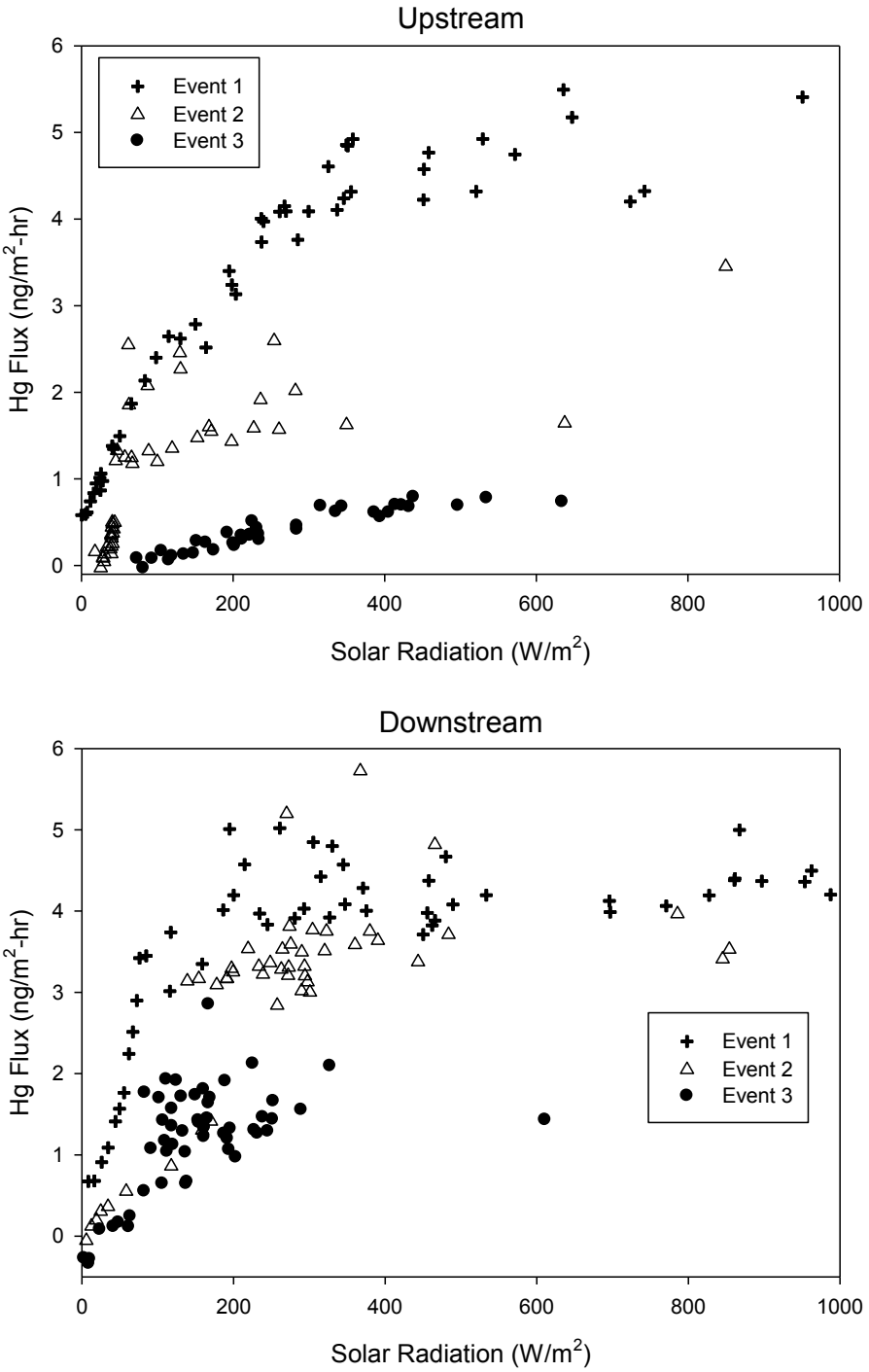

Figure 3.3 Elemental Hg volatilization as a function of solar radiation at upstream (upper panel) and downstream (lower panel) sites for all three sampling events. Note relationship at both upstream and downstream sites between solar radiation and Hg^0 volatilization (reported as flux) at low solar radiation (i.e., < 400 W m^{-2}).

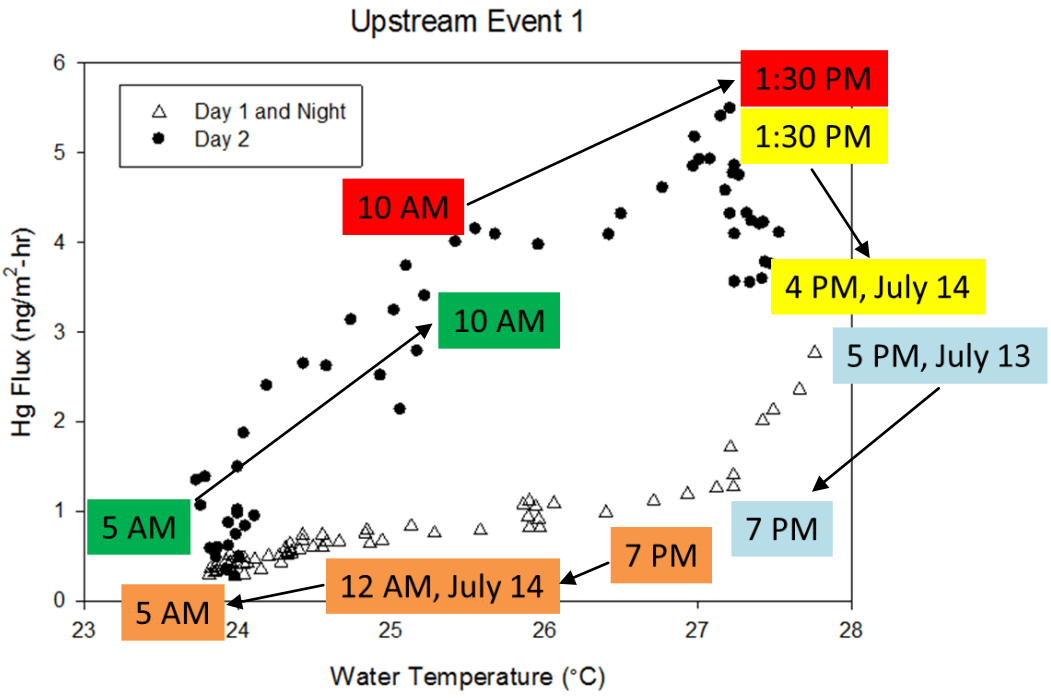

Figure 3.4 Elemental Hg volatilization (reported as flux) as a function of water temperature during 13-15 July 2010 event (Event 1). Note that time advances from right to left along the "Day 1 and Night" symbols (5 PM, July 13 to 5 AM, July 14; open triangle), and then from left to right along the "Day 2" symbols (5 AM, July 14 to 4 PM, July 14; closed circle).

responsible for the noted disparity between solar radiation and Hg^0 volatilization relative to water temperature and Hg^0 volatilization.

The suggestion that solar radiation drives Hg^0 volatilization has been reported elsewhere (Xiao et al. 1995; O'Driscoll et al. 2003a; O'Driscoll et al. 2007; Selvendiran et al. 2009). In some studies, the relationship between Hg^0 volatilization and solar radiation was strengthened by shifting solar radiation to some period approximately 60-90 minutes prior to the DGM value recorded (O'Driscoll et al. 2003a; Selvendiran et al. 2009). In this study, however, the relationship between solar radiation and Hg^0 volatilization was not strengthened by shifting solar

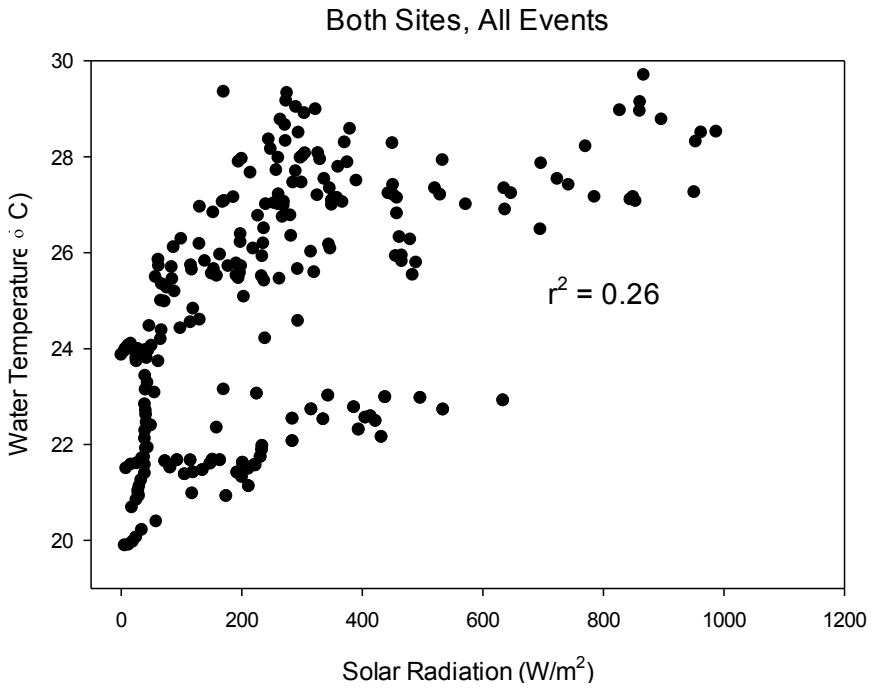

Figure 3.5 Water temperature as a function of solar radiation at both sites during all events.

radiation. A similar observation was made in another study performed on the St. Lawrence River (O'Driscoll et al. 2007). The experiments that exhibited stronger relationships with shifted solar radiations were conducted on lentic systems, whereas my experiment and that by O'Driscoll et al. (2007) were conducted on lotic systems. Perhaps the well-mixed nature of a river relative to a lake may increase exposure of Hg(II) to solar radiation and thus increase rates of photoreduction.

3.4.2 Effects of Zebra Mussels on Mercury Volatilization

The New York State Barge Canal Cut is particularly well-suited for analysis of the water quality signatures of zebra mussels, as there are no point-source loadings or noteworthy tributary inflows along this 1.7-km reach. In order to determine whether Hg^0 volatilization was different between the upstream site (i.e., above the dense concentration of zebra mussels) and the downstream site (i.e., below the dense concentration of zebra mussels), t-tests were attempted on the daytime Hg^0

volatilization data using SigmaPlot (Systat Software, Inc. 2008). However, the Hg^0 volatilization data were not normal, and efforts to achieve normality via transformations were not successful. The Mann-Whitney Rank-Sum Test is a non-parametric hypothesis test; as such, it does not require observations to follow any particular probability distribution, and was therefore applied to the dataset. Since Hg^0 volatilization values were almost non-existent overnight (see Figures 3.2.1, 3.2.2, and 3.2.3; pp. 28-30), testing was conducted on mid-day values, when solar radiation and Hg^0 volatilization values were strongest. Event 1 exhibited no significant difference between upstream and downstream values ($p = 0.531$). This result was likely influenced by a rain event that occurred the first afternoon of deployment at the upstream site. Lindberg et al. (2000) noted that rain resulted in immediate increases in DGM levels, likely due to inputs of photoreducible Hg(II) from rainwater. This hypothesis is supported in the Seneca River, as the measured DGM concentrations and calculated Hg^0 volatilization during and immediately following the rain event were the highest noted for all sampling events at both sites (Figures 3.2.1, 3.2.2, and 3.2.3; pp. 28-30), and likely influenced the lack of statistical difference between sites for Event 1. Events 2 and 3, however, did exhibit significant differences between upstream and downstream Hg^0 volatilization, with higher median Hg^0 volatilization noted at the downstream site for both events. In addition, when all daytime data from all events were compared, a significant difference was also noted, again with a higher median Hg^0 volatilization noted from the data collected at the downstream site. These results indicate that Hg^0 volatilization at the downstream site was significantly greater than Hg^0 volatilization at the upstream site. However, significant differences were also noted among solar radiation records at the two sites for all three events. These statistical tests were likewise conducted using the Mann-Whitney Rank-Sum Test due to lack of normality for the solar radiation record. In this case, the

median solar radiation values were higher at the downstream site for Events 1 and 2, but lower for Event 3. The variability in the record of solar radiation is attributed to differences in experimental conditions between the two sites, as discussed below.

Deployment conditions were not equivalent between the upstream and downstream sites: the upstream site was forested to the river's edge, whereas the downstream site was a privately owned lawn, largely clear of trees. Best efforts were made to place the weather station in the river as far from the bank as possible at the upstream site in order to record open-water conditions. River depth and encroachment upon the navigational channel precluded deployment more than 15-m from the bank. Nearby trees were well over 15-m tall, and thus shaded the weather station at certain times of the day. Since the water being sampled had flowed from further upstream, where it was fully exposed to incident solar radiation, the solar record provided by the weather station may not be completely representative. As a result, the importance of statistical differences observed in the solar radiation record between the upstream and downstream sites is unclear.

Varying responses of Hg^0 volatilization to both water temperature and solar radiation were observed at both upstream and downstream sites. At the upstream site, Hg^0 volatilization response to solar radiation differed noticeably among events, whereas responses were similar among events at the downstream site (Figure 3.3, p. 33). The maximum observed Hg^0 volatilization rates are displayed in Figure 3.6 (p. 39) for each event by site as functions of average mid-day (10:00-15:00) solar radiation. These data suggest that the maximum attainable Hg^0 volatilization is more strongly controlled by solar radiation at the upstream site, as indicated by the greater slope of the upstream site's regression line (0.015) versus the downstream site's

regression line (0.007), though limited sample size results in a lack of significance. The apparent difference in slope between upstream and downstream sites suggests an intervening effect. The only significant change in the channel between the sites is the dense zebra mussel population in the Cut. The documented water quality effects of this filter-feeding invader include significant clearing of the water column (Effler et al. 1996; Effler et al. 2004; Denkenberger et al. 2007). Therefore, I propose that the differences observed among events at the upstream site are the result of varying water quality signatures of hypereutrophic Cross Lake on the Seneca River immediately upstream of the Cut, with a specific emphasis on algal blooms (Effler et al. 2011). Further, the lack of apparent differences in the response of Hg^0 volatilization to solar radiation among the three events at the downstream site (Figure 3.3, p. 33) is likely due to the erasure of Cross Lake's signature by the clearing of the water column as it passes through the zebra mussel-infested Cut. Unfortunately, no field data exist for Cross Lake during my study period that could corroborate this speculation. However, these observations do indicate that the processing of the Seneca River water column by the zebra mussels may reduce Hg^0 volatilization limitation by solar radiation.

3.4.3 Atmospheric Mercury Exchange in the Seneca River

To support the reach-by-reach Seneca River mass balance estimates discussed in the subsequent sections of this chapter, all evasion values for the three summertime events discussed in the Chapter Section 3.4.1 were averaged. The resulting estimate of Hg evasion from the Seneca River is thus 1.3 ng m^{-2} hr^{-1} (or 11.4 μg m^{-2} yr^{-1}). This flux is assumed to apply to the entire year for purposes of mass balance estimates, and likely results in a positive bias, as Hg volatilization during the winter months is likely reduced due to ice cover, cold conditions, and reductions in incident solar radiation. Measurements do not currently exist for this system that account for

these seasonal effects. The seasonality of Hg volatilization is discussed further in Chapter 6. The estimate of 1.3 ng m^{-2} hr^{-1} generated here for the Seneca River is approximately 45% higher than the value noted for inland waters (0.9 ng m^{-2} hr^{-1}) in Chapter 6. However, the measurements in Chapter 6 are largely derived for lentic systems.

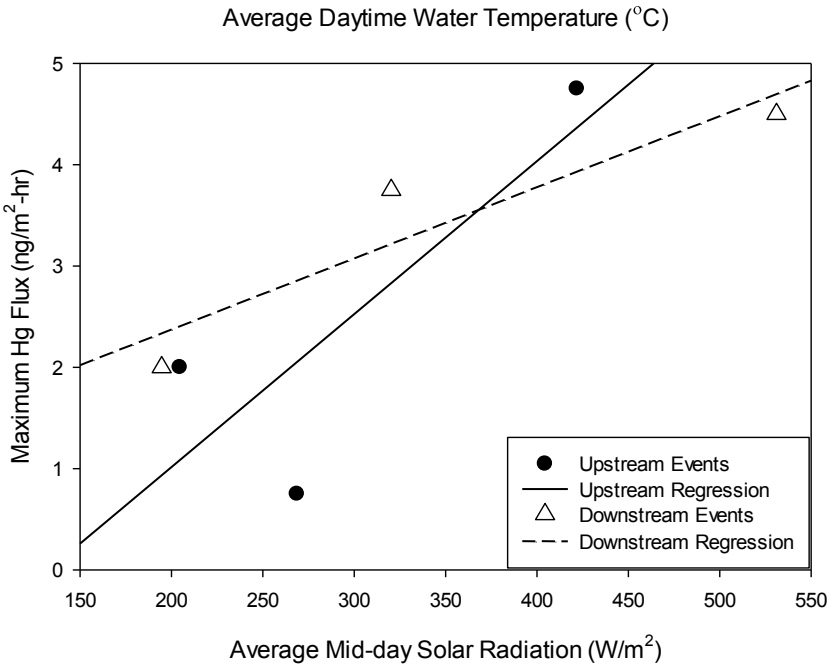

Figure 3.6 Maximum observed Hg^0 volatilization (reported as flux) as a function of average mid-day (i.e., 10:00-15:00) solar radiation. Elemental Hg volatilization displays greater dependence on solar radiation at the upstream site, suggesting solar radiation is less limiting at the downstream site. Correlations are strong but relationships are not significant due to small sample size. Mid-day solar radiation used to reduce bias from varying site conditions (i.e., forested banks vs. non-forested banks).

A GIS approach was used in conjunction with estimates of atmospheric Hg deposition generated from CMAQ (Bullock and Brehme 2002) to determine deposition rates of Hg(II) and particulate

Hg (Hg_P) to the Seneca River based on the Hg emission inventory for 2005. This analysis suggested deposition rates of 14.6 and 1.8 μg m^{-2} yr^{-1} for Hg(II) and Hg_P, respectively. These values were summed for a gross Hg deposition rate of 16.4 μg m^{-2} yr^{-1} to the Seneca River watershed. This deposition rate was used in conjunction with the Hg evasion rate noted above (11.4 μg m^{-2} yr^{-1}) to estimate net atmospheric exchange to each study reach of the Seneca River, as outlined in Table 3.2 and integrated with estimates of fluvial Hg flux in Chapter Sections 3.4.3, 3.4.4, and 3.4.5.

Table 3.2 Net atmospheric Hg exchange in the Seneca River. Note that negative values indicate net loss from the ecosystem and positive values indicate net deposition. Estimated fluvial Hg fluxes are included for comparison.

Reach	Length (m)	Width (m)	Area (m^2)	Evasion Flux (μg m^{-2} yr^{-1})	Gross Evasion (g yr^{-1})	Deposition Rate (μg m^{-2} yr^{-1})	Gross Deposition (g yr^{-1})	Net Atmospheric Exchange (g yr^{-1})	Fluvial Hg Flux (g yr^{-1})
B430 to B409	3,000	150	450,000	-11.4	-5	16.4	7	2	4,500
Cross Lake	--	--	9,000,000	-11.4	-103	16.4	148	45	--
B409 to B317	14,000	150	2,100,000	-11.4	-24	16.4	34	10	4,500
B317 to B224	19,000	150	2,850,000	-11.4	-32	16.4	47	15	5,200

3.4.4 Navigational Buoy 430 to 409

Previous work has focused on the effects of intervening Cross Lake on Seneca River water quality, and has indicated that during high-flow conditions the river short-circuits the lake by flowing straight through with minimal interaction between lake and river waters (Schindel et al. 1977). During low-flow conditions it is apparent that some mixing occurs, and a "signature" is imparted to the river water exiting the lake that is representative of lakewide surface water conditions (Effler et al. 2011). In this study, samples were collected from a depth of 3-m at

B430. At B409, samples were collected from depths of both 1-m and 3-m to assess stratification imparted to the river waters from the lake. The only significant differences between the 1-m and 3-m data were for THg and Chl_a: mean THg was significantly higher at 3-m, while mean Chl_a was significantly higher at 1-m. The elevated productivity of Cross Lake manifested itself by significantly higher values of Chl_a at B409 relative to B430, regardless of sample depth. Mean Chl_a levels increase by approximately 50% between B430 and B409 (Table 3.3, p. 44).

Cross Lake's presence had a significant effect on Hg in the Seneca River. At B430, approximately 80% of THg was associated with particulate material. At B409, however, THg_P made up only 60% of THg (Figure 3.7, p. 46). More significantly, mean THg_P concentrations decreased nearly 70% from 2.6 ng L^{-1} at B430 to 0.8 ng L^{-1} at B409, and overall mean THg concentrations decreased over 55% from 3.2 ng L^{-1} to 1.4 ng L^{-1}. These decreases likely result from the settling of particulate matter in Cross Lake due to reductions in flow velocity across the lake, as also evidenced by measures of T_n between the two sites: mean T_n decreased over 55% from 24.1 Nephelometric Turbidity Units (NTU) at B430 to 10.3 NTU at B409 (Table 3.3, p. 44). Based on these results, Cross Lake acts as a significant sink for fluvial loading of Hg from the Seneca River.

Bookman et al. (2008) noted a high Hg sedimentation rate (248.8 μg m^{-2} yr^{-1}) in Cross Lake relative to other regional lakes. This sedimentation rate equates to a yearly depositional Hg flux of 2.6 ± 0.1 kg yr^{-1}, based on the following assumptions: (1) the sedimentation rate is homogenous across the entire lake bottom, and (2) the area of the lake bottom is 15% (± 5%) greater than the surface area of the lake (i.e., 10.35 ± 0.45 km^2). It is likely that the majority of this sedimentation results from fluvial input of THg_P from the Seneca River, which contributes

approximately 98% of Cross Lake's inflow. Analysis of atmospheric Hg exchange suggests a net deposition of 5 μg m^{-2} yr^{-1}, or approximately 47 g yr^{-1} (Cross Lake plus the river reach; Table 3.2, p. 40). Fluvial Hg flux into Cross Lake was calculated at 13.3 kg yr^{-1}, and fluvial Hg export was estimated to be 4.5 kg yr^{-1}, suggesting a net Hg retention of 8.8 kg yr^{-1} (approximately 66%) in Cross Lake. Based on this estimate, the Hg sedimentation flux of 248.8 μg m^{-2} yr^{-1} (2.6 kg yr^{-1}) underestimates actual Hg sedimentation flux. Due to the rapid flushing rate of Cross Lake (i.e., 51 yr^{-1}; O'Donnell 2001) and the variable interaction of the Seneca River with the lake (Schindel et al. 1977; Effler et al. 2011), it is likely that sedimentation is not homogenous across the lake bottom. Bookman et al. (2008) developed their estimate from four cores collected from the northern half of Cross Lake. Effler and Carter (1987) noted higher net sedimentation rates in the area of the lake where the Seneca River passes through. It is likely that cores collected from the southern half of Cross Lake, where the Seneca River enters and exits, would exhibit higher rates of Hg sedimentation compared to a lake wide average.

3.4.5 Navigational Buoy 409 to 317

There was no significant difference between THg concentrations at B409 and B317, nor between THg_P concentrations at the bounding sites (Table 3.4, p. 44; Figure 3.7, p. 46). At B409, mean THg concentrations during the study were 1.1 ng L^{-1} in surface waters and 1.4 ng L^{-1} at 3-m depth. Water samples were only collected at 3m depth from B317, and the mean THg concentration was 1.2 ng L^{-1}. I hypothesized that the documented reductions in DO resources (Effler et al. 2004; Denkenberger et al. 2007; Effler et al. 2010) caused by the zebra mussel infestation in the Cut may support anaerobic Hg methylation. The data indicate an increase in MeHg across the reach (Figure 3.7, p. 46). Dissolved oxygen concentrations were significantly higher at B409 relative to B317 (Table 3.3, p. 44). Methylmercury concentrations at B409 were

0.037 and 0.034 ng L^{-1} at 1- and 3-m, respectively (Table 3.4, p. 44). At B317, mean MeHg concentrations were significantly higher at 0.087 ng L^{-1}. In addition, %MeHg as a fraction of THg was significantly higher at B317 (9%) than at B409 (4%). Other water quality indicators of the zebra mussel metabolism, notably the significant decrease in Chl_a between B409 and B317 (Table 3.3, p. 44), suggest the continued presence and activity of this invader during the study period. However, the lack of a shift in THg_P concentrations across this reach suggests either selective feeding by the zebra mussels with rejection of material with high particle-Hg associations, or efficient processing and egestion of THg_P.

Analysis of atmospheric Hg exchange suggests a net deposition of approximately 10 g yr^{-1} to the Seneca River between B409 and B317 (Table 3.2, p. 40). Fluvial Hg flux into the reach at B409 was estimated at 4.5 kg yr^{-1}, and fluvial Hg export past B317 was estimated to be 4.5 kg yr^{-1}, suggesting no net Hg retention between B409 and B317.

3.4.6 Navigational Buoy 317 to 224

Onondaga Lake waters have high specific conductance (SC; approximately 2,000 µS cm^{-1}; Effler et al. 2010) relative to the Seneca River (approximately 750 µS cm^{-1} upstream of the Onondaga Lake outlet; see Table 3.3, B317; p. 44), and therefore Onondaga Lake waters are relatively dense compared to the Seneca River. As a result of this density differential and the channelization of the river, unique bidirectional flow patterns often occur during low flow conditions at the Onondaga Lake outlet (Owens and Effler 1996), where river water will flow into the lake over the top of lake water, and lake water outflows plunge below the incoming river water. The plunging lake water has been documented to travel some distance upstream as well as downstream before fully mixing with the river water (Effler et al. 1984; Effler et al. 2010).

Table 3.3. Summary of 2007-2009 monitoring buoy data from the Seneca River. Descriptive statistics are limited to data collected on same dates as Hg grab samples.

Navigational Buoy–depth	DO (mg L^{-1})					Chl_a (µg L^{-1})					T_n (NTU)				
	Min	Max	Mean	Median	S.D.	Min	Max	Mean	Median	S.D.	Min	Max	Mean	Median	S.D.
B430 – 3m	3.5	9.5	7.4	7.6	1.5	4.2	22.4	10.9	9.0	5.2	10.7	91.8	24.1	16.3	21.4
B409 – 1m	6.8	13.2	9.0	8.7	1.7	8.2	63.8	16.5	12.9	13.1	6.0	14.5	9.7	9.7	2.4
B409 – 3m	6.4	11.6	8.4	8.0	1.4	5.0	58.2	12.6	9.7	12.0	7.0	15.0	10.1	10.3	2.1
B317 – 3m	4.4	8.8	6.8	7.2	1.3	1.9	12.0	5.9	4.8	3.5	3.8	45.9	10.7	7.2	10.5
B224 – 2.5m	3.4	8.1	6.2	6.4	1.0	1.7	28.9	6.8	4.6	6.9	1.1	88.9	10.1	3.0	22.1
Navigational Buoy–depth	**pH**					**T(°C)**					**SC (µS cm^{-1})**				
	Min	**Max**	**Mean**	**Median**	**S.D.**	**Min**	**Max**	**Mean**	**Median**	**S.D.**	**Min**	**Max**	**Mean**	**Median**	**S.D.**
B430 – 3m	7.6	8.3	7.9	7.9	0.2	19.2	26.1	23.0	22.9	1.8	615.3	936.3	761.5	780.7	75.2
B409 – 1m	7.7	8.6	8.3	8.3	0.3	20.4	26.8	23.7	23.5	1.8	539.0	860.0	734.6	761.0	80.1
B409 – 3m	7.7	8.7	8.2	8.1	0.3	20.3	26.8	23.4	23.3	1.7	540.0	858.0	738.2	766.0	81.8
B317 – 3m	7.4	8.3	7.8	7.7	0.2	19.8	27.0	23.6	23.6	1.8	642.7	826.0	747.6	764.3	54.5
B224 – 2.5m	7.4	7.8	7.6	7.6	0.1	19.9	26.6	23.5	23.4	1.6	734.5	1327.1	1021.1	1031.4	135.3

Table 3.4. Summary of 2007-2009 grab sample sampling depths and data from the Seneca River.

Navigational Buoy–depth	THg (ng L^{-1})					THg_D (ng L^{-1})					THg_P (ng L^{-1})				
	Min	Max	Mean	Median	S.D.	Min	Max	Mean	Median	S.D.	Min	Max	Mean	Median	S.D.
B430 – 3m	1.2	9.1	3.2	3.0	1.7	0.1	1.6	0.6	0.5	0.4	0.9	7.5	2.6	2.4	1.6
B409 – 1m	0.4	1.9	1.1	1.1	0.4	0.1	0.9	0.4	0.5	0.2	0.1	1.2	0.7	0.7	0.4
B409 – 3m	0.6	2.7	1.4	1.3	0.5	0.1	1.3	0.6	0.5	0.3	0.0	1.9	0.8	0.8	0.5
B317 – 3m	0.6	3.6	1.2	1.0	0.6	0.1	1.4	0.5	0.5	0.3	0.1	2.9	0.7	0.6	0.6
B224 – 1m	0.5	10.3	1.5	0.9	2.1	0.2	1.3	0.7	0.7	0.4	0.0	2.1	0.4	0.2	0.6
B224 – 3m	0.4	3.6	1.4	1.0	0.8	0.2	1.0	0.5	0.5	0.2	0.2	2.9	1.0	0.5	0.8

Navigational Buoy–depth	MeHg (ng L^{-1})				
	Min	Max	Mean	Median	S.D.
B430 – 3m	0.010	0.410	0.085	0.074	0.088
B409 – 1m	0.010	0.110	0.042	0.037	0.029
B409 – 3m	0.010	0.120	0.048	0.034	0.035
B317 – 3m	0.010	0.200	0.087	0.090	0.054
B224 – 1m	0.010	0.130	0.055	0.058	0.034
B224 – 3m	0.000	0.300	0.087	0.080	0.068

Due to the levels of Hg contamination in Onondaga Lake, it was hypothesized that the lake would contribute a significant amount of Hg to the river. At B224, water samples were collected from both the 1-m and 3-m depths. However, THg concentrations were not significantly different between B317 and B224 at either depth, nor were THg concentrations significantly different between the 1-m and 3-m depths at B224 (Table 3.4, p. 44; Figure 3.7, p. 46). The only significant difference noted between the 1-m and 3-m data at B224 was for THg_P; mean THg_P was significantly higher at 3-m (1.0 ng L^{-1}; Table 3.4, p. 44) than at 1-m (0.4 ng L^{-1}; Table 3.4, p. 44). Effler et al. (2010) noted infrequent thermal and chemical stratification extending from the Onondaga Lake outlet to B224, indicating that Onondaga Lake waters are generally mixed throughout the water column at this location. Profile data were collected manually on all days that Hg samples were collected; a review of SC data from these profiles indicated that the river water column was infrequently stratified during the sampling events. Dates exhibiting stratification showed no relationship to dates with greater differences between THg_P at the 1-m and 3-m depths. The elevated mean THg_P at 3-m may be a result of scour-related sediment resuspension. However, results of linear regression analysis of THg_P as a function of discharge at B224 were not significant at either 1-m or 3-m.

Analysis of atmospheric Hg exchange suggests a net deposition of approximately 15 g yr^{-1} to the Seneca River between B317 and B224 (Table 3.2, p. 40). Fluvial Hg flux into the reach at B317 was estimated at 4.5 kg yr^{-1}, and fluvial Hg export past B224 was estimated to be 5.2 kg yr^{-1}, suggesting a net Hg gain of 0.7 kg yr^{-1} between B317 and B224. It is quite likely that this additional Hg input is provided by the Onondaga Lake outlet. Also, Hg inputs from Onondaga Lake may be deposited to Seneca River sediments in this reach, particularly in light of the

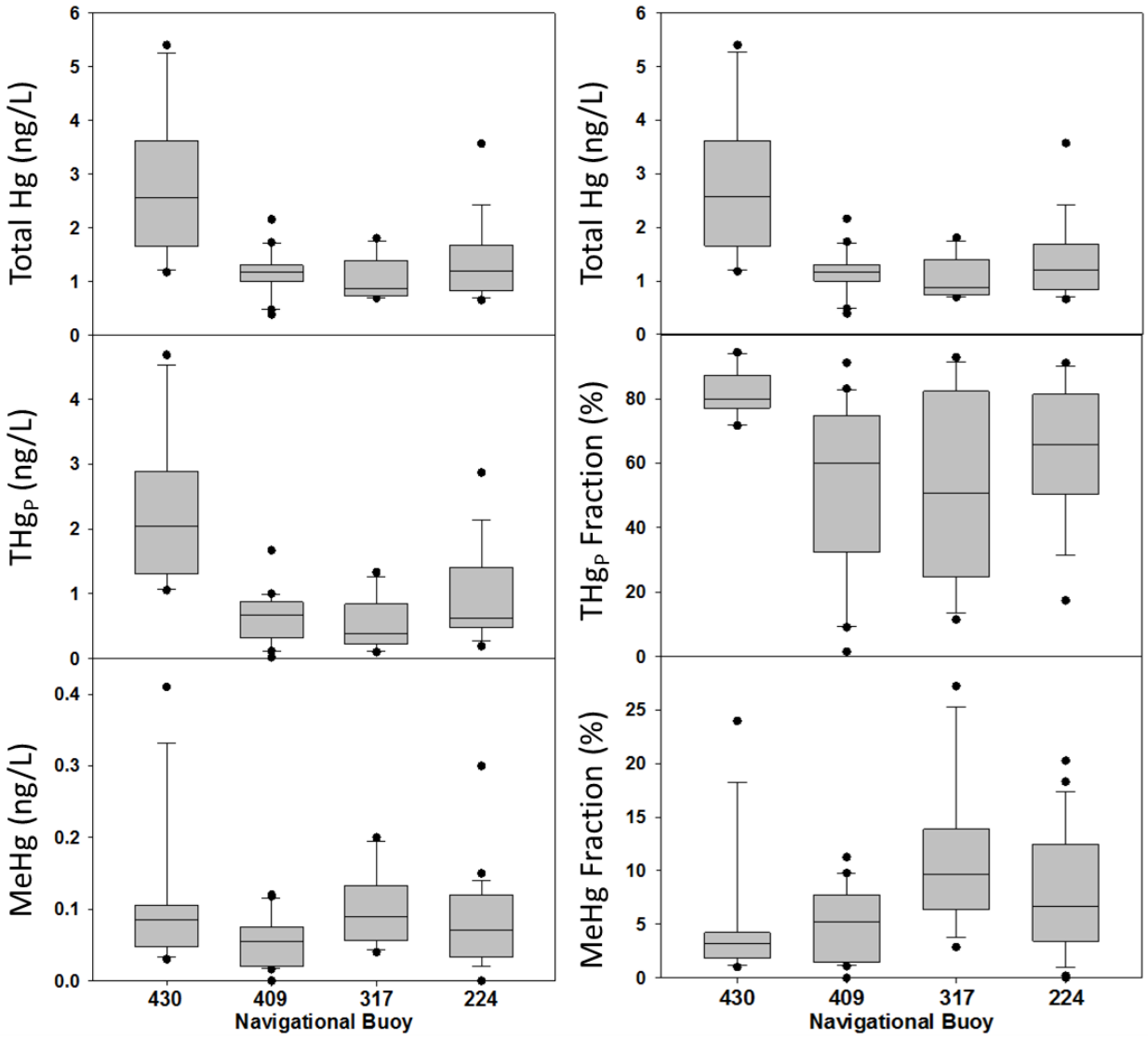

Figure 3.7 Total Hg, THg_P, and MeHg concentrations and fractions at Seneca River sampling locations: Navigational Buoys 430, 409, 317, and 224. Significant reductions in THg and THg_P occur between 430 and 409 (Cross Lake). Significant increases in MeHg occur between 409 and 317 (zebra mussels and Baldwinsville dam). No significant changes occur between 317 and 224 (Onondaga Lake).

bidirectional flow often observed. As a result, some Hg outputs from Onondaga Lake may not be recorded at B224.

3.4.7 Seneca River Watershed Analysis

At 8,935 km^2, the Seneca River watershed makes up over two-thirds (68.5%) of the greater Three Rivers watershed (13,045 km^2). Analysis of watershed land-cover is detailed further in Chapter 4, and land-use data were provided by Natural Resources Canada/Canadian Centre for Remote Sensing et al. (2010). Land-use in the Seneca River watershed consists primarily of agriculture (50%) and forest (35%), with urban areas (7%), open water (7%), and wetland (1%) making up the rest. Total Hg^0 evasion and Hg deposition for the Seneca River watershed and greater Three Rivers watershed were calculated based on an integration of land-use patterns with literature-based estimates of atmospheric Hg flux (Denkenberger et al. 2012), and direct estimates of Hg^0 volatilization from the Seneca River (section 3.4.3). For the Seneca River watershed, total Hg^0 evasion and Hg deposition were estimated at 131 and 173 kg yr^{-1}, respectively, or 74% and 66% of evasion and deposition in the greater Three Rivers watershed.

These estimates suggest that the Seneca River watershed is a net sink for atmospheric Hg at a rate of 42 kg yr^{-1}. Calculations of fluvial Hg flux (section 3.4.6) indicate that the Seneca River exports 5.2 kg yr^{-1} Hg to the Three Rivers. The watershed therefore retains over 85% (36.8 kg yr^{-1}) of atmospherically deposited Hg, over 20% (8.8 kg yr^{-1}) of which is deposited in Cross Lake via sedimentation. Note that this estimate ignores leaching of natural levels of Hg from the soils, which are expected to be low relative to atmospheric inputs (Nater and Grigal 1992). In a study of tributaries to the Chesapeake Bay, retention of atmospheric Hg in most watersheds was observed to be over 60% (Lawson et al. 2001). Similar to the effect of Cross Lake on Hg flux in the Seneca River, heightened retention was noted in rivers with intervening features that promote settling (Lawson et al. 2001).

Rivers with watersheds dominated by agriculture often exhibit high THg_P fluxes due to strong particle-Hg associations and erosional processes (Hurley et al. 1995; Babiarz et al. 1998; Balogh et al. 1998; Hurley et al. 1998b; Engstrom et al. 2007; Babiarz et al. 2012). Accordingly, Hg fluxes in the Seneca River are dominated by the THg_P fraction (Table 3.4, p. 44). This strong association of Hg with the particulate fraction has dynamic effects on Hg export from the watershed: strong particle-Hg relationships facilitate sedimentation, thereby reducing overall Hg export. Conversely, precipitation and other overland runoff events significantly increase Hg export via erosion and resuspension in rivers and watersheds with dominant THg_P fractions (Babiarz et al. 1998). In summary, the land-use patterns of the Seneca River watershed, along with intervening Cross Lake, are the dominant controls of Hg transport in the river and Hg flux from the watershed. Increases in urban or agricultural land-use patterns are expected to increase Hg flux in the watershed, along with the total fluvial Hg contribution of the Three Rivers watershed to Lake Ontario.

4. Lake Ontario Sub-Watershed Analysis

4.1 Introduction

Watersheds serve as sources of Hg to receiving waters. In this study, the results of two independent field-sampling programs have been combined into a bi-national study to explore Hg dynamics in the Lake Ontario basin, with an emphasis on Hg speciation and particle relationships from the watersheds of major tributaries. Results from these sampling efforts are presented here in the context of relationships between concentrations of Hg species and measures of hydrology, watershed land-cover, and ancillary chemistry. The relationships noted are used to explore watershed land-cover effects and controls on Hg speciation.

4.2 System Description

Tributaries sampled in Canada included the Niagara, Twenty Mile Creek, Credit, Humber, Ganaraska, and Trent; those sampled in the US included the St. Lawrence, Black, Salmon, Oswego/Three Rivers, and Genesee (Figure 4.1, p. 50). The study watersheds vary with respect to size, land-cover, and discharge (Table 4.1, p. 51). In Figures 4.2-4.10 (pp. 50, 53, 54, 56-60), land-cover is listed as provided by Natural Resources Canada/Canadian Centre for Remote Sensing et al. (2010). To support data analysis, land-cover categories were lumped as shown in Table 4.2 (p. 52). In Canada, the study watershed closest to the Niagara River is Twenty Mile Creek (Figure 4.2, p. 50). The Twenty Mile Creek watershed is the second smallest of those included in the study with respect to area (295 km^2) and with the Ganaraska has the smallest mean discharge during the study period (4 $m^3 s^{-1}$). The Twenty Mile Creek watershed consists mostly of agricultural lands (90%; Table 4.1, p. 51).

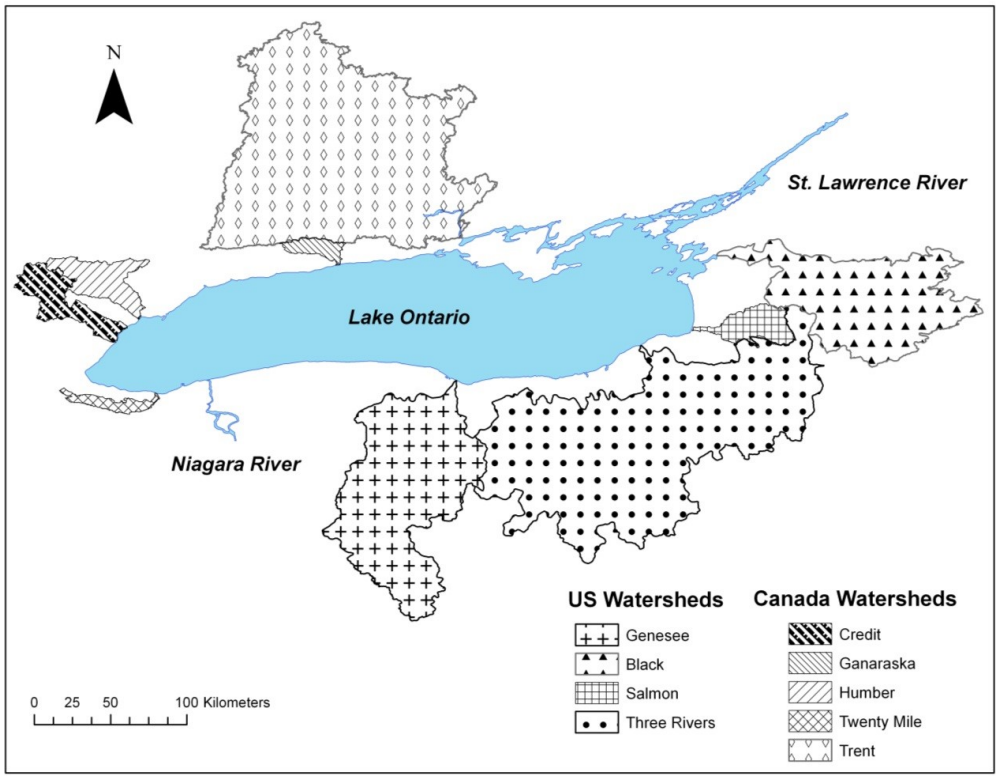

Figure 4.1 Lake Ontario and watersheds of study tributaries.

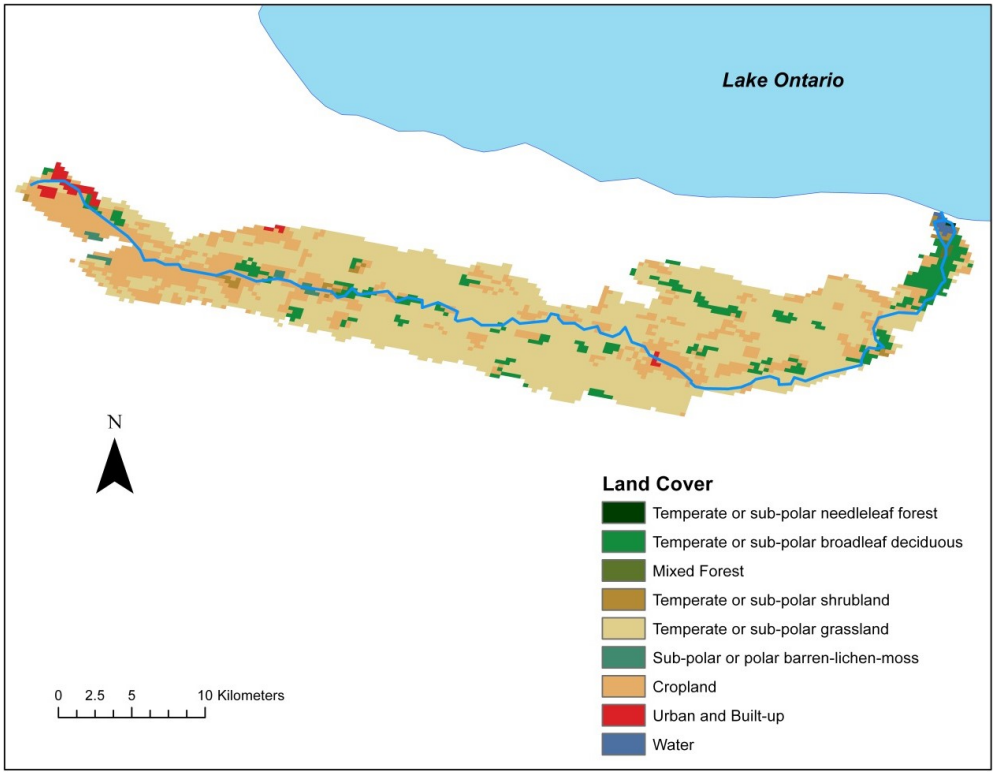

Figure 4.2 Twenty Mile Creek watershed and land-cover.

Table 4.1 Summary of study watershed characteristics.

Watershed	Notable Urban Centers within Watershed	Total Area (km^2)	Daily Discharge for Period of Record ($m^3 s^{-1}$)	Daily Discharge for Sampling Period		Areal Discharge for Sampling Period ($m^3 km^{-2} d^{-1}$)	Land-cover Percent Coverage				
				($m^3 s^{-1}$)	C.V.		Forest	Agriculture	Urban	Wetland	Water
Three Rivers	Syracuse, Oswego	13,045	195	200	0.7	1,325	43	42	7	3	6
Black	Watertown	5,015	120	124	0.7	2,137	78	12	2	6	2
Genesee	Rochester	6,550	80	78	0.9	1,032	51	43	5	0.5	0.7
Salmon	Pulaski	713	22	22	0.9	2,663	89	3	0.2	6	2
				Average of US Study Watersheds:			65	25	4	4	3
				Total Coverage in US Study Area:			53	35	5	3	4
Trent	Trenton	12,560	198	226	0.7	1,555	70	23	0.3	0.4	6
Credit	Mississauga	950	9	11	1.0	1,017	35	46	17	1	0.3
Humber	Toronto	910	6	9	1.5	881	31	53	16	0.2	0.06
Twenty Mile	none	295	3	4	2.3	1,202	9	90	1	0	0.3
Ganaraska	Port Hope	275	3	4	0.8	1,413	62	37	1	0	0.02
				Average of Canadian Study Watersheds:			41	50	7	0.3	1
				Total Coverage in Canadian Study Area:			54	38	4	0.4	3

Notes:

1. Sample period discharge for US rivers represents mean of 2009 and 2010 daily discharge estimates. Record periods vary.
2. Sample period discharge for Canada rivers represents mean of 2008 and 2009 daily discharge estimates. Record periods vary.
3. C.V. = coefficient of variation.

Table 4.2 Aggregate of land-cover categories used in this study.

Land-cover Description	Final Category
Temperate or sub-polar needleleaf forest	Forest
Temperate or sub-polar broadleaf deciduous	
Mixed Forest	
Temperate or sub-polar shrubland	
Sub-polar or polar shrubland-lichen-moss	
Cropland	Agriculture
Temperate or sub-polar grassland	
Sub-polar or polar grassland-lichen-moss	
Sub-polar or polar barren-lichen-moss	
Barren Lands	
Wetland	Wetland
Urban and Built-up	Urban
Water	Open Water

Note: Land-cover descriptions provided by Natural Resources Canada/Canadian Centre for Remote Sensing et al. (2010)

At approximately 950 km^2, the Credit River (Figure 4.3, p. 53) is the second largest of the study watersheds in Canada. The Credit is the most urbanized of the study watersheds (17%; Table 4.1, p. 51), and passes through Mississauga, part of the Greater Toronto Area, before it outlets to Lake Ontario. During the study period, the Credit River had a mean discharge rate of 11 $m^3 s^{-1}$. Aside from the urban land-cover mentioned, the Credit River watershed contains significant agricultural and forested lands (46% and 35%, respectively).

The Humber River watershed lies directly adjacent to and northeast of the Credit River watershed (Figure 4.4, p. 53). It is similar in size (910 km^2) and composition to the Credit River watershed. The Humber contains approximately the same distribution of urban land-cover (16%; Table 4.1, p. 51) and agricultural and forest coverage. The Humber passes through Toronto

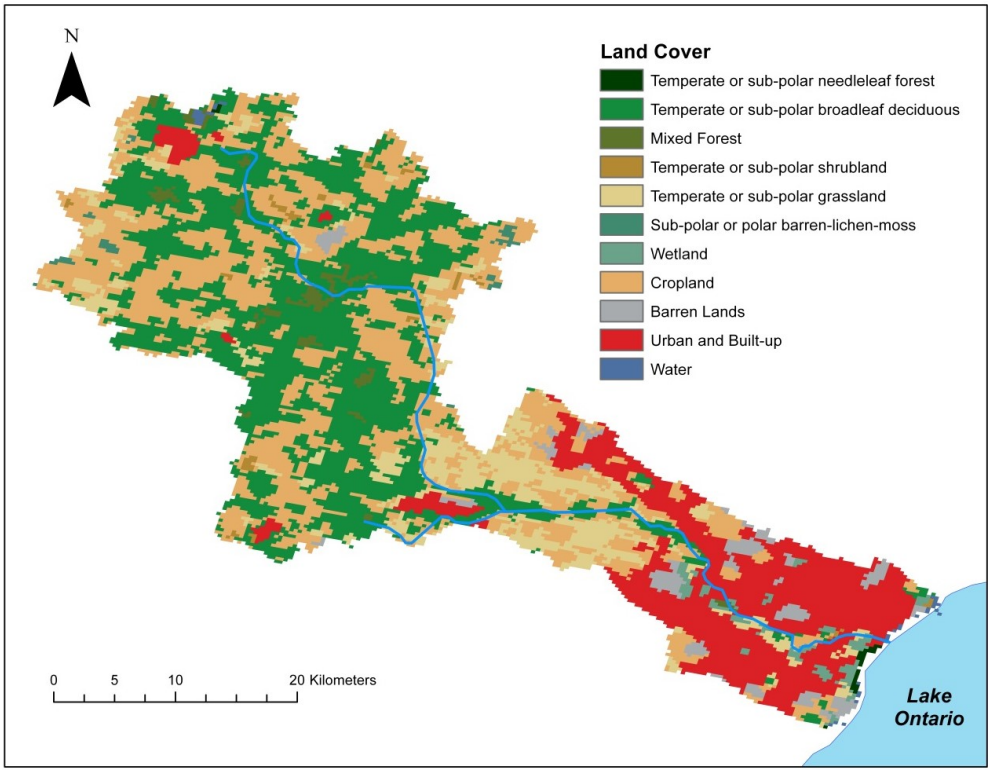

Figure 4.3 Credit River watershed and land-cover.

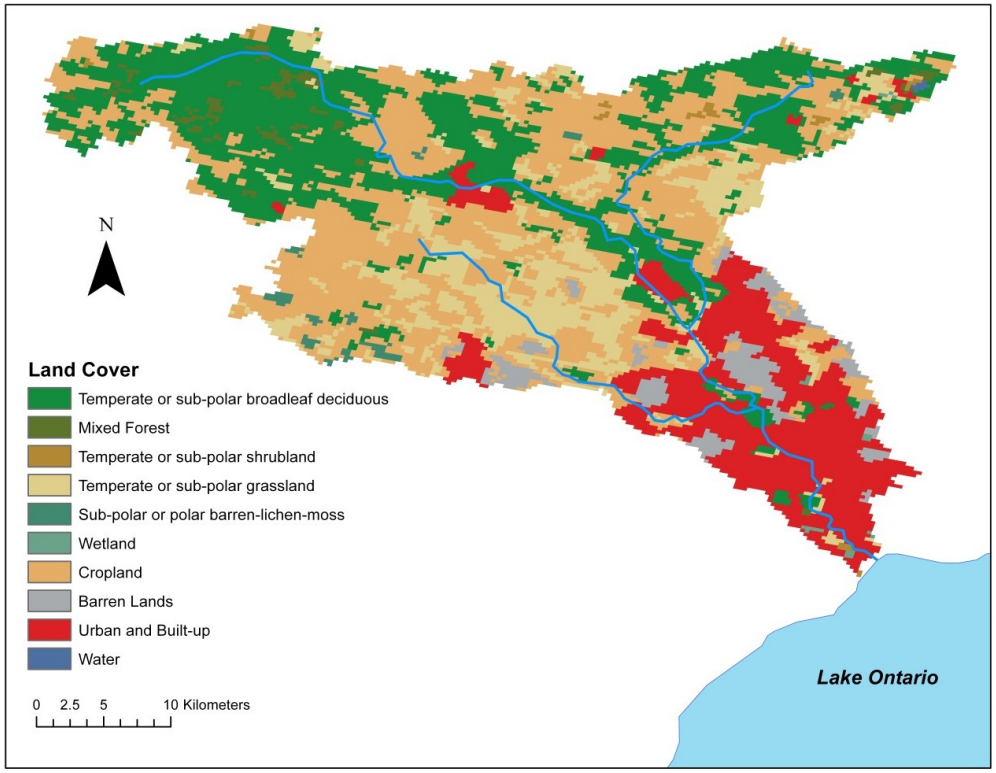

Figure 4.4 Humber River watershed and land-cover.

before it outlets to Lake Ontario, and exhibited a mean discharge rate of 9 m^3 s^{-1} during the study period.

The Ganaraska River watershed lies east of the Humber River watershed, and directly south of the western extent of the Trent River watershed (Figures 4.1, p. 49, and 4.5). At 275 km^2, the Ganaraska watershed is the smallest of all the study watersheds, though it is quite similar in size to the Twenty Mile Creek watershed. However, the land-cover of the Ganaraska differs from that surrounding Twenty Mile Creek in that nearly two-thirds of the watershed area is forested; the remainder is mostly agricultural land (Table 4.1, p. 51). The Ganaraska River empties into Lake Ontario at Port Hope, and had a mean discharge rate of 4 m^3 s^{-1} during the study period.

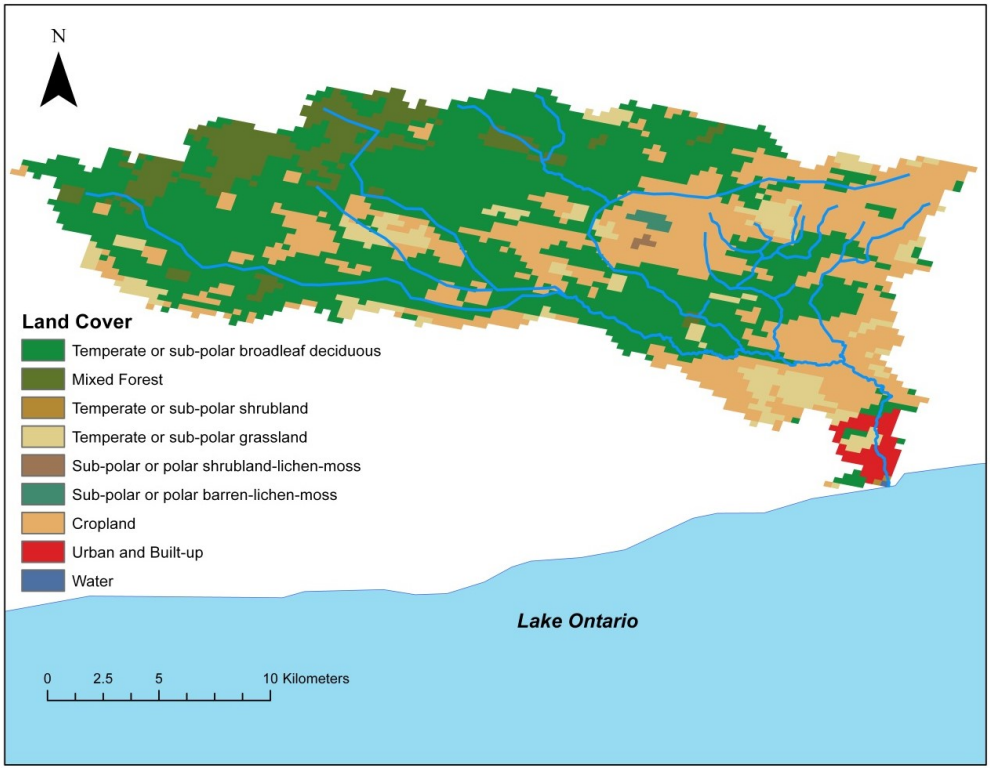

Figure 4.5 Ganaraska River watershed and land-cover.

The largest study watershed in Canada is the Trent River (Figure 4.6, p. 56). It is located immediately east of the Ganaraska River watershed, and at approximately 12,560 km^2, it covers over ten times the area of the next largest study watershed in Canada, and is the second largest of the sampled watersheds. Aside from size, the Trent River watershed is similar in composition to that of the Ganaraska – approximately two-thirds of the watershed is forested land, while nearly all of the remaining third is agricultural (Table 4.1, p. 51). The Trent River outlets at Trenton into the Bay of Quinte, near the northeastern shore of Lake Ontario. Current gauged discharge data are not available for the Trent River outlet. Discharge for the Trent was therefore composited from gauged subwatershed and discharge data provided by Ontario Power Generation. Discharge data for the Trent River over the Healey Falls Spillway was provided by Ontario Power Generation up to October 2, 2009. Approximately 9,090 km^2 of the 12,560 km^2 Trent River watershed is upstream of the Healey Falls Spillway. A gauged subwatershed of the Trent River that is below the Healey Falls Spillway is that of the Crowe River. Discharge data are available for the Crowe River at Marmora, Ontario, near the confluence of the Crowe River and the Trent River. The drainage area for the Crowe River at the gauging station is approximately 1,990 km^2. Daily discharge at Healey Falls Spillway was added to daily discharge from the Crowe River, representing 11,080 km^2 of the total 12,560 km^2 Trent River watershed (i.e., 88% of the total Trent River watershed). A scaling factor based on watershed area was then applied to estimate daily discharge for the entire Trent River. To estimate daily discharge data after October 2, 2009 (i.e., where data are not available from Ontario Power Generation at Healey Falls), the estimated total daily discharge of the Trent River was regressed against daily discharge from the Moira River at Foxboro, Ontario, which is adjacent to the Trent River. This regression relationship was used to develop a flow record for the Trent River after

October 2, 2009. Based on this approach, a daily discharge record was developed for the Trent River for the entire study period, and a mean discharge rate of 226 m^3 s^{-1} was estimated. This rate is over tenfold higher than any of the other Canadian study rivers.

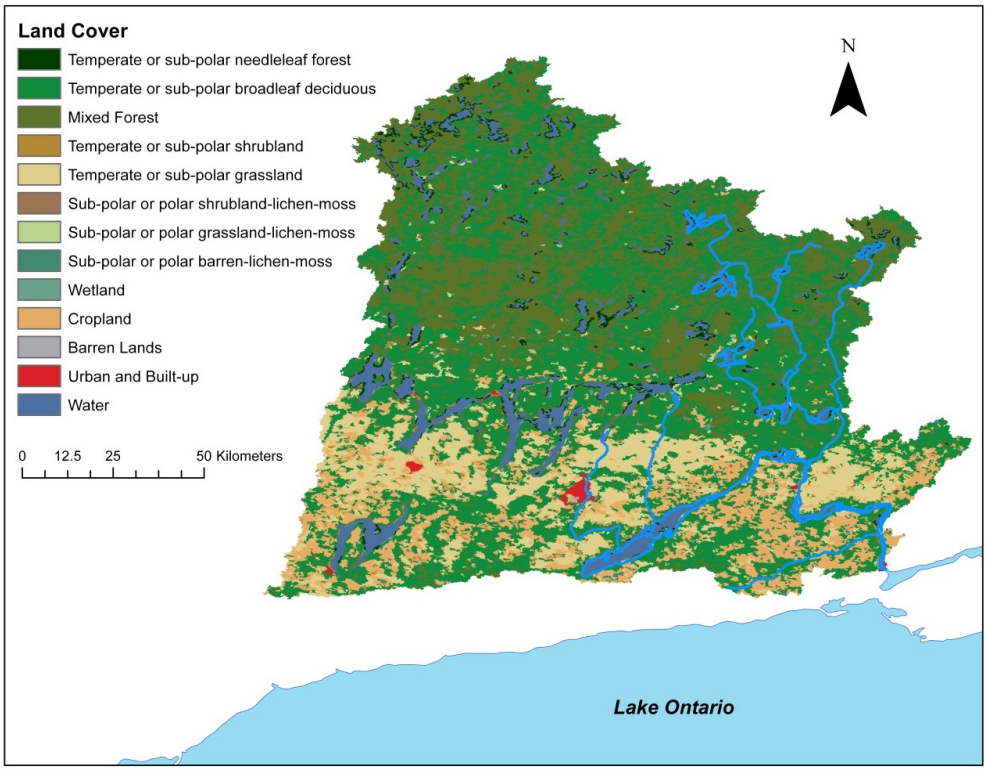

Figure 4.6 Trent River watershed and land-cover.

In the US, the study watershed closest to the Niagara River is that of the Genesee River (Figure 4.7, p. 57). With an area of 6,550 km^2, the Genesee watershed is over five times larger than any of the Canadian study watersheds, excluding the Trent, and is second in size of the study watersheds in the US. The Genesee watershed consists mostly of forested and agricultural lands (51% and 43%, respectively; Table 4.1, p. 51). Though urban land-cover makes up only 5% of the Genesee watershed, nearly 100% of the total urban land-cover consists of the city and attending suburbs of Rochester, which surround the last 25 kilometers of the river prior to

discharge into Lake Ontario. During the study period, the mean discharge of the Genesee River was 78 $m^3 s^{-1}$.

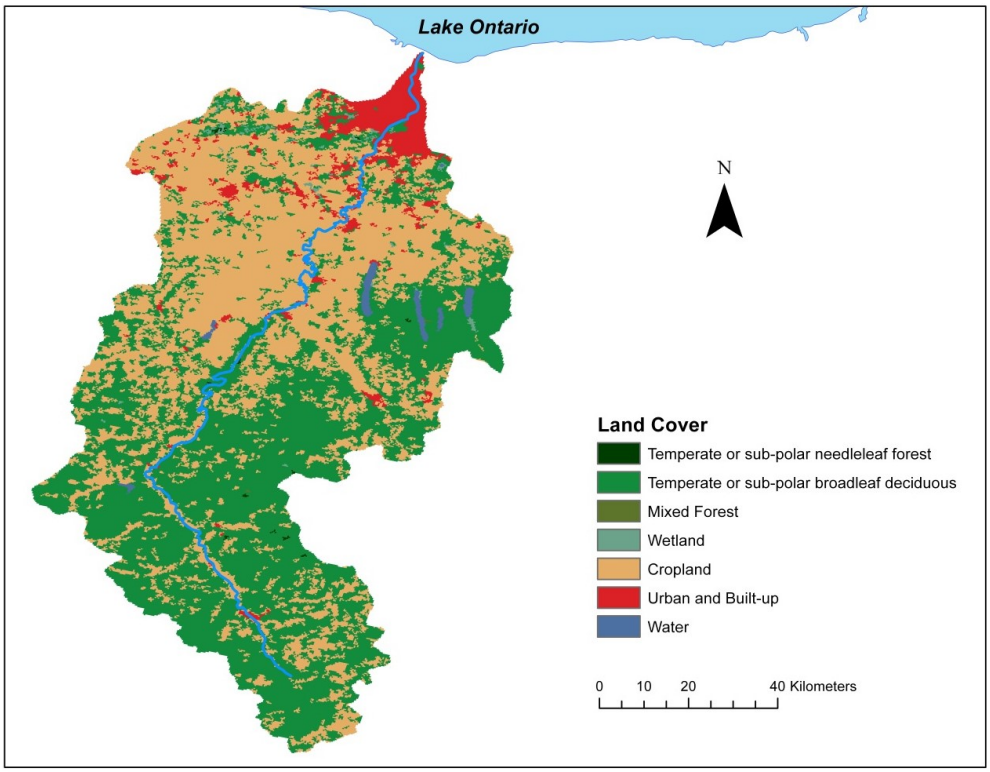

Figure 4.7 Genesee River watershed and land-cover.

The Three Rivers watershed lies adjacent to and east of the Genesee River watershed (Figure 4.8, p. 58). It consists of the combined watersheds for the Seneca River, which drains the Finger Lakes region, the Oneida River, and the Oswego River, which outlets to Lake Ontario at Oswego. At 13,045 km^2, the Three Rivers watershed is the largest study watershed. The mean discharge was the second highest during the study period, at 200 $m^3 s^{-1}$. Major land-cover is equally split between forested and agricultural lands (43% and 42%, respectively; Table 4.1, p. 51), and at 7%, urban land-cover is the highest of all US study watersheds.

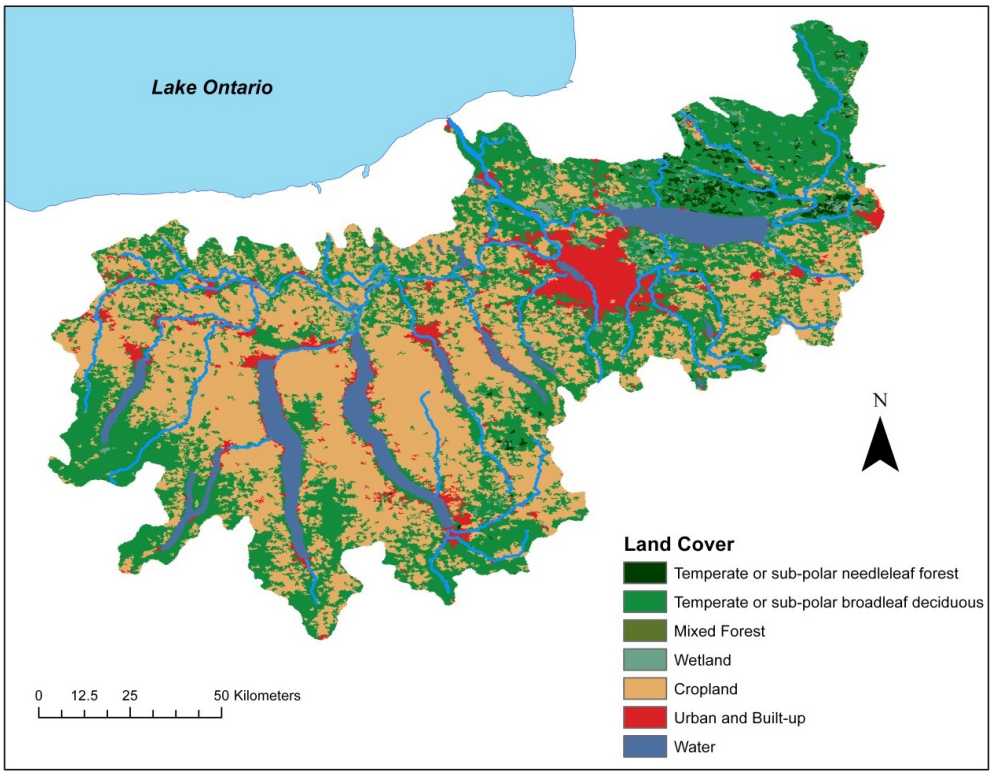

Figure 4.8 Three Rivers watershed and land-cover.

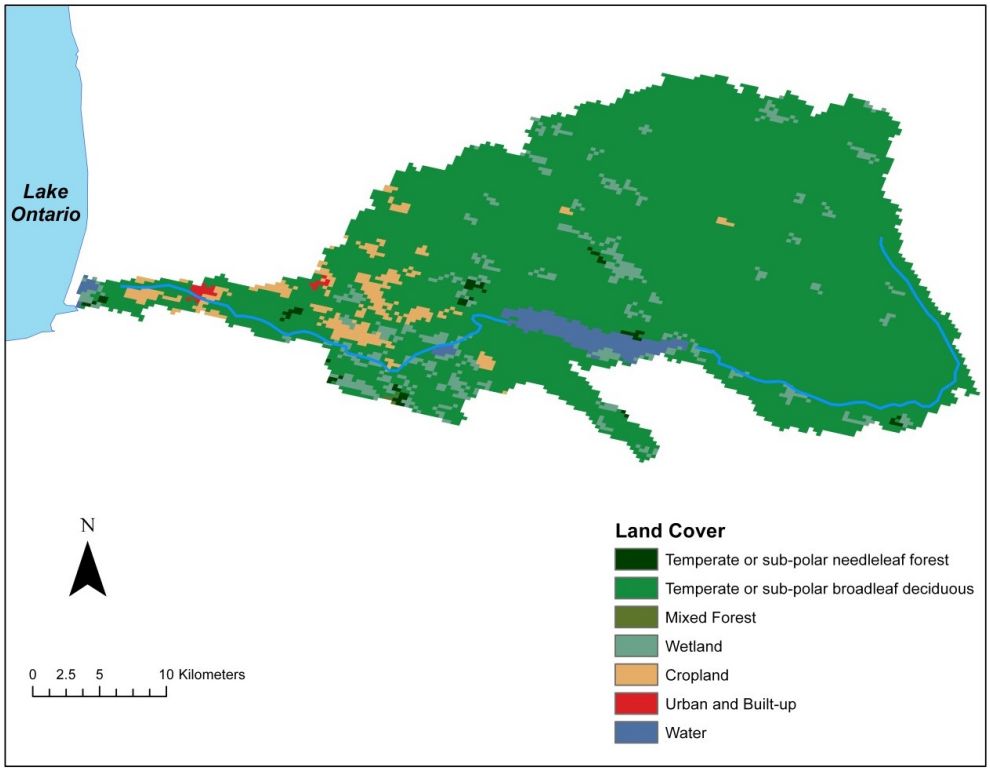

Figure 4.9 Salmon River watershed and land-cover.

The Salmon River watershed lies adjacent to and northeast of the Three Rivers watershed (Figure 4.9, p. 58). At 713 km^2, it is the smallest of the US watersheds. It is also the most heavily forested of the study watersheds (89%; Table 4.1, p. 51) and has a large wetland coverage (6%). Mean discharge during the study period was low relative to other US watersheds (22 $m^3 s^{-1}$), largely due to the small relative size of the watershed and the large forest cover.

The Black River watershed is adjacent to and north of the Salmon River watershed (Figure 4.10). It is the third largest study watershed in the US (5,015 km^2). Land-cover in the Black watershed is dominated by forest (78%; Table 4.1, p. 51), though this watershed and the Salmon has the greatest wetland coverage (6%). Mean discharge for the Black River during the study period was 124 $m^3 s^{-1}$.

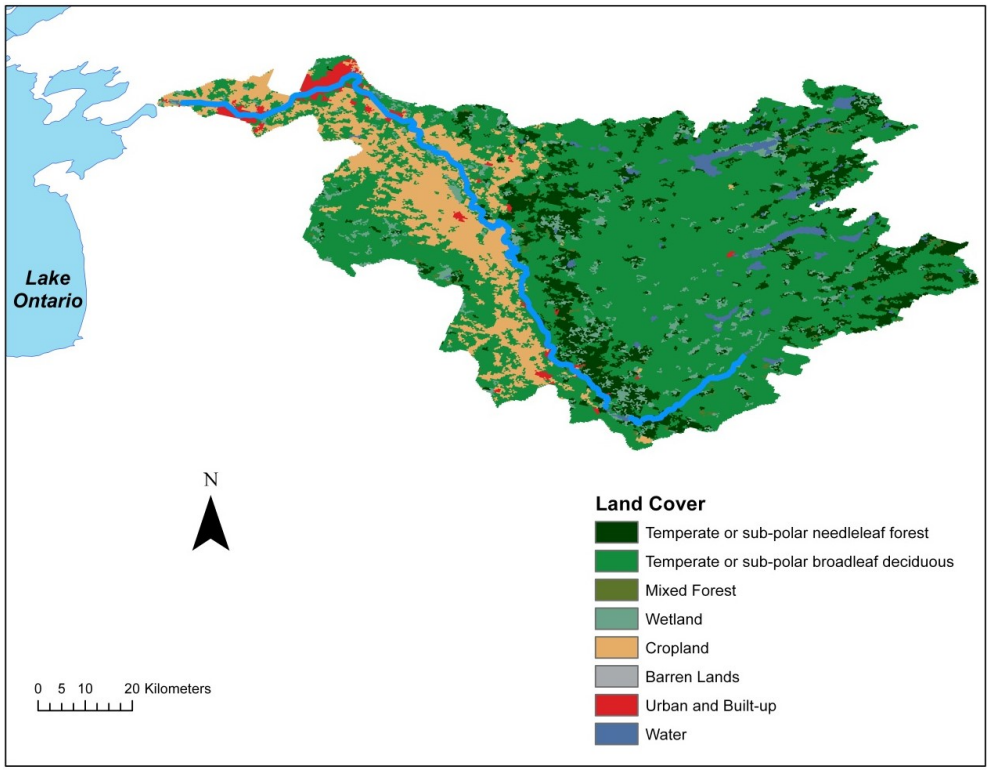

Figure 4.10 Black River watershed and land-cover.

In summary, land-cover and land-use patterns were variable and mixed within and among the study watersheds. Of the four land-cover categories, forest and agriculture dominated in both Canada and the US, and urban areas and wetlands were less significant. When the percent land-cover in the study watersheds in Canada is averaged, forest and agriculture coverage were similar at approximately 40% and 50%, respectively. Urban land-cover averages approximately 7%, water makes up an average of about 1%, and wetlands average less than 1%. On the other hand, when percent coverage in the US study watersheds was averaged, forest lands (~65%) were much higher than agricultural lands (~25%). Urban and wetland coverage average the same among the US study watersheds at approximately 3.5%, and water coverage averages about 3%.

4.3 Methods

Water samples were collected in both Canada and the US from the ten major tributaries into Lake Ontario and from the lake's outlet at the St. Lawrence River. Researchers from Canada and the US performed bimonthly sampling in Canada from June 2008 to December 2009, and in the US from June 2009 to May 2010. For purposes of the work presented in this chapter, the nine sampled tributaries located in the immediate watershed of Lake Ontario are discussed. Results from the Niagara and St. Lawrence rivers are presented here, but are discussed later in Chapter 5.

Sample collection was performed using trace metal clean protocols as described in Method 1669 (USEPA 1996). Analysis of US tributary samples was conducted at Syracuse University; analysis of Canadian tributary samples was conducted at the University of Toronto. Both laboratories used the same or similar methods for analysis. Upon arrival at the laboratory, 250-500 mL water sample aliquots were filtered through pre-cleaned 0.45-µm filters. Whole and

filtered water samples were then preserved using 4 mL L^{-1} 11.6 M trace metal grade hydrochloric acid. Sample analysis included supplementary chemistry (e.g., TSS, DOC). Total Hg analysis was conducted using CVAFS (Bloom, 1989; USEPA, 2002). Methylmercury determination was performed via aqueous phase ethylation with $NaB(C_2H_5)_4$, purge and trap separation and detection by CVAFS (Horvat et al. 1993a; Horvat et al. 1993b; Liang et al. 1994). Total particulate Hg was calculated as the difference between whole- and filtered-sample results; consequently, some reported THg_P concentrations are below THg and MeHg detection limits (0.20 and 0.02 ng L^{-1}, respectively). Supplementary water quality measures were analyzed using Standard Methods (Eaton et al. 1998): for DOC, the persulfate-ultraviolet oxidation method (5310C); for TSS, method 2540D.

The tributaries selected make up the majority of the non-Niagara fluvial inputs to Lake Ontario. In 2009, the volume discharged to the lake by the sampled tributaries represented approximately 90% of the flow at the lake's outlet (i.e., St. Lawrence River), and the Niagara River contributed approximately 91% of the sampled tributaries' inflow. Excluding the Niagara input, the remaining tributaries contributed the following percent total flows during the study period, in descending order: Trent (33%), Oswego/Three Rivers (29%), Black (18%), Genesee (12%), Salmon (3%), Credit (1.6%), Humber (1.4%), Ganaraska (0.7%), and Twenty Mile Creek (0.6%). Flow duration curves for the sampling period are shown in Figure 4.11 (p. 63). Samples were collected over a broad range of recorded flows, with no emphasis on any specific flow regime. Mean discharge during the sample period (2009-2010) was similar to the period of record for the US tributaries, while the Canadian tributaries averaged over 25% higher flows (2008-2009) than those on record (Table 4.1, p. 51). Overall, discharge was approximately 10%

higher in 2008 than 2009, and 2009 and 2010 were similar to each other and to the period of record.

Analysis of watershed land-cover characteristics was performed with a GIS approach. Land-cover data with 250-m spatial resolution from the North American Land Change Monitoring System were used to describe land-use patterns in each of the nine study watersheds (Natural Resources Canada/Canadian Centre for Remote Sensing et al. 2010). To facilitate analysis, the land-cover categories provided were generalized into the following groups: forest, agriculture, wetland, urban, and open water (detailed in Table 4.2, p. 52). Watershed boundaries for the US tributaries were developed from data provided by the New York State Department of Environmental Conservation (2000). Watershed boundaries for the Canadian tributaries were developed from data provided by the Ontario Ministry of Natural Resources (2011).

Statistical analysis was performed using SigmaPlot 11.0 (Systat Software, Inc. 2008). For tests of significance, α was set to 0.05 unless otherwise noted. For calculation of means, medians, and standard deviations, non-detect samples were assigned a value of one-half the detection limit of 0.20 ng L^{-1} for THg and 0.02 ng L^{-1} for MeHg. This approach was used to fill data gaps for less than 9% of all Hg analyses (91 of 1,020 samples), though the majority of non-detects occurred for MeHg analyses (77 of 440 samples), and are discussed later in the manuscript.

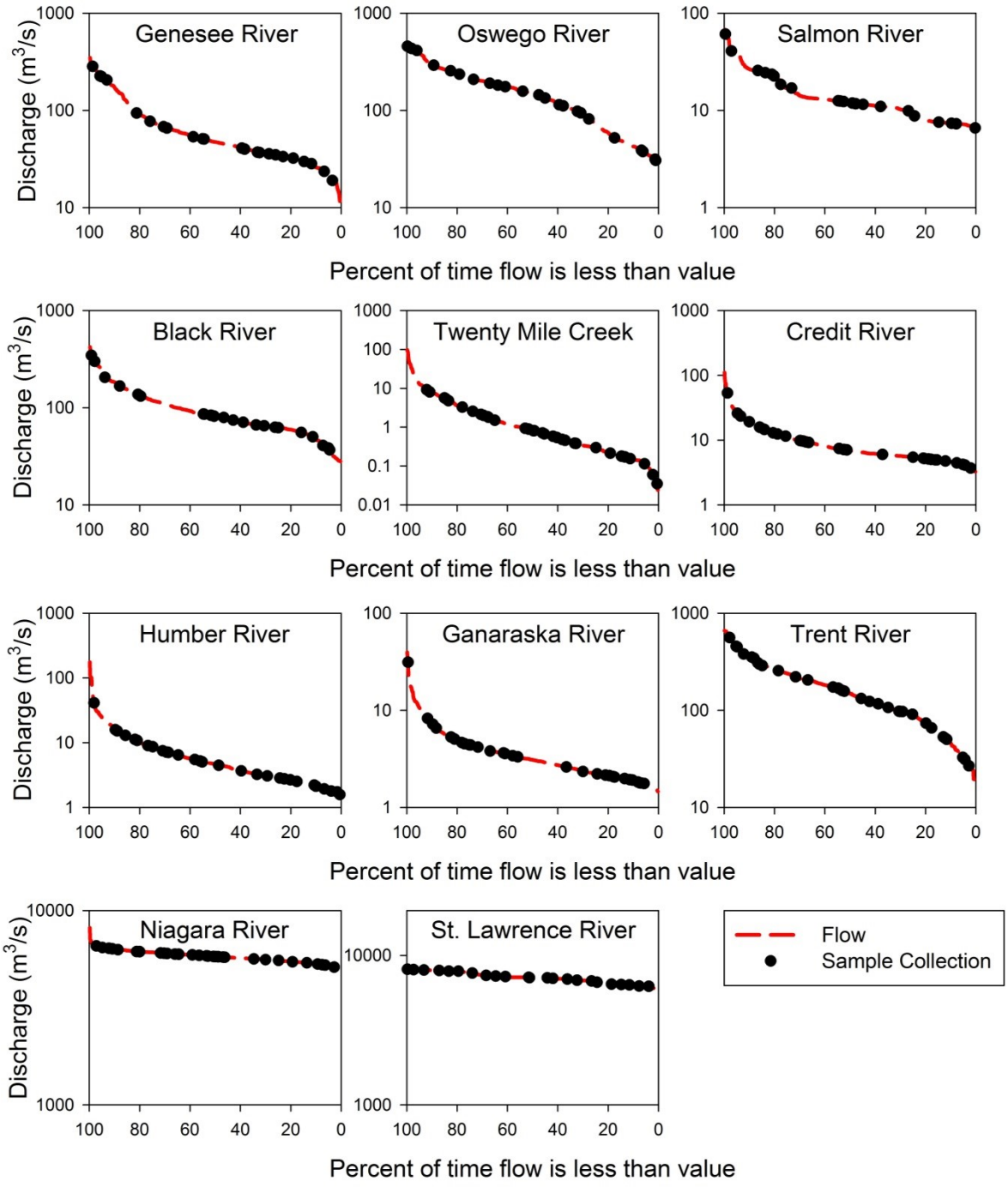

Figure 4.11 Flow duration curves for sampled tributaries. The conditions during sample collection over the range of flow conditions are shown.

4.4 Results and Discussion

4.4.1 Mercury Concentrations in Tributaries: Total Mercury

Mean THg concentrations in the study tributaries ranged from 0.9 ng L^{-1} in the Trent River to 2.6 ng L^{-1} in the Genesee River (Table 4.3, p. 65). The concentrations observed are generally low compared to those noted in studies of multiple rivers and streams in the Midwestern US (Babiarz et al. 1998; Hurley et al. 1998a; Balogh et al. 2005), but are similar to those sampled in Maine (Peckenham et al. 2003). Minimum THg concentrations for Lake Ontario study tributaries were typically less than 1 ng L^{-1} (range: 0.3 – 1.1 ng L^{-1}), while maximum THg concentrations varied nearly an order of magnitude with a range of 2.3 ng L^{-1} (Salmon River) to 14.0 ng L^{-1} (Genesee River). The maximum observation in the Genesee River was nearly two-fold higher than the next highest tributary (i.e., 7.5 ng L^{-1}; Twenty Mile Creek). This observation in the Genesee River, along with the next highest observation in the Genesee (11.2 ng L^{-1}), both occurred during sample collection on the rising limb of separate high-flow events. Of the nine study tributaries, six exhibited positive, significant relationships between flow and THg concentrations (Black, r = 0.57; Oswego, r = 0.61; Salmon, r = 0.73; Ganaraska, r = 0.73; Twenty Mile, r = 0.76; Genesee, r = 0.88).

Mean THg_D concentrations were less variable than THg, ranging from 0.5 ng L^{-1} (Ganaraska River) to 1.5 ng L^{-1} (Twenty Mile Creek). These concentrations of THg_D are similar to values noted in rivers and streams of the Midwestern US (Hurley et al. 1996; Balogh et al. 1998; Hurley et al. 1998a) and in tributaries to Sepetiba Bay, Brazil (Paraquetti et al. 2004). Minimum observations ranged from below detection (<0.20 ng L^{-1}) in several Lake Ontario study tributaries to 0.8 ng L^{-1} in the Black River. Maximum observations ranged from 1.2 ng L^{-1}

Table 4.3 Summary of concentrations of Hg fractions, TSS, and DOC for Lake Ontario tributaries.

Tributary	THg (ng L^{-1})				THg_D (ng L^{-1})				THg_P (ng L^{-1})				MeHg (ng L^{-1})				TSS (mg L^{-1})				DOC (mg L^{-1})			
	N	$\bar{x}$	M	SD	N	$\bar{x}$	M	SD	N	$\bar{x}$	M	SD	N	$\bar{x}$	M	SD	N	$\bar{x}$	M	SD	N	$\bar{x}$	M	SD
Genesee	23	2.6	1.0	3.5	23	0.7	0.6	0.4	23	2.0	0.6	3.3	21	0.05	0.04	0.05	23	52.5	15.2	95.9	21	3.6	3.3	1.2
Black	23	2.5	2.0	1.5	23	1.4	1.4	0.4	23	1.1	0.5	1.4	19	0.09	0.06	0.11	23	6.0	1.6	15.1	21	4.5	4.5	0.8
Twenty Mile	33	2.5	2.5	1.6	26	1.5	1.4	1.0	25	1.0	0.6	1.1	21	0.14	0.06	0.24	24	367.1	314.7	420.6	24	9.1	8.9	2.3
Humber	29	2.0	2.0	1.1	23	0.8	0.7	0.5	22	1.0	1.0	1.0	21	0.06	0.04	0.05	21	280.2	305.2	77.0	23	5.6	5.7	1.0
Credit	33	1.6	1.7	0.9	25	0.7	0.5	0.4	24	0.7	0.6	0.8	19	0.11	0.05	0.16	23	229.3	255.1	127.8	24	4.6	4.4	1.0
Salmon	23	1.4	1.3	0.3	23	1.1	1.1	0.3	23	0.3	0.2	0.3	21	0.10	0.09	0.10	23	2.5	1.0	3.2	21	3.4	3.2	0.6
Ganaraska	33	1.1	0.9	1.0	26	0.5	0.4	0.4	26	0.6	0.3	0.9	22	0.06	0.05	0.06	24	155.9	120.2	101.5	26	3.5	3.2	0.8
Oswego	23	1.0	0.7	0.6	23	0.6	0.5	0.3	23	0.4	0.2	0.5	20	0.11	0.05	0.19	23	3.8	2.2	4.8	21	3.9	4.0	0.4
Trent	33	0.9	0.6	0.6	26	0.6	0.5	0.3	26	0.3	0.2	0.2	17	0.07	0.02	0.11	24	146.0	94.4	106.1	26	5.9	5.9	1.2
Niagara	34	0.8	0.8	0.5	29	0.6	0.4	0.4	29	0.3	0.2	0.3	26	0.11	0.04	0.24	24	128.3	82.8	99.8	26	2.9	2.8	0.6
St. Lawrence	23	0.3	0.2	0.2	23	0.3	0.3	0.2	23	0.1	0.0	0.1	18	0.07	0.04	0.08	23	0.3	<0.10	0.3	21	2.1	2.0	0.2

Notes:

1. N = total number of samples
2. $\bar{x}$ = mean
3. M = median
4. SD = standard deviation

(Ganaraska River) to 3.7 ng L^{-1} (Twenty Mile Creek), although most THg_D maxima for the study tributaries fell on the low end of the range (i.e., between 1 and 2 ng L^{-1}). Differences between means and medians were generally small, suggesting minimal effects of flow events on THg_D (Table 4.3, p. 65). The lack of response of THg_D to flow was underscored by the few significant relationships between flow and THg_D in the study tributaries. Only two tributaries exhibited such a relationship, and in each instance the correlation is positive (Salmon, r = 0.62; Twenty Mile, r = 0.69).

Unlike THg and THg_D, which were analyzed directly, THg_P concentrations were obtained by calculating the difference between THg and THg_D. Similar to Babiarz and others (1998) noting for agricultural watersheds in Wisconsin, little variability was observed in THg_D concentrations; therefore the variability noted in THg for the study tributaries was largely a function of the THg_P fraction. Mean THg_P ranged from 0.3 ng L^{-1} (Trent River) to 2.0 ng L^{-1} (Genesee River). Results from the study tributaries were higher than estimates of THg_P observed in the Everglades (Cai et al. 1999), though this is to be expected due to the sheet flow, high DOC concentrations, and the wetland land-cover of that ecosystem. When compared to small forested watersheds in the northeastern US, mean THg_P concentrations from the study tributaries are generally similar (Dittman et al. 2010). On the other hand, my results are lower than THg_P concentrations noted for the Lower Fox River, Wisconsin (Hurley et al. 1998a), perhaps due to the heavy industrialization of that area. Minimum THg_P concentrations for tributaries in this study ranged from 0 to 0.02 ng L^{-1}. The range of maximum THg_P concentrations was similar to the range of maximum THg concentrations in the tributaries (0.8 – 13.4 ng L^{-1} for THg_P; 2.3 – 14.0 ng L^{-1} for THg), again underscoring the link between THg and THg_P. Total particulate Hg was correlated to flow more frequently than THg_D; six of the nine study tributaries exhibited significant,

positive relationships between THg_P and flow (Trent, r = 0.41; Black, r = 0.60; Oswego, r = 0.60; Twenty Mile, r = 0.62; Ganaraska, r = 0.83; Genesee, r = 0.87).

4.4.2 Mercury Concentrations in Tributaries: Methylmercury

Mean tributary MeHg concentrations (Table 4.3, p. 65) ranged from 0.05 ng L^{-1} (Genesee River) to 0.14 ng L^{-1} (Twenty Mile Creek), similar to those noted in Chesapeake Bay tributaries (Lawson et al. 2001), but lower than MeHg concentrations reported for streams and rivers in the Midwest (Babiarz et al. 1998; Balogh et al. 2003; Balogh et al. 2005). Although the mean THg concentration in the Genesee River was the highest of all tributaries sampled (i.e., 2.6 ng L^{-1}), the mean MeHg concentration at that site was the lowest. On the other hand, Twenty Mile Creek, which also had a relatively high mean THg concentration (i.e., 2.5 ng L^{-1}) for the study period, had the highest mean MeHg concentration. Minimum observed MeHg concentrations for all sampled tributaries were below detection limits (i.e., <0.02 ng L^{-1}). This condition occurred in approximately 31% of all tributary samples analyzed for MeHg. Maximum MeHg observations in the tributaries ranged from 0.14 ng L^{-1} in the Genesee River to 1.08 ng L^{-1} in Twenty Mile Creek. No tributaries exhibited a significant relationship between flow and MeHg. This lack of significant correlation between flow and MeHg may be partially due to limitations in the analytical detection of MeHg.

The ratio of MeHg as a fraction of THg (%MeHg) varied nearly four-fold among the study tributaries. The Genesee River had the lowest mean %MeHg (3.9%) for the study period, while the Trent River had the highest (13.8%). When median %MeHg values were considered, three of the nine tributaries fell within 5 to 7% MeHg (Ganaraska, 5.0%; Salmon, 6.7%; Oswego, 7.0%). Median %MeHg for the remaining six tributaries ranged between 2.7 and 3.8% (Credit, 2.7%; Twenty Mile, 2.7%; Black, 2.9%; Genesee, 3.0%; Humber, 3.1%; Trent, 3.8%). Note that

the Genesee River and Trent River, which had the lowest and highest mean %MeHg, respectively, had relatively similar median %MeHg values. The range of mean %MeHg values observed in this study are similar to those noted for streams and rivers in the midwestern US (i.e., 1 to 15%; Babiarz et al. 1998; Balogh et al. 2003; Balogh et al. 2005) and the northeastern US (i.e., 13-15%; Dennis et al. 2005). Though percent MeHg was highly variable within and among the study tributaries (standard deviations ranged from 3.6 to 30.3% MeHg), a seasonal variation was noted. Methylmercury ratios were higher in the spring relative to other seasons in the Genesee and Ganaraska rivers. In the summer, MeHg was a more dominant contributor in the Black, Salmon, Oswego, and Trent rivers. Study tributaries that had higher %MeHg in the fall relative to other seasons included Twenty Mile Creek, and the Credit and Humber rivers.

The aqueous- and particulate-phase MeHg datasets were not as complete as for other Hg species. This was a result of low sample volume and possible demethylation in some particulate-phase samples due to sample holding times despite acid preservation. Nevertheless, the available data suggested that MeHg was largely associated with the aqueous phase, which may explain the lack of relationships described earlier between flow and MeHg in the study tributaries. Due to analytical variability and typically very low MeHg concentrations, some filtered samples exhibited MeHg concentrations greater than MeHg concentrations in the corresponding unfiltered samples. As a result, the calculated mean %MeHg in the dissolved phase (i.e., the percent of unfiltered MeHg that is filterable) was virtually 100% in every tributary indicating that MeHg in Lake Ontario tributaries is predominantly dissolved.

4.4.3 Effects of Land-cover on Mercury Fractions

Flow-weighted fractions of THg_D, THg_P, and MeHg were similar across most study watersheds (Figure 4.12, p. 70), with THg_D and THg_P fractions typically falling between 45% and 55% of

THg, and MeHg evenly distributed between 1% and 9% of THg. However, three of the nine study watersheds (Genesee, Salmon, and Trent) did not follow this pattern, instead displaying dominant Hg associations with either the dissolved or the particulate phase. Mercury from the Genesee was primarily associated with the particulate phase (>80%). The Genesee watershed was the only one of the study watersheds where THg_P dominated the estimated Hg load. The GIS analysis indicated that the watershed surrounding the final 25 km of the tributary is almost exclusively urbanized. Urbanized watersheds are commonly linked to elevated THg_P loads due to localized industrial inputs and the lack of exposed soil to retain atmospheric Hg inputs (Hurley et al. 1995; Mason and Sullivan 1998; Lyons et al. 2006). Though both the Credit and Humber watersheds exhibit greater total urban land-cover than the Genesee, the urban coverage in the Canadian watersheds is more fragmented, with forested area in the lower reaches of each watershed in addition to riparian zones. These down-river forested reaches may serve as sinks for particulate matter, thereby attenuating watershed export (Peterjohn and Correll 1984). Such forested reaches are not as evident in the lower Genesee watershed.

The other two watersheds that did not exhibit comparable fractions of THg_P and THg_D were the Salmon and the Trent (Figure 4.12, p. 70). Flow-weighted Hg speciation in both of these watersheds was dominated by the dissolved fraction (75% and 65% for the Salmon and Trent, respectively; Figure 4.12, p. 70). Forested lands cover large portions of both watersheds, with the Salmon watershed being almost exclusively forested (~89%) and the Trent more mixed (70% forest, 23% agriculture). Land-cover in the Ganaraska watershed is similar to that in the Trent, though THg_P was slightly higher than THg_D for the Ganaraska (Figure 4.12, p. 70). The Ganaraska River has one impoundment located <5 km from the mouth of the tributary, although

the tributary in general is relatively shallow and swift-flowing. In comparison, the Trent River is heavily

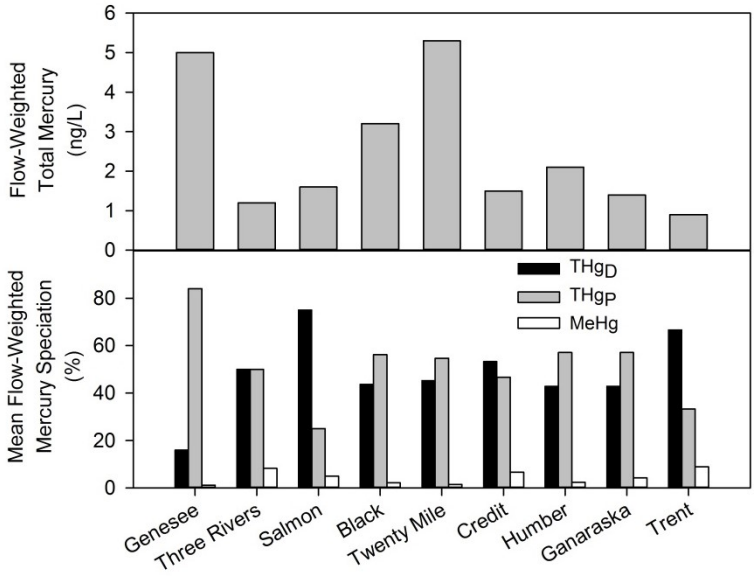

Figure 4.12 Annual volume-weighted mercury concentration and distribution of speciation for each tributary.

impounded, with at least eight dams in the final 25 km of the tributary, which would promote settling of particulate matter and associated Hg. The TSS was not significantly different between the Ganaraska and Trent, but DOC was significantly greater in the Trent River.

While it appears that characteristics of the tributary may influence the partitioning of Hg in the Trent River (e.g., impoundments promote settling of THg_P), it is likely that the nearly homogenous forest cover of the Salmon watershed contributes to the strong THg_D signature observed in that tributary by limiting particulate input. Similar Hg filter-phase associations were noted by Hurley et al. (1998b) in heavily forested watersheds. Although the Black River watershed has similar land-cover characteristics to the Salmon (i.e., nearly 80% forest cover), Hg

was more associated with the particulate-phase in the Black. A closer analysis of land-cover distribution in the watershed offered a possible explanation: agricultural lands cover about 12% of the Black River watershed. Although this is a relatively small area of land, nearly all of it is concentrated within a 10 km buffer immediately adjacent to the lower 100 km of the tributary. Agricultural land-cover is commonly linked to increased THg_P concentrations and loading (Hurley et al. 1995; Babiarz et al. 1998; Wang et al. 2004). It is plausible that the higher THg_P fraction noted in the Black River is a result of the localized agricultural activities noted in the watershed.

Regression analysis was performed on Hg fractions and percent land-cover. Only one relationship was significant. Methylmercury fraction was positively correlated to percent open water coverage ($r^2 = 0.56$). Loss of Hg mass from an ecosystem is linked to open water coverage (Burns et al. 2012), and photodemethylation processes can decrease MeHg in open water (Sellers et al. 1996; Bradley et al. 2011). The increases in MeHg fraction with increases in open water coverage may be a result not of increases in MeHg concentration, but instead decreases in THg concentration with relatively stable MeHg concentrations. Although the relationship between THg concentration and open water coverage in the study watersheds was weak and not significant ($r = -0.47$), it was nevertheless negative. In addition, MeHg concentrations were not significantly different among the study tributaries.

4.4.4 Linkages with Dissolved Organic Carbon and Total Suspended Solids

The transport of Hg species is often linked to organic carbon and suspended sediment characteristics (Dittman et al. 2010). The concentrations of DOC and TSS were analyzed to explore possible relationships with Hg in the sampled tributaries. For DOC, means and medians from all sampled tributaries were similar, suggesting little skew of observations among

tributaries, and standard deviations were relatively small (Table 4.3, p. 65). Mean values of DOC for the Salmon, Ganaraska, Genesee, and Oswego tributaries ranged between 3 and 4 mg C L^{-1}; the Black, Credit, Humber, and Trent tributaries ranged between 4.5 and 6 mg C L^{-1}; and the mean for Twenty Mile Creek was slightly over 9 mg C L^{-1}.

Total suspended solids characteristics were markedly more variable than DOC in the study tributaries. A very large range of mean TSS concentrations (2.5 – 367 mg L^{-1}) was evident. In addition, seven of the nine tributaries exhibited larger mean than median TSS values, with standard deviations at least 50% of the magnitude of the respective means. In fact, standard deviations for several tributaries were over 100% the magnitude of the respective means (e.g., Genesee, Black, Twenty Mile, Salmon, Oswego; Table 4.3, p. 65). This difference indicates the influence of high-flow events during the study period. An extreme example was the Genesee River, with a median TSS of 15 mg L^{-1} and a mean TSS threefold higher (53 mg L^{-1}). Study tributaries with substantially lower TSS values also exhibited this pattern: mean TSS concentrations for the Black and Salmon rivers (2.5 to 6 mg L^{-1}, respectively) were two or more times higher than median values. Interestingly, the two tributaries with the most urbanized watersheds exhibited a contrasting pattern. Both the Humber and Credit rivers, which pass through urban areas, had mean TSS concentrations lower than median TSS concentrations over the course of the study. Removal of the TSS data from a single high-flow event that occurred on the same date in both tributaries suggests a very weak TSS concentration-flow relationship with a negative slope, so it is possible that this pattern is the result of an effect of dilution.

Mercury is commonly mobilized in association with organic carbon (Driscoll et al. 1994; Driscoll et al. 1995; Schuster et al. 2008; Shanley et al. 2008; Demers et al. 2010; Dittman et al.

2010). The variable nature of DOC and TSS for each tributary during the study period is illustrated in Figure 4.13 (p. 74). The correlations between DOC and TSS in the study tributaries and between DOC and Hg in the literature suggest that increases in Hg may also result from increases in TSS. When viewed in its entirety, the dataset for this project indicated that a positive relationship may exist between THg and TSS in the study tributaries; however, the relationship was not statistically significant. A weak, positive correlation was evident between THg and DOC ($r = 0.32$) in the study tributaries.

Potential correlations between DOC, TSS, and Hg were explored further based on the THg_D and THg_P fractions. The only tributary that exhibited a significant relationship between THg_D and DOC (positive) was Twenty Mile Creek ($r = 0.59$). However, when viewed seasonally both the Black ($r = 0.88$) and Salmon ($r = 0.86$) rivers had positive, significant relationships between THg_D and DOC in the spring. A significant, positive relationship was also noted between THg_P and TSS in six of the nine study tributaries (Ganaraska, $r = 0.41$; Oswego, $r = 0.41$; Credit, $r = 0.66$; Salmon, $r = 0.71$; Black, $r = 0.73$; Genesee, $r = 0.94$). Some seasonality was apparent in the correlation between THg_P and TSS. Strong, significant relationships were evident in spring for the Black ($r = 0.99$) and Oswego ($r = 0.99$); in summer for the Salmon ($r = 0.97$), Genesee ($r = 0.97$), and Twenty Mile Creek ($r = 0.89$); in fall for the Salmon ($r = 0.94$), Twenty Mile Creek ($r = 0.98$), and Credit ($r = 0.83$); and in winter for the Black ($r = 0.99$), Salmon ($r = 0.86$), and Genesee ($r = 0.99$).

Due to the relationships noted between Hg, DOC, and TSS, regression analysis was performed to determine how DOC and TSS are affected by flow in the study tributaries. Results of the analysis varied considerably from tributary to tributary, with most exhibiting no discernible

correlation. Relationships between TSS and instantaneous discharge were positive and significant in three of the nine study tributaries (Salmon, r = 0.60; Black, r = 0.81; Genesee, r = 0.94). Data for the remaining tributaries indicated no significant relationship between TSS and flow. Relationships between DOC and flow were positive and significant in two of the nine study tributaries (Genesee, r = 0.52; Twenty Mile, r = 0.67). None of the other tributaries showed a significant relationship between DOC and flow.

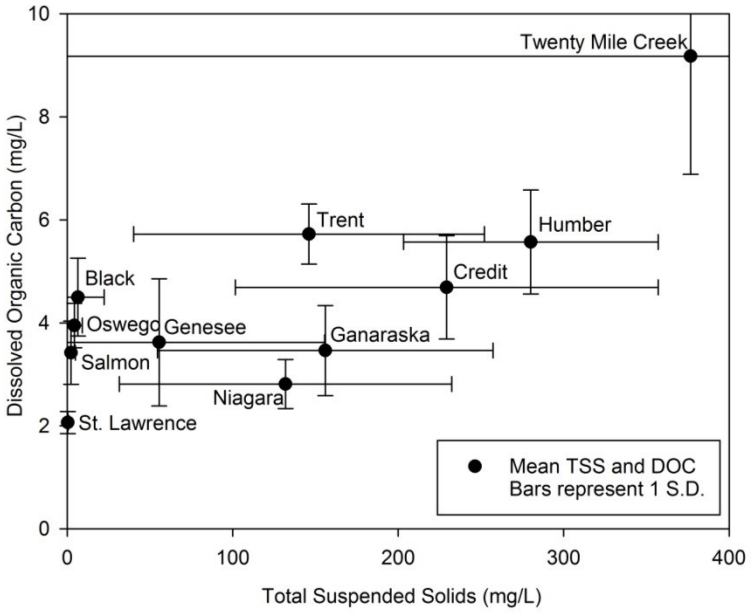

Figure 4.13 Dissolved organic carbon as a function of total suspended solids in the study tributaries. Several of the study watersheds show large variability in TSS.

4.4.5 Particle Partitioning of Mercury

The partitioning of Hg between TSS and water strongly influences Hg dynamics in lotic systems (Balogh et al. 1998; Brigham et al. 2009). Discharge events such as rainfall and snowmelt increase TSS in tributaries via flushing of overland particulate and sediment scour. Such events can accelerate Hg transport in tributaries where there exists a strong association between Hg and

TSS. Alternatively, increases in flow may result in little change in load rates if dilution of Hg concentrations occurs with increasing flow. A broad range of particle enrichment (PE; the Hg concentration of TSS, calculated as THg_P/TSS) was encountered in the sampled tributaries (0 – 67,650 ng Hg g^{-1} TSS). The dataset was strongly skewed, with some mean values being considerably larger than medians (e.g., Genesee, Black rivers; Table 4.4). In addition, a clear distinction was evident between the Canadian tributaries (mean range: 3.2 – 4.4 ng g^{-1}; median = 2.4 ng g^{-1}) and the US tributaries (mean range: 144 – 2,979 ng g^{-1}; median = 122.1 ng g^{-1}). Based on the available data, PE was significantly higher in US tributaries ($p < 0.001$; Mann-Whitney Rank Sum Test). Though THg_P concentrations in water were similar in Canadian and US tributaries, TSS concentrations were much higher in Canada relative to the US, resulting in a dilution effect on particle Hg content.

Table 4.4 Summary of particle Hg relationships in the study tributaries.

Tributary	THg				MeHg			
	PE (ng g^{-1})		Log K_d		PE (ng g^{-1})		Log K_d	
	Mean	Median	Mean	Median	Mean	Median	Mean	Median
Genesee	2,978.56	32.92	4.33	4.82	115.50	0.00	1.89	0.00
Black	857.28	317.22	5.40	5.38	24.74	0.00	2.37	0.00
Salmon	262.07	164.05	4.87	5.17	44.76	0.00	2.68	0.00
Oswego	143.98	107.11	4.61	5.28	29.32	0.69	2.98	2.36
Twenty Mile	4.36	1.55	2.98	3.33	0.03	0.00	1.31	0.60
Ganaraska	3.85	2.63	3.68	3.70	0.08	0.00	1.68	0.00
Humber	3.71	3.54	3.68	3.65	0.08	0.00	1.52	0.00
Trent	3.52	1.66	3.39	3.62	0.31	0.00	1.85	0.00
Credit	3.17	2.55	3.61	3.61	0.07	0.00	1.46	0.00

Increased retention of atmospherically deposited Hg in forested areas (i.e., US watersheds) relative to more urbanized and agricultural areas (i.e., Canadian watersheds) may support the elevated particle enrichment noted in the US watersheds in this study. Based on 2005 estimates of atmospheric Hg deposition derived from CMAQ (http://www.epa.gov/asmdnerl/EcoExposure/

depositionMapping.html; Bullock and Brehme 2002), Hg inputs from the atmosphere do not vary significantly among the study watersheds. However, Lyons et al. (2006) suggests that urbanized regions may retain lower percentages of atmospherically deposited Hg than other land-covers. In a study of midwestern states it was noted that forest floors exhibit higher Hg concentrations than surface mineral soils (Nater and Grigal 1992), largely as a result of higher organic matter content. Organic matter contains significant amounts of reduced sulfur sites that readily form complexes with Hg (Ravichandran 2004). The US watersheds average 50% more forested land-cover than the Canadian watersheds, while the Canadian watersheds exhibit 100% more agricultural and urban land-cover. Based on these observations, the higher Hg particle enrichment of the US watersheds may be influenced by differences in the land-cover between US and Canadian watersheds.

A similar pattern was evident for MeHg PE values. The Canadian tributaries exhibited a lower range of MeHg PE values (mean range: 0.03 – 0.31 ng g^{-1}; median = 0 ng g^{-1}) than the US tributaries (mean range: 24.7 – 115.5 ng g^{-1}; median = 0 ng g^{-1}). Due to the low and often non-detect MeHg analytical results, particulate MeHg values of zero were often calculated. This resulted in the zero values reported for medians on both sides of Lake Ontario (Table 4.4, p. 75), and the subsequent lack of significant difference between the US and Canadian tributaries (p = 0.078; Mann-Whitney Rank Sum Test).

Multiple linear regression was employed to explore the relationship between percent land-cover and mean particle enrichment. For this analysis, PE values had to be log-transformed to satisfy assumptions of normality. Following transformation, forward stepwise regression was carried out on the datasets. The only land-cover category found to have a statistically significant effect

was percent wetland coverage, and that applied only to log MeHg PE. The equation shown below represents this model ($r^2 = 0.46$):

$$\text{Log MeHg PE} = -0.636 + (0.400 * [\% \text{ Wetland}]) \quad \text{(Eq. 4.1)}$$

Though not significant at $\alpha = 0.05$, the best predictive model for log THg PE is represented by the following equation, which was also limited to percent wetland coverage ($r^2 = 0.38$):

$$\text{Log THg PE} = 0.970 + (0.298 * [\% \text{ Wetland}]) \quad \text{(Eq. 4.2)}$$

Distribution coefficients (K_d) may be used to assess the relative affinity of Hg for the particulate or the dissolved phase. Values of K_d can be useful in comparing particle-Hg relationships among different rivers (Babiarz et al. 1998). Commonly reported in logarithmic terms, K_d values for data in this study were calculated using the following equation:

$$K_d = C_p/C_f \quad \text{(Eq. 4.3)}$$

C_p represents a calculated value, the concentration of Hg on particles, in ng kg^{-1}, and C_f represents the measured concentration of THg_D in ng L^{-1}. Higher relative log K_d values therefore indicate a greater affinity for the particulate phase. For THg, mean log K_d values ranged from a low of 2.98 in the Twenty Mile Creek to a high of 5.40 in the Black River. Perhaps not surprisingly, based on PE observations, mean log K_d values were higher in the US tributaries relative to the Canadian tributaries, suggesting a greater particle affinity for Hg in the US watersheds. Relationships between land-cover and log K_d values were not readily discernible, with most watersheds having largely mixed land-use as discussed earlier. However, the only tributary with a mean log K_d less than 3.0, suggesting the lowest relative affinity with the

particulate phase, was Twenty Mile Creek. Twenty Mile Creek has the most homogenous land-cover of the watersheds studied, at ~90% agricultural cover. This observation fails to support the assertion that agricultural land-cover can increase THg_P. However, the mean DOC in the Twenty Mile Creek was the highest of all tributaries in the study, over 50% higher than the next highest tributary (Table 4.3, p. 65). This relatively high amount of DOC may cause preferential partitioning of Hg with dissolved organic matter in the Twenty Mile Creek, and hence influence the K_d. In Twenty Mile Creek, it is likely that atmospherically deposited Hg (largely Hg[II]) is preferentially complexed by DOC.

The log K_d values for MeHg were somewhat lower than for THg; mean values ranged from a low of 1.31 for Twenty Mile Creek to a high of 2.98 in the Oswego River. Tributaries with MeHg log $K_d > 2.0$ drained more forest-dominated watersheds, while those with log $K_d < 2.0$ drained more mixed watersheds, often with significant contributions from agricultural and urban lands. These patterns are different than what might be expected. As discussed in previous sections, positive relationships are commonly observed between agricultural land-use and particulate-phase associations, and also between forested land-use and dissolved-phase associations (Balogh et al. 1998). However, it is likely that particulate matter from forested watersheds has a higher organic carbon content, and as a result may offer preferential binding sites over particulate matter draining more agricultural or urban watersheds. POC has been shown to have an inverse relationship with TSS (Meybeck 1982), and TSS increases with agricultural and urban land-cover in the study watersheds (Tables 4.1 and 4.3, pp. 50 and 65, respectively). As discussed earlier, agricultural and urban lands retain lower percentages of atmospherically deposited Hg (Lyons et al. 2006), and forest floors have higher Hg concentrations than mineral soils, largely due to higher relative organic matter conent. The

higher particle-Hg associations for MeHg noted here for forested watersheds is likely due to the strong attraction of MeHg for organic matter.

The distribution coefficients presented here are similar to those presented elsewhere for THg (e.g., Hurley et al. 1994; Hurley et al. 1996; Mason and Sullivan 1997; Babiarz et al. 1998; Quémerais et al. 1998; Paraquetti et al. 2004). The MeHg K_d values for Lake Ontario tributaries are lower than those observed in some midwestern US studies (e.g., Mason and Sullivan 1997; Babiarz et al. 1998), and similar to those reported in a study conducted in the Everglades (Cai et al. 1999). The lower MeHg K_d values in this study may be an artifact of the strong observed affinity of MeHg for the dissolved phase in the sampled tributaries. Filtered MeHg results for the entire dataset had a mean of 0.07 ng L^{-1} and a median of 0.05 ng L^{-1}. Particulate MeHg estimates for the entire dataset had a mean of 0.04 ng L^{-1} and a median of 0 ng L^{-1}. A significant number of MeHg PE values were at or very close to zero due to analytically equivalent whole-water and filter-phase MeHg results. In fact, median MeHg PE values for eight of the nine sampled tributaries were zero. As previously mentioned, MeHg was difficult to thoroughly characterize in this ecosystem due to a majority of the observations having been very near to or below the detection limit (i.e., 0.02 ng L^{-1}).

With most watersheds having mixed land-cover, a multiple linear regression approach was used to determine relationships between percent land-cover and log K_d. For THg, a backward stepwise regression suggested that percent wetland was the only significant ($r^2 = 0.78$) predictor of THg log K_d, as follows:

$$\text{THg log } K_d = 3.53 + (0.277 * [\% \text{ Wetland}]) \qquad \text{(Eq. 4.4)}$$

Performing a backward stepwise regression for MeHg suggested that all land-cover variables could be used to predict MeHg log K_d ($r^2 = 0.97$). A forward stepwise regression proved more selective, indicating that percent wetland and percent water were most appropriately used to predict MeHg log K_d, and that the remaining land-cover categories did not contribute appreciably to predictive ability. The final model for MeHg log K_d ($r^2 = 0.82$) is:

$$\text{MeHg log } K_d = 1.47 + (0.147 * [\% \text{ Wetland}]) + (0.111*[\% \text{ Open Water}]) \quad \text{(Eq. 4.5)}$$

Interestingly, both models indicate positive relationships among the variables, suggesting an increased affinity for the particulate phase for THg with percent wetland coverage, and MeHg with percent wetland and percent open water coverage. The pattern noted with the wetland variable may be a result of increases in POC, and consequent increases in binding sites for Hg on particulate matter. The positive correlation between percent open water land-cover and the association of MeHg with the particulate phase is less clear, and may be coincidental.

5. Lake Ontario Mercury Mass Balance

5.1 Introduction

Lake Ontario is the fourth largest of the Great Lakes with respect to volume (1,640 km^3) and the fifth largest with respect to surface area (18,960 km^2). The direct watershed area of the lake is 64,030 km^2, for a watershed area to lake surface area ratio of 3.4 (the largest of the Great Lakes). The mean hydraulic residence time is estimated at 6 years, which is the second shortest of all the Great Lakes (Government of Canada and United States Environmental Protection Agency 1995).

The objective of this portion of the study was to build upon the results generated in Chapter 4 and improve the understanding of Hg cycling for Lake Ontario by quantifying fluvial loading of Hg, previously identified as a significant factor in the mass balance, yet largely unquantified. These critical data are then used in conjunction with estimates of atmospheric Hg exchange and Hg sedimentation to develop a comprehensive Hg budget for the lake.

5.2 Methods

Samples were collected from ten major rivers discharging into Lake Ontario and from the outlet at the St. Lawrence River. Rivers sampled in Canada included the Niagara, Twenty Mile Creek, Credit, Humber, Ganaraska, and Trent; those sampled in the US included the St. Lawrence, Black, Salmon, Oswego, and Genesee (Figure 4.1; p. 49). The volume discharged to Lake Ontario by these tributaries represents approximately 90% of the flow at the St. Lawrence River, with the Niagara River contributing approximately 91% of the measured tributary inflow during 2009. Samples were collected over a broad range of recorded flows, with no emphasis on any specific flow regime (Figure 4.11, p. 63). Mean discharge during the sampling period was similar to the period of record for the US tributaries, while the Canadian tributaries averaged

approximately 30% higher flows during the study period than the long-term mean (Table 4.1, p. 51). Bimonthly sampling was performed in Canada from June 2008 to December 2009, and in the US from June 2009 to May 2010. Discharge for all tributaries was generally higher in 2008 than either 2009 or 2010, supporting the higher relative flows recorded in the Canadian rivers over the study period.

Sample collection was performed using trace metal clean protocols (USEPA 1996). Either in the field or upon arrival at the laboratory, 250-500 mL water sample aliquots were filtered through pre-cleaned 0.45-µm filters. Whole and filtered water samples were then preserved using 4 mL L^{-1} 11.6 M trace metal grade hydrochloric acid. Sample analysis included ancillary chemistry (e.g., TSS, DOC). Analysis of US tributary samples was conducted at Syracuse University; analysis of Canadian tributary samples was conducted at the University of Toronto. Both laboratories used the same or similar methods for analysis. Total Hg analysis was conducted using CVAFS (Bloom 1989; USEPA 2002). Methylmercury determination was performed via aqueous phase ethylation with $NaB(C_2H_5)_4$, purge and trap separation and detection by CVAFS (Horvat et al. 1993a; Horvat et al. 1993b; Liang et al. 1994). Total particulate Hg concentrations, flux, and yield were calculated as the difference between whole- and filtered-sample results; consequently, some reported THg_P concentrations are below the THg detection limit (0.20 ng L^{-1}). Ancillary water quality measures were analyzed using Standard Methods (Eaton et al. 1998): for DOC, the persulfate-ultraviolet oxidation method (5310C) and for TSS, method 2540D.

For calculation of means, medians, standard deviations, and mass balances, non-detect samples were assigned a value of ½ the detection limit of 0.20 ng L^{-1} for THg and 0.02 ng L^{-1} for MeHg. This approach was used to fill data gaps for less than 9% of all Hg analyses.

The mass transport of Hg species was estimated by coupling fluvial concentration measurements with discharge data available from USGS and Environment Canada stations. Calculations were performed using $FLUX_{32}$ software, version 3.03 (Walker 1987). The $FLUX_{32}$ model utilizes daily discharge rates (where available) in conjunction with analyte concentrations to estimate material fluxes. Multiple calculation methods are provided in the software package, allowing the user to choose the one that best suits the flow and concentration characteristics of each tributary. Mean daily discharge data are available for most of the tributaries in this study, with the exceptions of the St. Lawrence River (weekly data only) and the Trent River. Daily discharge for the Trent River was composited from a gauged subwatershed and discharge data provided by Ontario Power Generation, as described in Chapter Section 4.2. Sample data are available for most analytes on a biweekly basis between June 2008 and December 2009 for Canada and June 2009 and May 2010 for the US. Estimates of fluxes for Hg species in this study generally displayed only small relative variations among most calculation methods. Disregarding the flux estimates for Twenty Mile Creek (which has a small watershed and flashy flow characteristics; Table 4.1, p. 51), the mean variation for estimates of THg flux based on different calculation methods was approximately 10%. Flux estimates for Twenty Mile Creek varied considerably (i.e., over 100%) due to the variable flow regime of the Creek and differences in how each calculation method handles the concentration-flow relationship. In the end, the calculation method was individually selected for each tributary based on the lowest coefficient of variation

reported for each method by $FLUX_{32}$, and by the general agreement of multiple calculation methods.

Retention coefficients (R) for Lake Ontario were estimated for all analytes using the following equation:

$$R = (\text{flux in} - \text{flux out})/(\text{flux in}) \qquad \text{(Eq. 5.1)}$$

The R values were calculated on a solely riverine ($R_{riverine}$) basis, including dissolved ($R_{dissolved}$), particulate ($R_{particulate}$), and MeHg fractions (R_{methyl}), on an atmospheric basis (R_{atmos}), and on an atmospheric plus riverine (R_{total}) basis. Though values of $R_{riverine}$ and R_{atmos} greatly oversimplify retention and loss of Hg from Lake Ontario, they are nevertheless provided to indicate relative retention and loss from different sources. Analysis of watershed land-cover characteristics was performed with a GIS approach as discussed in Chapter 4, and is summarized in Table 4.1 (p. 51). Watershed yields were calculated based on estimates of flux, according to the following equation:

$$\text{Watershed Yield} = \text{flux} / \text{watershed area} \qquad \text{(Eq. 5.2)}$$

Statistical analysis was performed using SigmaPlot 11.0 (Systat Software, Inc. 2008) and alpha was set to 0.05 for significance in all statistical tests.

5.3 Results and Discussion

5.3.1 Total Mercury Flux

The yearly THg flux estimates were highly variable among the study rivers (Figure 5.1, p. 86; Table 5.1, p. 87). While some of this variation can be attributed to differences in Hg

concentration, the major driver of Hg loading rates to the lake is river discharge. Although the Niagara River had the lowest average THg concentration of the inflowing tributaries (0.8 ng L^{-1}; Table 4.3, p. 65), its THg flux (154 kg yr^{-1}) dominated the fluvial THg load to Lake Ontario, constituting nearly 80% of the annual total. The next closest fluvial source of THg to the lake was the Black River (13 kg yr^{-1}). The smallest contributor was the Ganaraska River, which supplied THg at a rate of 0.2 kg yr^{-1} during the study period. Based on these estimates, the total fluvial THg load was approximately 197 kg yr^{-1} to Lake Ontario. The St. Lawrence River is the sole fluvial export for Lake Ontario (assuming groundwater seepage constitutes a negligible mass flux of Hg). Total Hg export from the lake was estimated to be 68 kg yr^{-1}. The mean THg concentration for the St. Lawrence River (0.3 ng L^{-1}; Table 4.3, p. 65) was lower than any of the inflowing rivers, including the Niagara River. Therefore, similar to fluvial THg loads, the magnitude of THg export via the St. Lawrence River is driven by water flux. Summed together, the riverine THg flux estimates indicated net fluvial retention of approximately 129 kg yr^{-1} THg ($R_{riverine}$ = 0.65; Table 5.2, p. 88).

5.3.2 Dissolved Mercury Flux

Estimates of THg_D flux are similar to THg flux estimates because the total annual THg_D load was likewise dominated by the Niagara River (105 kg yr^{-1}). As was observed with THg estimates, the next highest contributor was the Black River (5.5 kg yr^{-1}) and the lowest contributor was the Ganaraska River (0.1 kg yr^{-1}). Total dissolved Hg export via the St. Lawrence River (67 kg yr^{-1}) constituted over 95% of total fluvial Hg loss from Lake Ontario. Unlike most of Lake Ontario's tributaries, the Hg in the St. Lawrence River consisted almost entirely (i.e., > 90%) of the dissolved fraction. The riverine mass balance of THg_D for the lake suggests fluvial retention of approximately 56 kg yr^{-1} ($R_{dissolved}$ = 0.45; Table 5.2, p. 88).

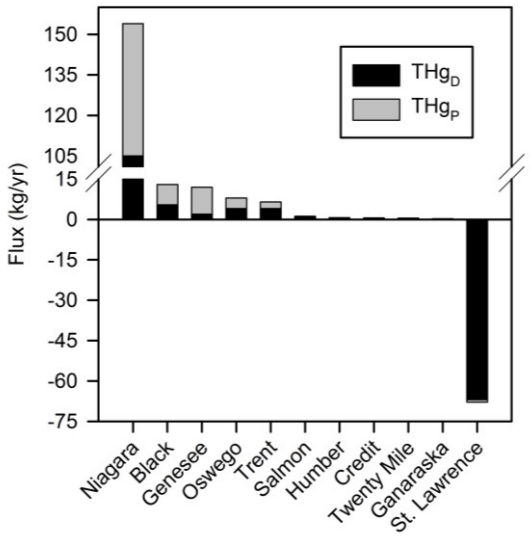

Figure 5.1 Summary of fluvial Hg flux into and out of Lake Ontario for the study period.

5.3.3 Particulate Mercury Flux

Total particulate Hg loads to the lake were also dominated by the Niagara River (i.e., 50 kg yr^{-1}), despite the Niagara having the lowest mean THg_P concentration of all sampled tributaries (i.e., 0.3 ng L^{-1}; Table 4.3, p. 65). Unlike THg and THg_D fluxes to the lake, where the contribution of the Niagara River was nearly fifteen- to twenty-fold higher than the next largest tributary source, THg_P flux from the Niagara was not as dominant relative to other fluvial sources. The next highest source of THg_P to Lake Ontario was the Genesee River at 10 kg yr^{-1}, followed by the Black River (7.5 kg yr^{-1}) and the Oswego River (3.9 kg yr^{-1}). Interestingly, net THg_P loads to the lake exceeded net THg_D loads. Gross THg_D loads to the lake were approximately 60% higher than gross THg_P loads. However, over 95% of the fluvial THg_P load was retained in the lake (i.e., 75 kg yr^{-1}; $R_{particulate}$ = 0.99; Table 5.2, p. 88), emphasizing the role of Lake Ontario as a depositional basin for Hg. Note that while this calculation depicts net THg_P transport, undoubtedly some THg_P is produced within the lake.

Table 5.1 Summary of Hg fluxes and yields for rivers and outlet of Lake Ontario.

Watershed	Watershed Area (km^2)	Flux and Yield													
		THg				THg_D				THg_P[3]		MeHg			
		($kg\ yr^{-1}$)	($g\ km^{-2}\ yr^{-1}$)	C.V.	S.D.	($kg\ yr^{-1}$)	($g\ km^{-2}\ yr^{-1}$)	C.V.	S.D.	($kg\ yr^{-1}$)	($g\ km^{-2}\ yr^{-1}$)	($kg\ yr^{-1}$)	($g\ km^{-2}\ yr^{-1}$)	C.V.	S.D.
Niagara	--	154	--	0.1	15.52	105	--	0.1	14.35	49	--	20	--	0.5	9.57
Oswego	13,045	8.0	0.6	0.2	1.55	4.1	0.3	0.2	0.71	3.9	0.3	0.6	0.05	0.48	0.35
Trent	12,560	6.5	0.5	0.1	0.86	4.1	0.3	0.2	0.63	2.4	0.2	0.6	0.04	0.44	0.24
Genesee	6,550	12	1.8	0.2	2.51	2.0	0.3	0.1	0.25	10	1.5	0.1	0.02	0.32	0.04
Black	5,015	13	2.6	0.2	2.19	5.5	1.1	0.1	0.28	7.5	1.5	0.3	0.05	0.24	0.06
Credit	950	0.5	0.6	0.1	0.04	0.3	0.3	0.1	0.03	0.3	0.3	0.04	0.04	0.43	0.02
Humber	910	0.6	0.7	0.1	0.06	0.3	0.3	0.1	0.03	0.4	0.4	0.02	0.02	0.23	0.004
Salmon	713	1.2	1.6	0.1	0.07	0.9	1.2	0.1	0.08	0.3	0.4	0.06	0.08	0.24	0.01
Twenty Mile	295	0.5	1.8	0.2	0.08	0.3	1.0	0.1	0.04	0.2	0.7	0.01	0.03	0.21	0.002
Ganaraska	275	0.2	0.9	0.4	0.10	0.1	0.3	0.3	0.02	0.2	0.5	0.01	0.03	0.16	0.001
St. Lawrence	--	68	--	0.1	8.12	67	--	0.08	5.59	0.9	--	17	--	0.27	4.47

Notes:

1. C.V. = coefficient of variation.
2. S.D. = standard deviation.
3. THg_P is the calculated difference between THg and THg_D. As a result, measures of variation are not reported for THg_P.

Table 5.2 Summary of flux estimates and retention coefficients for Lake Ontario.

Basis		Flux In (kg yr^{-1})	Flux Out (kg yr^{-1})	Retention Coefficient (*R*)
Riverine[(1)]	THg_D	122	67	0.45
	THg_P	74	1	0.99
	MeHg	22	17	0.22
	THg	197	68	0.65
Atmospheric	Hg_P + Hg(II)[(2)]	233	0	1.00
	Hg^0 [(3)]	300	410	-0.37
	THg	533	410	0.23
Total	THg	730	478	0.35

Notes:

1. This study.
2. CMAQ (Bullock and Brehme 2002).
3. LOADS (Lai et al. 2007).

5.3.4 Methylmercury Flux

Methylmercury fluxes for the study period were substantially smaller than all other forms of Hg. The MeHg flux from the Niagara River (i.e., 20 kg yr^{-1}) was far greater than any of the other tributaries. The next closest MeHg input was for the Oswego River at 0.6 kg yr^{-1}, over an order of magnitude less than the Niagara's contribution. Methylmercury fluxes from the remaining US study rivers were all higher than the Canadian tributaries except for the Trent River. At 0.6 kg yr^{-1}, the Trent River contributed approximately the same amount of MeHg as the Oswego River. The observed spatial distribution of MeHg fluxes reflects variation in river discharge. The smallest US tributary (Salmon River) contributed approximately twice the volume of water to Lake Ontario than the second largest Canadian study tributary (Table 4.1, p. 51). The gross fluvial MeHg load to the lake was estimated at 22 kg yr^{-1}. Export via the St. Lawrence River was estimated to be 17 kg yr^{-1}, for a net fluvial retention of 5.0 kg yr^{-1} MeHg (R_{methyl} = 0.22; Table 5.2). As with other Hg forms, while Lake Ontario is a net sink for MeHg inputs, likely

some production of MeHg occurs within the water column and sediments of the lake (Eckley and Hintelmann 2006; Achá et al. 2012).

5.3.5 Watershed Mercury Yield and Land-cover

Annual THg yields ranged from a low of 0.5 g km^{-2} yr^{-1} (Trent River watershed) to a high of 2.6 g km^{-2} yr^{-1} (Black River watershed); THg_D yields ranged from 0.3 g km^{-2} yr^{-1} (all watersheds but Black, Salmon, and Twenty Mile) to 1.2 g km^{-2} yr^{-1} (Salmon watershed); THg_P yields ranged from 0.2 g km^{-2} yr^{-1} (Trent watershed) to 1.5 g km^{-2} yr^{-1} (Black and Genesee watersheds); and MeHg yields ranged from 0.02 g km^{-2} yr^{-1} (Humber and Genesee watersheds) to 0.08 g km^{-2} yr^{-1} (Salmon watershed) (Table 5.1, p. 87). Only MeHg yield estimates were normally distributed – all others were positively skewed.

Watershed yields of THg, THg_D, THg_P, and MeHg were modeled by regression analysis with percent land-cover (forest, agriculture, wetland, urban, open water) for each of the watersheds. Three of the four significant relationships observed suggest land-cover controls on MeHg yield. Of these three, two were positive (forest, $r^2 = 0.39$; wetland, $r^2 = 0.73$); and one was negative (agriculture, $r^2 = 0.43$). The observed relationship between increases in wetland coverage and increases in watershed yields of MeHg is consistent with others in the literature (Hurley et al. 1995; St. Louis et al. 1996; Driscoll et al. 1998; Grigal 2002; Warner et al. 2005). The positive link between MeHg and forest cover is not as common in the literature, though some studies suggest that a MeHg pulse occurs from litterfall inputs in forested catchments (St. Louis et al. 2001; Balogh et al. 2003). Note that a positive relationship exists between forest and wetland cover ($r^2 = 0.44$). The correlation between MeHg and forest cover may therefore be coincident with the link observed between forest and wetland cover. Finally, the inverse relationship between agricultural land-use and MeHg yield seen in this study is not frequently noted in the

literature, though Kamman et al. (2005b) documented a positive correlation between sediment MeHg concentrations expressed as a percentage of THg and agricultural land-cover in waterbodies of northeastern North America. There was a significant negative relationship between percent wetland coverage and percent agricultural coverage among the Lake Ontario watersheds ($r^2 = 0.50$), as well as a significant negative relationship between percent forest coverage and percent agricultural coverage ($r^2 = 0.94$). The relationship observed between MeHg yield and agricultural land-use may therefore be coincident with land-use dynamics: study watersheds with higher agricultural land-cover had less wetland and forest coverage. Driscoll et al. (2012) described a dampening of MeHg production resulting from nutrient loading to coastal ecosystems, where subsequent increases in biomass decrease MeHg trophic transfer by dilution. In addition, they noted that increases in carbon deposition from higher rates of primary production can result in reductions in methylation rates. A similar process may also be occurring in study watersheds with higher relative agricultural land-cover.

Wetlands are typically important sources of natural organic matter to connected surface waters (Mulholland and Kuenzler 1979; Eckhardt and Moore 1990). A positive relationship was evident between watershed yield of THg_D and percent wetland coverage in the study. Strong associations between THg_D and DOC are regularly reported in the literature (Schuster et al. 2008; Shanley et al. 2008). There was also a weak, though significant, positive relationship between DOC and THg_D for the entire dataset ($r^2 = 0.27$). However, there were no significant relationships between either percent wetland or wetland area and measures of DOC in the study watersheds. This lack of a pattern may be a result of the relatively small (i.e., $\leq 6\%$) amount of wetland coverage for the study watersheds and, hence, a very small range of percent wetland area among the watersheds. Also, there is likely an additional small amount of wetland coverage

that escapes the resolution (i.e., 250-m) of the land-cover data or low-lying terrain that escapes wetland classification, yet still affects stream water chemistry and that of adjacent water bodies (Driscoll et al. 1998).

5.3.6 Atmospheric Mercury Fluxes to Lake Ontario

Unfortunately, detailed measurements of atmospheric exchange and sediment deposition are not available for Lake Ontario for the study period. However, to help put the fluvial measurements into perspective, I summarize reports in the literature on atmospheric Hg fluxes. The CMAQ (Bullock and Brehme 2002) model has been used to develop estimates of particulate and ionic atmospheric Hg deposition on a 12 km grid. In order to estimate deposition for Lake Ontario based on the CMAQ output, a GIS approach was used to analyze depositional rates for each of the 12 km squares over the lake based on the Hg emission inventory for 2005. These rates ranged from a low of 7.0 $\mu g\ m^{-2}\ yr^{-1}$ Hg (near the central-northern shore and the outlet) to a high of 19.4 $\mu g\ m^{-2}\ yr^{-1}$ Hg (in the vicinity of the western end of the lake). The resulting mean of all squares covering the lake (12.3 $\mu g\ m^{-2}\ yr^{-1}$ Hg) was applied for budget estimates. Based on a total open water area of 18,960 km^2 for Lake Ontario, this analysis suggests a particulate and ionic Hg input of approximately 233 kg yr^{-1} to the lake via wet and dry deposition. Gaseous Hg^0 exchange was estimated based on a field study performed on Lake Ontario between April 2002 and July 2003. Gross deposition and emission of Hg^0 were estimated at 300 and 410 kg yr^{-1}, respectively (Lai et al. 2007). Combining these estimates with the CMAQ values for particulate and ionic deposition results in a net atmospheric THg flux of 123 kg yr^{-1} to the lake (R_{atmos} = 0.23; Table 5.2, p. 88), which is similar in magnitude to the fluvial THg flux from the Niagara River (i.e., 154 kg yr^{-1}).

5.3.7 Sedimentation of Mercury in Lake Ontario

There are few empirical data for lake-wide THg sedimentation rates. Data from a single dated sediment core collected in the western basin of Lake Ontario in 2008 suggest a recent THg net sedimentation rate of approximately 190 $\mu g\ m^{-2}\ yr^{-1}$ (Drevnick et al. 2012). This value results in a THg flux to the sediments on the order of 4,000 kg yr^{-1} when applied across the entire lake bottom (assuming a lake bottom area of approximately 20,000 km^2). This estimate doubles to approximately 8,000 kg yr^{-1} when using sedimentation rates based on cores collected in 1981 (Pirrone et al. 1998). Decreases in anthropogenic Hg emissions over the past two decades (Drevnick et al. 2012) support reductions in THg sedimentation. However, in light of the net estimates of atmospheric plus fluvial THg flux to the lake (total = 252 kg yr^{-1}), these values almost certainly greatly overestimate total net Hg deposition to sediments. Sedimentation across the lake bottom is not homogenous, making a basin-wide estimate of net THg sedimentation based on sediment cores a challenge. Thomas et al. (1972) indicate that sedimentation is limited to the three major sub-basins of the lake (i.e., Niagara, Mississauga, Rochester); this has been more recently been modified to include the Kingston sub-basin (Kaur et al. 2012). Oliver et al. (1989) suggested that little net sediment accumulation occurs outside these sub-basins. Estimates of the combined area of these four sub-basins range from 8,660 km^2 to 11,390 km^2 (Oliver 1984; Kaur et al. 2012). Application of the more recent net sedimentation estimate from Drevnick et al. (2012) to this range of depositional area results in a net THg sedimentation flux of approximately 1,660 to 2,180 kg yr^{-1}. Though this range is approximately half the value of that calculated from application of Hg fluxes from individual cores to the entire lake bottom, it is still high relative to my estimates of fluvial and atmospheric THg loads to the lake.

None of the above studies discuss the effects of sediment re-suspension, though it can be assumed that sedimentation rates developed from sediment cores represent net sedimentation. In a recent modeling effort, gross THg sedimentation was estimated at approximately 3,530 kg yr^{-1} (Ethier et al. 2012). Ethier et al. (2012) also estimated re-suspension of sediment THg for areas of the lake bottom likely to be affected by atmospheric conditions and water currents (i.e., the nearshore zone), and found this flux to be approximately 3,370 kg yr^{-1}. The balance between these values suggests an approximate net THg sedimentation flux of 160 kg yr^{-1} to lake sediments, a value that is on the same order of magnitude as my net sum estimate of atmospheric and fluvial THg flux to the lake (i.e., 252 kg yr^{-1}). Further, total solids deposition to Lake Ontario sediments have been estimated at approximately 4.26×10^9 kg yr^{-1} (DePinto et al. 2004). Assuming all Hg sedimentation results from THg_P, particle enrichment (i.e., PE; the concentration of Hg on particles) for solids contributing to sedimentation is estimated at 38 ng g^{-1}. This value is well within the range of PE observed for the riverine dataset reported in this study (median = 4.9 ng g^{-1}; mean = 470 ng g^{-1}).

6. Great Lakes Basin Atmospheric Mercury Budget

6.1 Introduction

Given the importance of Hg^0 evasion to the overall mass balance of watersheds, in this chapter I review the literature on surface-air fluxes of Hg^0 in terrestrial and freshwater aquatic environments and provide a synthesis of these studies. The focus of this analysis is the Great Lakes Basin (GLB). Overall Hg^0 losses from the GLB are estimated, and these fluxes are compared with estimates of Hg emissions and inputs from wet, dry and litterfall Hg deposition through a synthesis of the best available information in the published literature.

6.2 Literature Review of Mercury Evasion Estimates

This review of Hg^0 evasion studies is organized by land-cover type: forest, agriculture, grassland, urban, wetlands, inland lakes, and the open waters of the Great Lakes. Based on this review, rates of Hg^0 evasion were selected for each land-cover, and used to calculate Hg evasion for the GLB. For the purpose of this analysis, Hg fluxes discussed and selected for scaling purposes are net gaseous exchange values (i.e., flux values presented account for both gaseous Hg deposition and emission).

Surface Hg^0 fluxes are influenced by diel and seasonal variability under environmental conditions. Variables that have been found to be important in influencing fluxes include solar radiation, temperature, precipitation and atmospheric turbulence and chemistry (summarized in Gustin et al. 2008; Stamenkovic et al. 2008). There is considerable variation in estimates of Hg^0 evasion for various land-cover types. This large overall variability occurs due to large temporal variability over the time of day and season, relatively large spatial variability, and substantial differences in the nature and intensity of measurements among studies. For example, Poissant et

al. (2004) observed a greater than 50% increase in Hg^0 volatilization from the same wetland site under dry conditions compared to when it was flooded. Moreover, soil temperature became a more important controller of Hg^0 evasion than solar radiation during the dry period. While some studies have suggested that prolonged soil moisture might inhibit Hg^0 evasion (Schroeder et al. 2005; Selvendiran et al. 2008b), others have noted elevated Hg^0 evasion rates immediately following precipitation events (Lindberg et al. 1999; Engle et al. 2001; Eckley et al. 2011). Marked spatial variability has also been documented in the literature. Eckley and Branfireun (2008) noted an approximate four-fold difference in Hg^0 evasion between some pavement sites in Toronto, and suggested this difference was a result of different pavement compositions.

Some studies have measured Hg^0 flux during different seasons to establish an annual ecosystem flux which accounts for temporal variability, whereas other studies conduct measurements over a range of days (or hours) during a single season. Several studies have identified that flux increases with temperature and solar radiation and as a result, fluxes are higher during the daytime than at night and generally higher in the summer than in winter (Gabriel et al. 2006; Choi and Holsen 2009a; Eckley et al. 2011); however, some studies have also identified that lower solar radiation under deciduous canopies and lower soil moisture content results in lower summertime fluxes (Kuiken et al. 2008; Hartman et al. 2009). Because several studies have shown diel Hg^0 fluxes to generally follow a pattern similar to solar elevation, measurements conducted only during daylight hours will greatly overestimate mean daily emissions (e.g., Chapter 3; Engle et al. 2001; Gustin et al. 2003; Gabriel et al. 2006). Therefore, for land-cover types where multiple studies have been conducted, selection of data that incorporate daily and seasonal variability in developing annual flux estimates has been prioritized, as well as studies from within/near the GLB.

Surface Hg^0 fluxes can be measured/modeled using several approaches. For soils, dynamic flux chambers (DFC) and micrometeorological methods (MM) are the most common techniques and for aquatic ecosystems, DFCs and purge/trap methods are routinely applied. Additionally, both Hg^0 detectors and mathematical models used to estimate Hg^0 evasion vary. Studies that compare different techniques used to measure flux suggest that the methodological approach and operating parameters influence the magnitude of the calculated flux (Gustin et al. 1999; Rolfhus and Fitzgerald 2001; Eckley et al. 2010). Therefore, because there is no standard protocol for conducting measurements of gaseous Hg^0 flux, some component of the variability in Hg^0 fluxes among landscapes reported is a function of differences in flux measurement techniques. To minimize this artifact, flux datasets that used similar methodological approaches were selected as part of this review. For soil surfaces, fluxes measured using DFCs were available for all surface types and were prioritized for scaling. For aquatic surfaces, where DFC measurements were available they were selected; however for some surfaces only purge/trap data were available and applied for scaling.

Note that in many of the studies reviewed it was assumed that soil Hg^0 evasion during periods of snow cover is minimal. While this may be true for the soil itself, studies have reported substantial rates of Hg^0 evasion from snowpack (e.g., Lalonde et al. 2002; Ferrari et al. 2005). A considerable portion of the GLB is snow-covered during the winter season. Few studies were found that estimated Hg^0 evasion from snowpack in the GLB (Schroeder et al. 2005), and many of the emission studies reviewed had no or limited measurements during winter. Additional studies are necessary to quantify Hg^0 emission from the snow cover period in the GLB.

6.2.1 Forests

Fluxes (based on DFC) from a deciduous forest in the Adirondack region of New York were selected for scaling forest lands that incorporated diel measurements conducted during each season (Choi and Holsen 2009a; Table 6.1, p. 98). The seasonal flux data were then scaled annually to account for seasonal changes in canopy coverage in the summer and snow coverage in the winter; expressed as an annual hourly average this flux was 0.8 ng m^{-2} hr^{-1}. Other studies of Hg flux from North American forests using DFCs include Carpi and Lindberg (1998) and Zhang et al. (2001) both of which measured spring/summer daytime-only fluxes from the soil beneath a deciduous forest in Tennessee (flux range: 2 to 7 ng m^{-2} hr^{-1}) and Michigan (average flux: 1.4 ±1.4 ng m^{-2} hr^{-1}) and Schroeder et al. (2005) which measured summertime fluxes from forest soil in Nova Scotia (flux average: 1.1 ng m^{-2} hr^{-1}). While the Choi and Holsen (2009a) flux value appears lower than measurements from other studies, this is because their value incorporates diel and seasonal variability, whereas the other studies do not. During warm, sunny conditions, Choi and Holsen (2009a) measured Hg^0 fluxes that were in excess of 10 ng m^{-2} hr^{-1}, which is of similar magnitude as measured during peak emissions in the other studies.

6.2.2 Agricultural Lands

Agricultural lands include areas used for crop production. Grasslands, including areas used for livestock pasture, are discussed in the *Grasslands* section. Using the DFC method, Carpi and Lindberg (1998) measured Hg^0 fluxes from a simulated plowed agricultural field in Tennessee (vegetation was manually removed from the surface before measurements were conducted) and found fluxes ranging from -0.66 to 44.8 ng m^{-2} hr^{-1}. This large range incorporates values at different sample locations (two different fields) and levels of daytime solar radiation. The fluxes from the Nelson field site in Carpi and Lindberg (1998) are considered more representative of

Table 6.1 Summary of terrestrial Hg fluxes measured in or near the Great Lakes Basin. Note: some studies only measured Hg fluxes during the daytime—to estimate diel fluxes from daytime measurements, a Gaussian distribution was assumed following the methods of Engle et al. (2001) and Nacht and Gustin (2004). All estimated diel fluxes are presented in italics in the Table. For land-covers where multiple DFC measurements exist, a potential range of values is given in parenthesis that reflects diel and seasonally adjusted flux estimates.

Land-cover	Site Description	Season	Method	Daily flux (ng m^{-2} d^{-1})	Hourly flux (ng m^{-2} hr^{-1})	Flux used for scaling (ng m^{-2} d^{-1})	Soil THg Conc. (ng g^{-1})	Reference
Forest	Deciduous forest-- Adirondacks, NY, USA	Spring	DFC	15	0.64[a]	19 (Potential range: 6.2 to 33)	81.9 ± 24.7	Choi and Holsen 2009a; Choi and Holsen 2009b
		Summer		32	1.34[a]			
		Fall		19	0.77[a]			
		Winter		22	0.09[a]			
		Annual Ave.		19	0.80[b]			
	Deciduous forest-- Oak Ridge, TN, USA	Spring/ Summer	DFC	*10 to 33**	2.0 to 7.0[c]		469 ± 75	Carpi and Lindberg 1998
	Forest-- Nova Scotia, Canada	Summer	DFC	*8.5*	1.1[c]		150 - 330	Schroeder et al. 2005
	Deciduous forest— Upper Peninsula Michigan, USA	Summer	DFC	*22*	1.4 ±1.4[c]		69 - 98	Zhang et al. 2001
	Deciduous forest— Standing Stone State Forest, TN, USA	Spring	DFC	0	0.0 ± 0.3[c]		92	Kuiken et al. 2008
		Summer		3.1	0.4 ± 0.3[c]			
		Fall		7.0	0.9 ± 0.6[c]			
		Winter		4.7	0.6 ± 0.5[c]			
		Annual Ave		*6.2*	0.4 ± 0.5			
Agriculture	Disturbed soil— Tennessee, USA	Spring/ Summer	DFC	*82 to 230*	12 ± 5.4 to 45 ± 5.2[c]	58 (Potential range: 82 to 230)	61 ± 19 to 111 ± 14	Carpi and Lindberg 1998
	Cropland-Maryhill, Ontario, Canada	Fall	MM	2.4	0.1 ± 0.2[d]		400[e]	Cobbett and Van Heyst 2007
	Cropland- Minnesota, USA	Spring	MM	230	9.67[d]		24.8 ± 4.2	Cobos et al. 2002

Land-cover	Site Description	Season	Method	Daily flux (ng m^{-2} d^{-1})	Hourly flux (ng m^{-2} hr^{-1})	Flux used for scaling (ng m^{-2} d^{-1})	Soil THg Conc. (ng g^{-1})	Reference
Agriculture (cont'd)	Snow covered rural soil—Elora, Ontario, Canada	Winter	DFC	*1.0*	0.09 ± 0.03[c]		NA	Schroeder et al. 2005
Grassland	Pasture, Ontario and Quebec, Canada	Summer	DFC	43*	3.0[d]	40 (Potential range: 36 to 43)	6	Schroeder et al. 2005
			MM	26	1.1[d]		47	
			MM	70	2.9[d]		100	
	Pasture—Upper Peninsula Michigan, USA	Summer	DFC	*36**	7.6 ±1.7[c]		16	Zhang et al. 2001
	Wisconsin	Not specified	DFC	7.2	0.3± 0.07[d]		<10 to 28	Ericksen et al. 2006
Urban	Pavement—Toronto, Ontario, Canada	Summer	DFC	*4.3**	1.0[f]	Pavement: 3.6 (Potential range: -0.24 to 4.3) Soil: 55.2 (Potential Range: 29 to 62)	16	Eckley and Branfireun 2008
	Soil—Toronto, Ontario, Canada	Summer	DFC	*29**	6.2[f]		61	
	Pavement—Tuscaloosa, Alabama, USA	Spring	DFC	139	5.8[a]		Not measured	Gabriel et al. 2006
		Summer		264	11[a]			
		Fall		26	1.1[a]			
		Winter		34	1.4[a]			
		Annual Ave		62	2.6			
	Soil—Tuscaloosa, Alabama, USA	Spring	DFC	-0.48	-0.02[a]		25 to 47	
		Summer		0.48	0.02[a]			
		Fall		-3.6	-0.15[a]			
		Winter		2.2	0.09[a]			
		Annual Ave		-0.24	-0.01			

[a]Median value from diel measurements

[b]Annual estimate adjusted (+20%) to account for limited UVB permeability of polycarbonate chamber

[c]Hourly average measurements during daytime/sunlight conditions.

[d]Diel average

[e]Concentration after biosolids application

[f]Median value from daytime measurements conducted at several locations

*Adjusting this value to account for seasonal variability based on the findings of Choi and Holsen (2009a)

the GLB because the Hg concentration of the soil (61±19 ng g^{-1}) was similar to values measured from crop and pastureland within the GLB (see Table 6.1, p. 98). Because these measurements were conducted during the spring/summer daytime conditions, they needed to be adjusted to account for diel and seasonal flux variability. Flux measurements obtained during only specific periods of the day can be extrapolated to diel averaged fluxes assuming a Gaussian distribution (Engle et al. 2001; Nacht and Gustin 2004). Using the daytime sunny conditions average flux of 12.5 ng m^{-2} hr^{-1} to represent noontime emissions, and the average from measurements obtained in the shade to represent nighttime fluxes (-0.66 ng m^{-2} hr^{-1}), to fit a Gaussian distribution resulted in an estimated diel flux of 3.4 ng m^{-2} hr^{-1}. Furthermore, since this flux was measured during the spring/summer, it is not representative of fall and winter emissions. If a similar decrease in fluxes is assumed during the fall as was observed from the seasonal measurements from a GLB forest (Choi and Holsen 2009a), then the diel autumn Hg^0 fluxes are estimated to be 2.7 ng m^{-2} hr^{-1}. During the winter, Schroeder et al. (2005) measured low fluxes (0.09 ± 0.03 ng m^{-2} hr^{-1}) from an agricultural area in Southern Ontario covered in snow. Averaging these fluxes by their respective seasonal time intervals results in an estimated annual average flux from GLB cropland of 2.4 ng m^{-2} hr^{-1}. Several studies have shown that Hg^0 fluxes increase following surface disturbance, however these elevated emissions are temporary and fluxes return to pre-disturbance levels within a week after soil disturbance (Gustin et al. 2003; Eckley et al. 2011). While the results of Carpi and Lindberg (1998) indicate that Hg^0 fluxes from agricultural lands can be elevated during periods of active plowing/harvesting, it is not clear from their study how long the emissions remained elevated. In the annual average flux applied for scaling, the fluxes from the disturbed surfaces from Carpi and Lindberg (1998) were applied over a 6 month period, which may be an overestimation of the emissions during this period depending on how often the

fields are disturbed from farming activities and how long the emissions remained elevated following surface disturbances. Other MM measurements of Hg^0 fluxes on agricultural lands found values ranging from an average autumn diel flux of 0.1 ± 0.2 ng m^{-2} hr^{-1} at an Ontario cropland field (Cobbett and Van Heyst 2007) to an average spring diel flux of 9.67 ng m^{-2} hr^{-1} at a Minnesota cropland field (Cobos et al. 2002). The large range in reported Hg^0 fluxes for croplands does not appear to be related to differences in soil Hg concentrations, which were highest in the Cobbett and Van Heyst (2007) study where the fluxes were the lowest; instead variations in Hg^0 fluxes may reflect varying levels of surface disturbance associated with agricultural activity.

Analysis of GLB Hg^0 evasion (see below) suggests that agricultural lands account for more than 50% of total Hg evasion from the GLB. It is not clear from these studies when and for how long Hg^0 evasion rates are elevated from agricultural lands. Elevated Hg^0 evasion rates also may reflect high rates of carbon mineralization and Hg(II) cycling associated with land disturbance or materials added to agricultural lands. Based on the literature review and the elevated rates associated with this review, there is a clear need for more rigorous evasion studies on agricultural lands, quantifying rates and climatic and landscape level drivers that control evasion rates.

6.2.3 Grasslands

For grasslands/pastures, Schroeder et al. (2005) used both the DFC and MM techniques to measure average diel summertime Hg^0 fluxes in Ontario (3.0 and 1.1 ng m^{-2} hr^{-1} respectively) and Quebec (MM only: 2.9 ng m^{-2} hr^{-1}) and Zhang et al. (2001) used a DFC to measure mid-day summer fluxes from the Upper Peninsula in Michigan (7.6 ± 1.7 ng m^{-2} hr^{-1}). While the values from Zhang et al. (2001) appear much larger than those from Schroeder et al. (2005), this difference is likely due to the fact that the latter considered diel conditions. Assuming the

Gaussian flux distribution the diel flux from Zhang et al. (2001) was estimated to be 2.6 ng m^{-2} hr^{-1}, which is similar to values of Schroeder et al. (2005), suggesting that these measurements are representative of grassland emissions. Ericksen et al. (2006) measured diel fluxes with a DFC from grasslands in Wisconsin and found that some fluxes were similar in magnitude to those of Schroeder et al. (2005) and Zhang et al. (2001) (maximum flux: 3.5 ng m^{-2} hr^{-1}), but overall Ericksen et al. (2006) reported a much lower mean flux of 0.3 ± 0.07 ng m^{-2} hr^{-1} (the season these measurements were conducted is not reported). Their lower flux may be a function of their grassland site being under forest cover and not exposed to direct sunlight, which is not a typical condition for grasslands. As such, an average of the Schroeder et al. (2005) and Zhang et al. (2001) values were used for scaling in the overall GLB analysis (i.e., 2.8 ng m^{-2} hr^{-1}). Because this value represents summer conditions, it was adjusted to be seasonally representative as was described for the agricultural lands resulting in an annual estimated average flux of 2.0 ng m^{-2} hr^{-1}. This value is slightly lower, but of similar magnitude as the fluxes reported for agricultural cropland. Similar rates of Hg^0 evasion are anticipated for agricultural lands and grasslands of the GLB, as both land-covers are exposed to full solar radiation (i.e., limited canopy cover, which can decrease emissions). The slightly lower fluxes from the grasslands may reflect the lower level of disturbance these surfaces encounter relative to croplands.

6.2.4 Urban Lands

Urban areas largely consist of impervious surfaces, such as pavement, and pervious soils. Eckley and Branfireun (2008) used DFCs to measure fluxes from both types of surfaces from several locations from a major urban center within the GLB (Toronto, Ontario). The median fluxes they reported were based on summertime daytime measurements (1.0 and 6.2 ng m^{-2} hr^{-1} for pavement and soil, respectively). Using the Gaussian distribution to estimate diel Hg^0 fluxes,

values of 0.3 and 2.0 ng m^{-2} hr^{-1} for pavement and soil are estimated, respectively. These values are similar to a more intensive diel and seasonal sampling campaign conducted from urban soils and pavement from outside of the GLB (Tuscaloosa, Alabama; Gabriel et al. 2006). Gabriel et al. (2006) found a median annual flux of -0.01 ng m^{-2} hr^{-1} for pavement, and 2.64 ng m^{-2} hr^{-1} for urban soils. The similarity in flux magnitudes may be due to similar soil Hg concentrations between the two sites (Table 6.1, p. 98). The measurements of Eckley and Branfireun (2008) included good spatial coverage. In contrast, Gabriel et al. (2006) characterized temporal variability (which was based on a single location). However, because the magnitude of measurements from these two studies is similar, they have been averaged to obtain values for urban lands of the GLB that are both spatially and temporally representative (pavement: 0.15 and soil: 2.3 ng m^{-2} hr^{-1}). Urban lands of the GLB are assumed to be 40% impervious surfaces and 60% pervious land (Akbari et al. 2003). The relatively few urban evasion studies in the GLB, as well as the spatial heterogeneity noted in Eckley and Branfireun (2008) (i.e., median values at six sample sites in one city ranging from below detection limit to 5.2 ng m^{-2} hr^{-1}), suggests that additional research is needed to better characterize Hg emissions from urban environments.

6.2.5 Wetlands

Of the three surface-air Hg-flux studies for wetlands reviewed, two used DFCs (Poissant et al. 2004; Selvendiran et al. 2008b) while the other applied MM gradients (Lindberg and Meyers 2001). Poissant et al. (2004) compared Hg^0 evasion from a wetland in Quebec during a flooded period with values during a dry period. Diurnal measurements were made during both periods; the median values were calculated from both daytime and nighttime measurements. They found a median Hg^0 flux of 0.83 ng m^{-2} hr^{-1} during the dry period (August to September, 1999), and a median Hg^0 flux of 0.5 ng m^{-2} hr^{-1} during the flooded period (May 2000). Selvendiran et al.

(2008b) found a similar pattern from a riparian zone in the Adirondack region of New York. During flooded conditions, net volatilization was -1.3, -3.9, and -3.6 ng m^{-2} hr^{-1} for spring, summer and fall, indicating deposition; during drier conditions, net volatilization was observed (3.8 ng m^{-2} hr^{-1}). They also evaluated a beaver meadow, estimating an annual Hg^0 evasion flux of 0.52 ng m^{-2} hr^{-1}. This estimate included both seasonal and diurnal measurements from a wetland in close proximity to the GLB, and as a result may be more representative of the annual evasion rate for wetlands in the GLB. Note, however, the differences observed between flooded and dry conditions at different wetlands. Seasonal changes, as well as periods of drought or elevated precipitation, could have considerable effects on Hg^0 evasion rates from wetlands.

6.2.6 Lakes (Inland)

In addition to the MM gradient and DFC methods typically used for Hg^0 evasion work on soils, estimates of evasion from aquatic environments include the use of a purge and trap system (e.g., Chapter 3; O'Driscoll et al. 2003b). While DFC and MM methods measure net Hg^0 exchange, the purge and trap methods measure DGM, and use models to determine air-water Hg^0 exchange. Selvendiran et al. (2009) applied the purge and trap system to estimate Hg^0 evasion from Arbutus Lake in the Adirondacks, New York. They developed an annual estimate of Hg^0 evasion from the lake surface, 0.89 ng m^{-2} hr^{-1}. During the study, mean daytime evasion was 1.6 ng m^{-2} hr^{-1} and mean nighttime evasion was estimated at 0.7 ng m^{-2} hr^{-1}. The value proposed as an annual estimate accounts for diel as well as seasonal variation. Vandal et al. (1991) developed an annual estimate of Hg^0 evasion (0.17 ng m^{-2} hr^{-1}) for seepage lakes in Wisconsin. All other studies provided estimates specific to the study period, or did not define a study period: O'Driscoll et al. (2003a) noted a daytime range of 2.1 to 3.8 ng m^{-2} hr^{-1} during the summer for two lakes in Nova Scotia; Xiao et al. (1991) developed a mean daily estimate of 7.9 ng m^{-2} hr^{-1}

during the warmer season for four lakes in Sweden; Wollenberg and Peters (2009) noted a range of 0.14 to 20.95 ng m^{-2} hr^{-1} from a dimictic lake in eastern Pennsylvania during fall turnover. Of these, the Selvendiran et al. (2009) estimate, which accounts for both diurnal and seasonal variations, was used to represent Hg^0 evasion from inland lakes in the GLB. Of the literature reviewed, Hg^0 evasion estimates for inland lakes exhibit the greatest variability in methodological approach. It is therefore difficult to reconcile values across a region and objectively compare Hg evasion values among different lakes.

6.2.7 Great Lakes

Estimates of gaseous Hg^0 evasion from the surfaces of the Great Lakes have largely been developed using data collected from grab samples that were promptly analyzed for DGM. Four recent studies were reviewed, and the only one not employing grab samples simply estimated gaseous Hg evasion by difference to close a Hg^0 budget (i.e., Rolfhus et al. 2003). That study estimated an annual Hg^0 volatilization rate of 1.0 ng m^{-2} hr^{-1} from Lake Superior. The remaining studies reviewed focused on Lake Superior, Lake Ontario and Lake Michigan.

Jeremiason et al. (2009) estimated evasional Hg^0 fluxes for Lake Superior and Lake Michigan, with annual values of 0.22 and 0.75 ng m^{-2} hr^{-1}, respectively. Vette et al. (2002) also studied Lake Michigan, and found a similar estimate of 0.89 ng m^{-2} hr^{-1}. Due to the more recent observations that are based on DGM measurements, the estimates of Jeremiason et al. (2009) were used to represent Hg^0 evasional flux from both Lake Superior and Lake Michigan in this analysis. As part of an atmospheric deposition study for Lake Ontario, Lai et al. (2007) estimated an annual Hg^0 evasion rate of 0.66 ng m^{-2} hr^{-1}. This was the only report in the literature for Lake Ontario, and was therefore used to represent that lake's annual Hg^0 emission rate. No studies were found for either Lake Huron or Lake Erie. However, since Lake Huron

and Lake Michigan are geologically considered the same body of water (Great Lakes Environmental Research Laboratory 2006), the Lake Michigan Hg^0 evasion rate was used to represent Lake Huron as well. Due to the proximity of Lake Ontario and Lake Erie, the Hg^0 evasion rate for Lake Ontario was used for Lake Erie. More studies on Hg evasion from the Great Lakes would be beneficial, particularly with respect to Lakes Erie and Huron, and also to estimate localized influences of large river discharges and urban centers.

6.3 Relative importance of Hg evasion for the Great Lakes Basin

A GIS approach was utilized to attempt to place estimates of rates of Hg^0 evasion in the context of the Hg dynamics across the GLB. Values of Hg^0 evasion rates for land-cover type were used based on the literature review discussed above. These rates were applied to the distribution of land-cover for the GLB from USGS Global Land Cover Characterization (Table 6.2, p. 107). Due to the limited number of evasion studies that have been conducted for certain land-cover types, land-cover classes have been lumped to describe forests, agricultural lands, grasslands, urban lands, inland waters including lakes, reservoirs, rivers and wetlands; and the individual Great Lakes. Rates of Hg^0 evasion for the GLB are compared with: values of Hg emissions for the US and Canada for 2005; wet Hg deposition for 2002-2008 obtained from the Mercury Deposition Network (Risch et al. 2012b); estimates of Hg dry deposition calculated from the CMAQ model (Bullock and Brehme 2002) for 2001; and forest litterfall Hg deposition in the GLB.

Litterfall Hg deposition was estimated by litter studies conducted by forest type (Demers et al. 2007; Risch et al. 2012a) and GIS forest cover. For the U.S., forest cover type data were available by tree species association classes from the USGS (e.g., maple-birch-beech, spruce-fir,

oak-hickory). Litterfall Hg deposition rates for forest species classes were multiplied by the land area of these classes for the U.S. area of the GLB. Unfortunately a comparable GIS of tree species association classes are not available for Canada. As a result, the forest cover classes in the USGS Global Land Cover Characterization for Canada were used (discussed above for land-cover classes), which include hardwood, conifer and mixed forest cover classes. The mean litterfall Hg deposition reported in Risch et al. (2012a) was used for conifer and mixed forest classes. It was assumed in the GLB in Canada that the hardwood forest class is largely comprised of maple-birch-beech forest class and therefore the data for that forest association class in Risch et al. (2012a) was selected. Values of litterfall Hg deposition for forest species association classes in the U.S. and the three forest cover classes in Canada were summed. Note that forest lands represent 37% of the Great Lakes watershed area (Table 6.2). The total litterfall Hg deposition estimated for forest lands was prorated to the entire GLB. Total Hg deposition was estimated as the sum of wet Hg deposition, dry Hg deposition and litterfall Hg deposition (Driscoll et al. 2007a).

Table 6.2 Area of land-cover types, areal Hg evasion rate for land-cover type, and total and percentage of Hg evasion by land-cover type for the Great Lakes Basin.

Land-cover	Area		Hg Evasion Rate		Total Hg Evasion ($kg\ yr^{-1}$)	Percentage of Total Hg Evasion
	(km^2)	(% of total)	($\mu g\ m^{-2}\ yr^{-1}$)	($ng\ m^{-2}\ hr^{-1}$)		
Urban	9,420	1	12.6	1.4	120	1.5
Agricultural	202,600	27	21	2.4	4,260	55.0
Grassland	198	0.03	17.5	2.0	35	0.4
Forest	277,700	37	7.0	0.8	1,900	25.1
Inland waters	24,200	3	7.8	0.9	190	2.4
Great Lakes	244,160	32	4.9	0.6	1,190	15.4
Total	760,000	100	10.2	1.2	7,700	100

This analysis suggests an overall Hg^0 evasion for the GLB of about 7.7 Mg yr^{-1}, corresponding to an areal rate of 10.2 μg m^{-2} yr^{-1} (Tables 6.2 and 6.3, pp. 106 and 108, respectively). Total Hg^0 evasion is distributed among the various land-cover types (Table 6.2, p. 107; Figure 6.1, p. 110). As the areal evasion rates reported in the literature for urban lands, agricultural lands and grasslands are greater than the other land-cover types and the region as a whole, these land-cover types had a disproportionate contribution to the total emissions. Evasion from agricultural lands, grasslands and urban lands is estimated to have contributed 55%, 0.4% and 1.5% to the total, respectively. Forest land contributed a relatively large fraction of total Hg^0 evasion (25.1%) due to its large area of the GLB. Inland waters and the Great Lakes also contributed to the total Hg^0 evasion of the GLB (2.4 and 15.4%, respectively). It appears that areal evasion rates from inland waters (7.8 μg m^{-2} yr^{-1}) are somewhat greater than the Great Lakes (4.9 μg m^{-2} yr^{-1}). The lower value for the Great Lakes is in part due to lower areal rates for Lake Superior (1.9 μg m^{-2} yr^{-1}).

Total direct anthropogenic Hg emissions for 2005 for the GLB were 10.2 Mg yr^{-1}, which corresponds to an areal flux of 13.4 μg m^{-2} yr^{-1} across the entire GLB (Table 6.3, p. 109). Of these emissions about 60% are as Hg^0 and 40% occurred as oxidized Hg. The Hg emissions in the GLB represent 8.8% of the total anthropogenic Hg emissions for the U.S. and Canada (115.3 Mg yr^{-1}). The Great Lakes themselves are 32% of the area of the GLB. As a result of this relatively large fraction of open water area, the total and areal fluxes of anthropogenic Hg emissions give the appearance of being relatively low. Note however, there are numerous Hg emission sources in close proximity to the GLB. As 50, 100 and 200 km buffers adjacent to the GLB are considered, there is a considerable increase in total Hg emissions to a value of 30.2 Mg yr^{-1} for the GLB plus a 200 km buffer or 26.2% of the Canadian and U.S. total Hg emissions (Table 6.3, p. 109). Increasing the buffer area from 50 to 100 and to 200 km around the GLB

Table 6.3 Comparison of rates of Hg evasion estimated for the Great Lakes Basin with direct total Hg emissions (including Hg^0 and oxidized [ox] Hg), wet, dry and litter Hg deposition. Note that total Hg deposition is the sum of wet, dry and litter deposition. Because many emission sources are proximate to the Great Lakes Basin also included are direct total Hg emissions for the GLB plus for the lands within 50, 100 and 200 km buffer areas. Note that areal fluxes are prorated across the entire GLB (plus any buffer area), including the Great Lakes.

Flux	**Total Hg flux (kg yr^{-1})**	**Areal Hg flux (µg m^{-2} yr^{-1})**
Evasion	7,700	10.2
Direct anthropogenic emissions	10,185 (ox 4,100, Hg^0 6,100)	13.4
Direct emissions with 50 km buffer	14,608 (ox 5,200, Hg^0 9,500)	14.2
Direct emissions with 100 km buffer	19,200 (ox 7,500, Hg^0 11,700)	15.2
Direct emissions with 200 km buffer	30,200 (ox 12,900, Hg^0 17,300)	17.1
Wet deposition	6,100	8.1
Dry deposition	7,400	9.8
Litter deposition	2,400	3.1
Total deposition	15,900	21.0

direct, increases the areal fluxes of total anthropogenic Hg emissions over these areas from 14.2 to 15.2 to 17.1 µg m^{-2} yr^{-1}, respectively (Table 6.3), demonstrating the importance of emission sources adjacent to the Great Lakes watershed. Note that these proximate emission sources are highly relevant to Hg dynamics for the GLB because they are within the spatial scale for deposition of oxidized species of Hg emissions (reactive gaseous Hg and particulate Hg; Driscoll et al. 2007b). Within the GLB plus the 200 km buffer region, emissions of oxidized Hg are 12.9 Mg yr^{-1}, or 43% of total Hg emissions. This pattern indicates that regional and local scale Hg emissions are undoubtedly important to the ecosystem effects of Hg deposition for the GLB (Drevnick et al. 2012). For the GLB, direct anthropogenic Hg emissions are somewhat

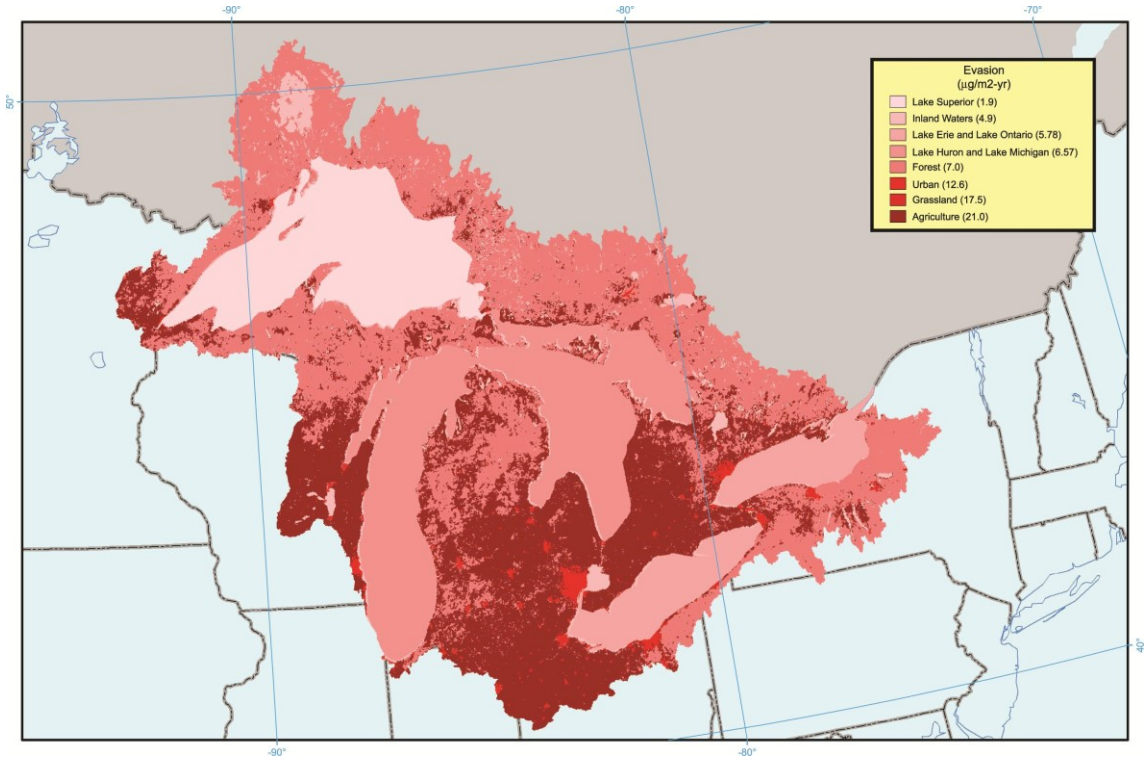

Figure 6.1 Map of the Great Lakes Basin showing rates of elemental mercury evasion.

greater but comparable in magnitude to this study's estimate of Hg re-emissions indicating that re-emission (i.e., evasion) is an important pathway of Hg to the atmosphere.

Rates of Hg^0 evasion are found to be less than total atmospheric Hg deposition, within the uncertainty of this analysis. From the MDN, 6.1 Mg wet Hg deposition for the GLB, or an areal rate of 8.1 µg m^{-2} yr^{-1}, are estimated. This input is somewhat less than this study's estimate for Hg^0 evasive losses. Estimated dry Hg deposition from USEPA CMAQ simulations for 2001 is 7.45 Mg yr^{-1} or 9.8 µg m^{-2} yr^{-1}, somewhat greater than the estimate of wet Hg deposition for the GLB. The estimate of litterfall Hg deposition for forest lands of the Great Lakes watershed generated from this literature review is 2.37 Mg yr^{-1}, for an areal rate of 8.3 µg m^{-2} yr^{-1}. As forest cover is 36%, this flux is prorated to 3.1 µg m^{-2} yr^{-1}over the entire GLB. The sum of the estimates of these three deposition fluxes is 15.95 Mg yr^{-1} or 21.0 µg m^{-2} yr^{-1}, more than double

the estimate of evasion Hg losses. Quémerais et al. (1999) observed fluvial Hg losses for Lake Ontario of 0.112 Mg yr^{-1} for 1995 to 1996, suggesting a total fluvial Hg loss of approximately 0.15 μg m^{-2} yr^{-1} from the entire GLB. In contrast, I estimate a fluvial outflow of THg of 0.068 Mg yr^{-1} from Lake Ontario or 0.09 μg m^{-2} yr^{-1} (Chapter 5) for 2008-2010, approximately a decade after Quémerais et al. (1999). This marked decrease in THg outflow shows the response of the GLB and Lake Ontario to recent decreases in Hg inputs. This analysis also indicates that the GLB is currently a net sink for atmospheric inputs of Hg.

7. Recommendations for Future Work

Considerable research has been conducted on the Seneca River. However, prior to the work reported here, there was no information on Hg transport and transformations in the river despite its fluvial connection to Hg-contaminated Onondaga Lake. The database that exists as a result of this work was generated prior to the commencement of remedial activities at Onondaga Lake intended to address the severe Hg contamination in the lake. During this study, it was estimated that Onondaga Lake contributed an additional 15% to the fluvial Hg load of the Seneca River. A future sampling and analysis program is therefore recommended to assess the impacts of Onondaga Lake remedial activities on Hg levels in the Seneca River.

A common, recurring theme observed in this research and throughout the literature is that patterns of land-use and distribution in a watershed play a significant role in Hg speciation and transport. More specifically, the relative amounts of different land-cover types are not the only important aspect driving land-cover effects on Hg fate and transport. The location of different types of land-cover relative to the river are at least as important, as noted in this study with the down-river tracts of forested land in the Humber and Credit Rivers potentially serving as THg_P sinks, and the down-river tracts of agricultural land immediately adjacent to the Black River potentially serving as a THg_P source. Future studies addressing the effects of watershed land-use on riverine Hg fate and transport should consider land-use immediately adjacent to the river, and be cognizant of the fact that some land-cover patterns may escape the resolution of available land-cover models. For example, wetlands may exist immediately bordering a river and be too small to be resolved by commonly available land-cover databases. However, wetlands are key sources of MeHg and can also serve to increase THg_D levels, thereby increasing the fraction of bioavailable Hg in waters.

In addition to watershed land-cover controls on Hg, it was observed that in-river physical characteristics can have important effects on the mass transport of Hg species. An example of anthropogenic in-river characteristics occurs in the Trent River, where concentrations of THg_P were lower than expected. The Trent River is heavily impounded in the last 25 km prior to discharging into Lake Ontario, and the impoundments likely promote THg_P deposition. A natural example of in-river characteristics is observed in the Seneca River, where intervening Cross Lake supports removal of over 65% of the mass flux of Hg from the Seneca River. This signature of reduced Hg flux is sustained over 60 km downriver, past the Three Rivers junction to the outlet of the Oswego River. Mercury flux increases somewhat between the outlet of Cross Lake and the mouth of the Oswego River, likely due to inputs from Onondaga Lake and the Oneida River, but is still approximately 40% lower at the mouth of the Oswego River (8.0 kg yr^{-1}) than at the outlet of Cross Lake (13.3 kg yr^{-1}). Cross Lake therefore significantly reduces the Hg load of this river to Lake Ontario. The data collected in this study support a robust assessment of the effects of Cross Lake on Hg transport in the Seneca River. However, the same assessment cannot be made for the effects of impoundments on Hg transport in any of the study rivers. It is recommended that future studies be conducted immediately above and below impoundments to quantify their effects on Hg transport and speciation. Such studies would be particularly informative in rivers where existing impoundments are proposed for decommissioning and removal. It is plausible to assume that impoundments serve as a sink for fluvial THg_P.

Budget constraints and resource limitations make it important to focus investigations on the more significant components of a mass balance. Results of this study suggest that increases in light penetration as a result of zebra mussel metabolism may increase volatilization (i.e., loss) of Hg

from the Seneca River. However, confounding factors during field analysis (e.g., weather, canopy cover) introduced uncertainty to estimates of the effects of zebra mussel metabolism on Hg^0 volatilization. Moreover, estimates of atmospheric Hg deposition were found to be slightly larger, though similar in magnitude, to average Hg^0 volatilization rates from the Seneca River. Based on the level of effort required to measure Hg^0 volatilization in the field, these activities are not recommended unless Hg^0 volatilization is presumed to be a large component of an ecosystem's Hg mass balance. In the case of the Seneca River, the surface area does not allow for significant volatilization relative to the fluvial mass transport of Hg. The results of the work presented here are helpful in showing that volatilization does not represent a significant loss mechanism of Hg from rivers of this size. In addition, it is worth noting that application of the Hg^0 volatilization rate generated from a literature review for inland waters (reported in Chapter 6) over the volatilization rate measured in the field would have had no measurable effect on the reach-by-reach mass balance estimates reported for the Seneca River in Chapter 3. Elemental Hg volatilization would represent a much more significant portion of a mass balance for a quiescent system with large surface area (e.g., a lake or wetland), and such a system would be a more appropriate application for such intensive field efforts.

The importance of event sampling was underscored by the Lake Ontario tributary study. Total Hg concentrations were observed to increase 5-fold over average concentrations in response to elevated runoff from snow-melt or precipitation. The THg flux during such events can represent a significant portion of the yearly flux. Failure to characterize the response of THg transport to such events can result in severe underestimation of THg flux to receiving waters. Future studies should target several runoff events, with a concentrated rate of sample collection prior to the

event, during the rising limb, and following the peak, to adequately assess ecosystem response and support accurate flux estimates.

When viewed independently, the components of atmospheric Hg exchange (Hg_P, Hg(II), and Hg^0 deposition, and Hg^0 volatilization) are the largest factors of the Hg mass balance in Lake Ontario. Similar results have been observed in other Great Lakes (e.g., Mason and Sullivan 1997; Landis and Keeler 2002; Rolfhus et al. 2003). However, when summed to represent net atmospheric Hg exchange (i.e., 123 kg yr^{-1} deposition), these values are comparable to fluvial loading from the Niagara River (i.e., 154 kg yr^{-1}). Prior to the research conducted as part of this dissertation, the total fluvial load of Hg was largely unquantified. Other researchers have developed robust mathematical models to estimate the transport and transformations of Hg within Lake Ontario (Ethier et al. 2012). It is recommended that the results of the Lake Ontario sampling effort reported in this dissertation be integrated into these models and used for further calibration and verification.

It is recommended that future Hg studies be conducted on Lakes Huron and Erie, as there is a striking paucity of Hg data on these systems. Further, although open-water studies may provide important estimates of whole-lake Hg concentrations in any or all of the Great Lakes, it is recommended that future Hg studies conducted on any of the Great Lakes focus on near-shore areas. These areas support a significant amount of the lakes' biota. As a result of this and the more accessible nature of near-shore areas, they are the most likely pathways of human and wildlife exposure to Hg. Although the fluvial Hg loads to Lake Ontario from the adjacent study watersheds are small relative to the Niagara River and atmospheric inputs, tributaries have strong controls on nearshore areas, and tributary inputs appear to remain in the nearshore zones rather

than being exported into open waters of the lake (Howell et al. 2012; Makarewicz et al. 2012a). As noted in this dissertation, riverine Hg inputs are largely particulate-related and are likely to settle in near-shore areas, where secondary processes such as resuspension, remineralization, and methylation will then play a much more important role (Hurley et al. 1998b). In addition, Makarewicz et al. (2012b) noted a thin band of water with unique chemistry isolated to the nearshore zone of Lake Ontario, specifically in late spring and summer. Rolfhus et al. (2003) suggested tributary MeHg loading is possibly more available to biota, as they noted elevated Hg concentrations in biota during the spring season. Rolfhus et al. (2003) also noted that MeHg is diffuse in open waters of Lake Superior, yet at times orders of magnitude higher in nearshore zones. It is therefore prudent to focus future research efforts in these areas.

In addition to a focus on near-shore zones, the variability noted in Hg concentrations within and among the watersheds of this study underscores the importance of an aquatic sampling and analysis plan for any study intending to evaluate Hg dynamics. Dependence on land-cover characteristics or surrogate measures to accurately estimate Hg transport characteristics is unlikely to be reliable. Though land-cover and surrogate measures may be used to develop plausible hypotheses and assumptions related to watershed Hg export, the results of this study indicate little reliable predictive relationships between them and estimates of Hg dynamics.

Efforts to further improve the efficiency, accuracy, and precision of ultra-low level (i.e., picogram per liter; pg L^{-1}) MeHg analysis would be welcome and would support further research on the cycling of this key form of Hg. The process has been greatly simplified in the Syracuse University laboratory, yet it is still apparent that limitations in detection limits as well as evidence of demethylation hindered estimation of MeHg flux in this study, and some of the

available data suggested conflicting results: MeHg was found to be almost exclusively associated with the aqueous phase for the Lake Ontario tributary study, but was observed to be almost exclusively associated with the particulate phase in samples collected from the Seneca River. Improvements in detection limits, at a minimum, would serve to confirm this observation, and may provide insight into any potential causes.

The analysis presented in this dissertation suggests that the GLB is currently a net sink for atmospheric inputs of Hg. Interestingly, though atmospheric Hg exchange is inconsequential when viewed relative to the smallest scale of the research presented here (i.e., reaches of the Seneca River), it becomes the most important element of any mass balance at larger scales (i.e., watersheds, Lake Ontario, GLB). In the GLB, the research presented here determined that direct anthropogenic Hg emissions (e.g., incinerators, coal-fired power plants) are similar in magnitude to estimates of Hg re-emissions (i.e., Hg^0 volatilization, or evasion), indicating that re-emission is an important pathway of Hg to the atmosphere. Based on this importance, methodological standardization of Hg^0 volatilization measurements is needed, and additional studies utilizing this standardized approach should be conducted on all significant land-cover surfaces in the GLB, including snow, agricultural lands, urban lands, inland lakes, and the Great Lakes (particularly Lakes Erie and Huron).

The data presented in this dissertation represent the largest Hg database for the Lake Ontario basin, and are a result of the first binational effort to develop a Hg dataset for Lake Ontario. The findings discussed provide insight into Hg fate and transport within the Seneca River, and have allowed for the development of a Hg budget for the Lake Ontario basin. It is suggested that the results from the Lake Ontario portion of this project be used in support of the development of a

more comprehensive proposal to investigate Hg dynamics in the Lake Ontario basin. For future studies it will be important to evaluate variation between wet and dry years. Further, a spatially robust sediment sampling program involving dated sediment cores would be helpful to improve the current understanding of Hg sedimentation and re-suspension in the lake.

8. Conclusions

8.1 Seneca River

Total particulate Hg is the dominant form of Hg in the Seneca River. In addition, it is clear that Cross Lake serves an important role for Hg transport in the Seneca River. Total Hg flux from the Seneca River to the Oswego River, and ultimately Lake Ontario, is reduced by approximately 65% due to the loss of THg_P to intervening Cross Lake, presumably largely via sedimentation. Throughout the study reach, Hg is largely associated with the particulate fraction (i.e., greater than 50%). This association facilitates removal via settling dynamics in intervening quiescent systems (e.g., Cross Lake). Methylmercury concentration and %MeHg significantly increase across the reach between B409 and B317 (0.048 ng L^{-1} to 0.087 ng L^{-1}, and 4% to 9%, respectively), likely due to zebra mussel metabolism. However, THg_P concentrations are unaffected by the zebra mussels. Further, the Onondaga Lake outlet likely contributes some Hg to the Seneca River. Although mean concentrations of THg are not significantly different between sites upstream and downstream of the outlet, flux estimates suggest an approximate 15% increase in THg load to the river between B317 and B224 (i.e., upstream and downstream of the Onondaga Lake outlet). No other significant point sources exist over this reach of the river. Elemental Hg volatilization rates are limited by solar radiation and water temperature, and it appears that zebra mussels may dampen these limitations via clearing of the water column. Regardless of any effect of zebra mussels on Hg^0 volatilization, atmospheric Hg exchange represents a negligible component of a Hg mass balance for river reaches. The Seneca River watershed is a net sink for atmospheric inputs of Hg at a rate of 42 kg yr^{-1}, and the watershed efficiently retains this Hg (>85%), while exporting approximately 5 kg yr^{-1} via the Three Rivers confluence.

8.2 Lake Ontario Sub-Watershed Analysis

Watershed characteristics have complex and mixed effects on Hg dynamics in the study tributaries. Total particulate Hg accounts for the bulk of the variability observed in THg concentrations; Hg associated with the dissolved fraction is less variable, and makes up a smaller fraction of the total Hg load from Lake Ontario's immediate watershed (i.e., not including the Niagara River). As a result, Hg entering Lake Ontario from tributaries is strongly influenced by the partitioning between Hg and particles, and therefore by any phenomena that affect particle transport. Mixed land-use among most of the study watersheds confounds discernible patterns. A stronger affinity of both Hg and MeHg for the particulate phase is noted in some tributaries draining watersheds that are more forest-dominated, though in general MeHg is more associated with the dissolved phase in all study tributaries. Mercury fractionation is similar across most watersheds, though localized land-cover patterns appear to have an effect on Hg speciation. For example, significant amounts of agriculture or urban land-cover adjacent to tributaries favor higher particulate fractions, though forested reaches may serve to attenuate such signatures. Wetlands and forested reaches may also serve to enrich the particle-Hg concentrations (i.e., C_p).

Physical characteristics within the tributaries also seem to affect speciation. Total dissolved Hg fractions are favored in heavily impounded tributaries such as the Trent, while THg_P fractions are favored in shallower, swifter flowing tributaries such as the Ganaraska, though both watersheds exhibit similar land-cover patterns. Land-cover did not prove to be a reliable predictor of PE in the study watersheds, though weak, positive relationships were noted between percent wetland cover and log-transformed values of THg PE and MeHg PE. On the other hand, percent wetland cover was a strong predictor of log K_d for both THg and MeHg, and percent open water was also linked to MeHg log K_d (positive relationships in each case). These positive relationships are

counter to what was expected, as they suggest a greater affinity for the particulate phase occurs with greater coverage of wetland or open water.

8.3 Lake Ontario Mass Balance

For many contaminants, the Niagara River is the main source to Lake Ontario (Oliver 1984; Oliver et al. 1989). In contrast, atmospheric exchange appears to be an important input and loss of Hg to and from Lake Ontario. The data collected in this study represent the most comprehensive dataset for Hg in Lake Ontario tributaries. Given the uncertainties and year-to-year variation, atmospheric and fluvial fluxes of Hg to and from the lake are similar in magnitude. Lake Ontario is clearly a net sink for Hg inputs (R_{total} = 0.35; Table 5.2, p. 88). The Hg fluxes from tributaries are largely driven by river discharge. Therefore, significant variation in inflows from tributary watersheds as a result of wet or dry years may result in widely varying Hg loads. In addition, atmospheric emissions of Hg for the Lake Ontario source area and atmospheric Hg deposition have been decreasing since the mid-1980s (Drevnick et al. 2012). These changes have driven decreases in atmospheric Hg loading but also have likely contributed to decreases in riverine inputs. The marked decreases in sediment Hg deposition for Lake Ontario and the other lower Great Lakes and decrease in fluvial losses of THg from Lake Ontario are also suggestive of decreases in point Hg inputs.

Lake Ontario is clearly not at steady-state with respect to Hg inputs. With anticipated future decreases in Hg emissions from the Mercury and Air Toxics Standards and possibly the United Nations Environment Programme (UNEP) Minamata Hg treaty, it is hypothesized that atmospheric Hg inputs will eventually decrease to values below fluvial inputs. The long hydraulic residence time of the lake (i.e., 6-8 years) and the dynamic physical nature and

potential bioavailability of Hg provides for complex cycling patterns that challenge a simplistic input-output view of Lake Ontario (Ethier et al. 2012; Kaur et al. 2012). The data presented here provide robust Hg input estimates for further characterization of the response of the lake to decreases in, and the shifting nature of, Hg inputs.

8.4 Great Lakes Basin Evasion Synthesis

Rates of Hg^0 evasion have been synthesized from a comprehensive literature review to develop an estimate of annual Hg^0 evasion from the GLB. This literature review identifies the need for standardized analytical and reporting methods for Hg^0 evasion measurements. In addition, specific land-cover areas would benefit from increased research efforts, particularly agricultural lands, where few studies have been conducted, and Lakes Erie and Huron, which appear to be unstudied relative to Hg^0 evasion. Some difficulty arises in synthesizing Hg^0 evasion rates from the literature due to seasonal and diel changes in evasion rates, coupled with methodological variations between studies. There is a need for additional measurements of Hg^0 evasion in the winter and from snowpack. Within the GLB, areal evasion rates for urban, agricultural, and grasslands are greater than other land-cover types, and the estimate for evasion in the region as a whole. Agricultural, forest, and the Great Lakes together contribute approximately 95% of the region's total Hg evasion, due in large part to the high areal coverage of the Great Lakes and forest, and both coverage and evasion rates of agricultural land. In conjunction with mass balance elements of the GLB, this analysis indicates that the GLB is a net sink for atmospheric inputs of Hg.

9. Appendices

9.1 Seneca River Data

Table 9.1 Analytical results of mercury sampling at Navigational Buoy 430 in the Seneca River (43.100129, -76.498893).

Sample Date	THg (ng L^{-1})	THg_D (ng L^{-1})	MeHg (ng L^{-1})
2007			
6/27/2007	4.19	—	0.07
7/25/2007	4.19	—	0.09
8/8/2007	2.83	0.63	0.09
8/29/2007	1.49	0.28	0.06
9/12/2007	2.98	0.16	0.08
9/26/2007	1.18	0.12	0.04
2008			
6/25/2008	2.65	—	—
7/8/2008	3.50	0.99	0.15
7/22/2008	5.41	0.72	—
8/5/2008	2.31	0.42	0.11
8/21/2008	2.71	—	0.09
9/5/2008	3.99	0.87	0.04
9/18/2008	1.71	0.37	0.41
9/30/2008	1.82	0.46	0.03
2009			
6/16/2009	3.39	0.29	ND (0.02)
6/30/2009	3.23	1.00	—
7/14/2009	2.97	0.41	0.027
7/28/2009	3.17	0.42	0.073
8/11/2009	9.08	1.57	0.080
8/25/2009	4.00	0.56	0.071
9/10/2009	2.38	0.54	ND (0.02)
9/22/2009	1.40	0.48	—

Notes:

1. ND is non-detect. Detection limit provided in parentheses.
2. "—" denotes insufficient sample volume for analysis or loss of sample.

Table 9.2 Analytical results of mercury sampling at Navigational Buoy 409 in the Seneca River (43.104011, -76.445517).

Sample Date	THg (ng L^{-1})		THg_D (ng L^{-1})		MeHg (ng L^{-1})	
	1-m	3-m	1-m	3-m	1-m	3-m
2007						
6/27/2007	0.75	2.18	—	—	0.04	0.09
7/25/2007	1.87	1.08	—	—	0.02	0.02
8/8/2007	1.07	1.20	0.51	0.47	—	0.12
8/29/2007	1.31	1.14	0.42	0.29	0.07	0.06
9/12/2007	0.99	1.04	0.09	0.18	0.05	0.07
9/26/2007	0.48	0.58	0.16	0.11	0.04	0.05
2008						
6/25/2008	—	1.30	—	1.28	—	—
7/8/2008	0.98	1.47	0.85	0.60	0.11	0.02
7/22/2008	1.54	1.73	0.54	0.93	—	—
8/5/2008	1.03	1.31	0.88	0.95	0.07	0.06
8/21/2008	1.37	1.40	—	—	0.02	0.02
9/5/2008	0.39	1.23	ND (0.20)	0.54	ND (0.02)	0.12
9/18/2008	1.17	1.26	—	1.15	0.09	0.06
9/30/2008	1.14	2.16	0.49	0.49	0.05	—
2009						
6/16/2009	0.83	1.20	ND (0.20)	0.25	0.01	0.03
6/30/2009	1.73	2.71	0.51	0.81	—	—
7/14/2009	1.33	1.49	0.34	0.75	0.03	0.02
7/28/2009	0.74	1.41	0.35	0.33	0.01	0.03
8/11/2009	1.68	1.59	0.56	0.54	0.04	0.03
8/25/2009	1.25	1.77	0.53	0.55	0.06	ND (0.02)
9/10/2009	0.90	1.04	0.52	0.55	ND (0.02)	ND (0.02)
9/22/2009	1.04	1.31	0.54	0.66	0.02	—

Notes:

1. ND is non-detect. Detection limit provided in parentheses.
2. "—" denotes insufficient sample volume for analysis or loss of sample.

Table 9.3 Analytical results of mercury sampling at Navigational Buoy 317 in the Seneca River (43.144022, -76.312571).

Sample Date	THg (ng L^{-1})	THg_D (ng L^{-1})	MeHg (ng L^{-1})
2007			
6/27/2007	1.06	—	0.06
7/25/2007	0.70	—	0.07
8/8/2007	0.88	0.56	0.18
8/29/2007	0.70	0.33	0.05
9/12/2007	1.15	0.16	0.13
9/26/2007	0.71	0.12	0.05
2008			
6/25/2008	1.51	0.67	—
7/8/2008	1.81	1.43	0.11
7/22/2008	0.83	0.74	—
8/5/2008	0.81	0.61	0.09
8/21/2008	0.95	—	0.09
9/5/2008	0.89	0.44	0.13
9/18/2008	0.73	0.51	0.20
9/30/2008	1.40	ND (0.20)	0.04
2009			
6/16/2009	0.56	0.24	—
6/30/2009	1.15	0.47	—
7/14/2009	1.08	0.40	0.03
7/28/2009	0.68	0.39	0.09
8/11/2009	3.55	0.66	0.09
8/25/2009	1.36	0.71	0.13
9/10/2009	1.66	0.57	ND (0.02)
9/22/2009	1.63	0.65	ND (0.02)

Notes:

1. ND is non-detect. Detection limit provided in parentheses.
2. "—" denotes insufficient sample volume for analysis or loss of sample.

Table 9.4 Analytical results of mercury sampling at Navigational Buoy 224 in the Seneca River (43.197093, -76.283007).

Sample Date	THg (ng L^{-1})		THg_D (ng L^{-1})		MeHg (ng L^{-1})	
	1-m	3-m	1-m	3-m	1-m	3-m
2007						
6/27/2007	0.91	0.85	—	—	0.02	0.03
7/25/2007	10.33	1.54	—	—	0.02	0.13
8/8/2007	1.17	1.83	0.56	0.32	—	0.30
8/29/2007	0.86	0.81	0.27	0.42	0.10	0.12
9/12/2007	1.67	2.14	0.17	0.19	0.06	0.12
9/26/2007	0.66	1.45	0.17	0.15	0.09	ND (0.02)
2008						
6/25/2008	—	1.55	—	1.01	—	0.12
7/8/2008	1.00	3.57	1.07	0.70	0.04	0.08
7/22/2008	1.20	1.68	1.31	0.50	—	—
8/5/2008	0.71	0.74	0.24	0.44	0.13	0.15
8/21/2008	0.47	0.72	—	—	0.06	0.08
9/5/2008	1.09	0.44	0.9	—	0.02	0.03
9/18/2008	0.79	1.40	1.07	0.48	0.06	0.09
9/30/2008	1.20	0.90	0.41	0.40	0.06	0.04
2009						
6/16/2009	0.84	0.62	0.25	0.29	ND (0.02)	0.03
6/30/2009	0.96	2.00	0.92	0.59	—	—
7/14/2009	0.85	0.96	0.63	0.45	0.09	0.12
7/28/2009	0.72	0.78	0.85	0.60	0.02	—
8/11/2009	3.05	3.36	0.96	0.66	0.07	0.06
8/25/2009	0.82	0.59	0.72	0.30	0.08	0.09
9/10/2009	0.89	0.89	0.76	0.54	0.04	ND (0.02)
9/22/2009	0.78	0.96	0.59	0.77	0.02	0.05

Notes:

1. ND is non-detect. Detection limit provided in parentheses.
2. "—" denotes insufficient sample volume for analysis or loss of sample.

9.2 Lake Ontario Tributary Data

Table 9.5 Analytical results of mercury sampling at St. Lawrence River. Samples collected and analyzed by Syracuse University from Cape Vincent Public Boat Launch in Cape Vincent, NY (44.133256, -76.322039).

Sample Date	THg ($ng\ L^{-1}$)	THg_D ($ng\ L^{-1}$)	MeHg ($ng\ L^{-1}$)	$MeHg_D$ ($ng\ L^{-1}$)	TSS ($mg\ L^{-1}$)	DOC ($mg\ L^{-1}$)
6/17/2009	0.43	0.55	0.08	0.12	0.51	2.25
7/1/2009	0.29	0.51	0.08	0.06	0.22	2.40
7/21/2009	0.22	0.28	0.12	0.14	0.81	2.02
8/12/2009	0.70	0.65	0.35	0.19	ND (0.10)	2.03
8/27/2009	0.56	0.58	—	ND (0.02)	ND (0.10)	2.20
9/10/2009	0.29	0.35	—	ND (0.02)	0.74	1.97
9/23/2009	0.20	0.39	—	0.27	0.84	2.17
10/8/2009	0.22	0.26	—	ND (0.02)	ND (0.10)	2.02
10/21/2009	0.35	0.40	ND (0.02)	ND (0.02)	ND (0.10)	2.70
11/11/2009	ND (0.20)	0.21	0.15	0.12	0.23	2.16
11/25/2009	0.20	0.25	0.03	0.05	ND (0.10)	2.05
12/9/2009	ND (0.20)	0.27	0.14	0.15	0.34	—
12/23/2009	0.20	0.14	—	0.11	ND (0.10)	—
1/13/2010	0.23	0.38	0.08	0.10	ND (0.10)	1.82
1/27/2010	0.35	0.30	ND (0.02)	ND (0.02)	0.61	2.09
2/10/2010	0.38	0.20	0.04	ND (0.02)	ND (0.10)	1.88
2/24/2010	0.51	0.27	ND (0.02)	ND (0.02)	0.81	2.22
3/10/2010	0.73	ND (0.20)	ND (0.02)	0.30	ND (0.10)	1.83
3/24/2010	0.50	0.32	ND (0.02)	0.03	ND (0.10)	1.86
4/2/2010	ND (0.20)	ND (0.20)	0.03	0.03	ND (0.10)	1.87
4/26/2010	ND (0.20)	0.27	0.07	0.08	ND (0.10)	1.92
5/12/2010	ND (0.20)	ND (0.20)	0.03	0.03	ND (0.10)	1.83
5/26/2010	ND (0.20)	ND (0.20)	0.04	0.02	ND (0.10)	2.05

Notes:

1. ND is non-detect. Detection limit provided in parentheses.
2. "—" denotes insufficient sample volume for analysis or loss of sample.
3. TSS is total suspended solids.
4. DOC is dissolved organic carbon.

Table 9.6 Analytical results of mercury sampling at Black River. Samples collected and analyzed by Syracuse University from the Vanduzee St Bridge, Watertown, NY (43.985309, -75.924580).

Sample Date	THg ($ng\ L^{-1}$)	THg_D ($ng\ L^{-1}$)	MeHg ($ng\ L^{-1}$)	$MeHg_D$ ($ng\ L^{-1}$)	TSS ($mg\ L^{-1}$)	DOC ($mg\ L^{-1}$)
6/17/2009	1.77	1.36	0.18	0.26	4.48	4.79
7/1/2009	2.45	1.57	0.23	ND (0.02)	2.34	4.47
7/21/2009	2.76	1.87	—	0.25	3.12	5.96
8/12/2009	2.51	1.85	0.43	0.36	1.10	5.44
8/27/2009	2.53	2.11	ND (0.02)	0.09	2.53	5.08
9/10/2009	6.48	1.72	0.09	0.11	1.06	4.74
9/23/2009	1.25	1.23	—	0.09	1.34	4.22
10/8/2009	3.54	1.04	—	ND (0.02)	6.30	5.69
10/21/2009	1.94	1.51	ND (0.02)	0.08	1.60	5.17
11/12/2009	1.56	1.16	0.08	0.03	0.25	5.10
11/25/2009	3.09	1.60	ND (0.02)	0.02	1.87	4.88
12/9/2009	2.78	1.52	ND (0.02)	ND (0.02)	3.98	—
12/23/2009	2.00	1.17	0.20	0.05	1.19	—
1/13/2010	1.19	0.91	0.05	0.06	1.11	3.42
1/27/2010	6.91	1.30	ND (0.02)	ND (0.02)	72.49	4.24
2/10/2010	1.46	1.09	—	ND (0.02)	ND (0.10)	3.95
2/24/2010	1.24	0.92	ND (0.02)	0.07	0.64	3.47
3/10/2010	1.13	0.76	ND (0.02)	0.10	1.12	3.38
3/24/2010	4.16	1.56	0.06	ND (0.02)	21.88	4.39
4/2/2010	1.90	1.43	0.07	0.06	2.28	3.85
4/26/2010	1.65	1.33	0.13	0.12	1.20	3.62
5/12/2010	2.71	2.09	0.14	0.15	5.40	4.70
5/26/2010	1.46	0.97	0.04	0.08	1.42	3.89

Notes:

1. ND is non-detect. Detection limit provided in parentheses.
2. "—" denotes insufficient sample volume for analysis or loss of sample.
3. TSS is total suspended solids.
4. DOC is dissolved organic carbon.

Table 9.7 Analytical results of mercury sampling at Salmon River. Samples collected and analyzed by Syracuse University from the NYS DEC public fishing area off Rt. 2A in Pulaski, NY (43.550032, -76.093674).

Sample Date	THg ($ng\ L^{-1}$)	THg_D ($ng\ L^{-1}$)	MeHg ($ng\ L^{-1}$)	$MeHg_D$ ($ng\ L^{-1}$)	TSS ($mg\ L^{-1}$)	DOC ($mg\ L^{-1}$)
6/17/2009	1.43	1.20	0.16	0.20	0.82	3.27
7/1/2009	1.54	1.37	0.11	ND (0.02)	0.98	2.86
7/21/2009	1.44	0.74	0.11	0.12	4.32	3.22
8/12/2009	1.21	1.05	0.45	0.27	1.30	3.44
8/27/2009	1.35	1.16	0.06	0.08	1.32	3.95
9/10/2009	1.18	0.72	—	0.03	6.76	3.46
9/23/2009	1.23	1.11	0.21	ND (0.02)	0.77	3.66
10/8/2009	1.53	1.09	ND (0.02)	ND (0.02)	4.34	4.32
10/21/2009	1.57	1.33	ND (0.02)	0.06	1.41	4.94
11/12/2009	1.10	0.98	0.18	0.18	0.24	4.27
11/25/2009	1.08	1.03	0.13	0.02	0.33	4.25
12/9/2009	2.22	0.95	ND (0.02)	0.04	11.34	—
12/23/2009	1.31	0.89	ND (0.02)	0.11	0.81	—
1/13/2010	1.31	0.51	ND (0.02)	0.04	0.77	3.17
1/27/2010	2.33	1.34	0.12	ND (0.02)	9.91	3.57
2/10/2010	1.69	1.17	ND (0.02)	ND (0.02)	0.99	3.14
2/24/2010	1.22	1.07	—	0.07	0.45	2.96
3/10/2010	1.25	0.90	ND (0.02)	0.06	1.83	2.64
3/24/2010	1.86	1.89	0.14	0.04	6.07	3.21
4/2/2010	1.35	1.11	0.02	0.02	0.34	2.79
4/26/2010	1.13	0.97	0.09	0.12	0.96	2.79
5/12/2010	1.20	1.09	0.08	0.07	0.34	2.98
5/26/2010	0.88	0.93	0.12	0.04	1.24	2.89

Notes:

1. ND is non-detect. Detection limit provided in parentheses.
2. "—" denotes insufficient sample volume for analysis or loss of sample.
3. TSS is total suspended solids.
4. DOC is dissolved organic carbon.

Table 9.8 Analytical results of mercury sampling at Oswego River. Samples collected and analyzed by Syracuse University from East Cayuga St, Oswego, NY (43.459496, -76.509756).

Sample Date	THg ($ng\ L^{-1}$)	THg_D ($ng\ L^{-1}$)	MeHg ($ng\ L^{-1}$)	$MeHg_D$ ($ng\ L^{-1}$)	TSS ($mg\ L^{-1}$)	DOC ($mg\ L^{-1}$)
6/17/2009	1.36	0.55	0.47	0.24	2.79	3.98
7/1/2009	1.10	0.78	0.09	ND (0.02)	2.25	3.48
7/21/2009	0.69	0.43	0.10	ND (0.02)	2.65	4.10
8/12/2009	1.27	1.11	0.78	0.19	2.80	4.10
8/27/2009	1.26	1.06	ND (0.02)	0.05	19.16	4.76
9/9/2009	0.74	0.64	0.25	ND (0.02)	8.03	4.11
9/23/2009	0.74	0.86	0.04	0.12	2.26	4.86
10/8/2009	0.50	0.47	—	0.20	2.22	2.96
10/21/2009	0.73	0.56	—	0.16	1.54	4.39
11/12/2009	1.98	0.33	—	0.03	2.67	3.75
11/25/2009	0.55	0.27	0.03	0.05	0.57	4.32
12/8/2009	0.63	0.30	0.08	0.03	1.54	—
12/23/2009	0.44	0.40	0.08	0.03	0.36	—
1/13/2010	0.37	0.55	0.06	0.15	ND (0.10)	4.08
1/27/2010	1.73	0.55	ND (0.02)	0.05	9.50	4.01
2/9/2010	0.48	0.38	0.03	0.02	0.61	3.46
2/23/2010	0.41	0.56	0.03	0.04	0.27	3.73
3/9/2010	0.47	0.40	ND (0.02)	0.03	1.03	3.65
3/24/2010	3.00	1.42	0.04	0.03	13.35	4.04
4/1/2010	1.34	0.63	0.06	0.09	5.94	3.60
4/23/2010	0.75	0.47	0.07	0.05	1.19	4.04
5/11/2010	1.23	0.53	0.03	0.04	6.92	3.66
5/25/2010	0.55	0.37	ND (0.02)	0.03	0.77	3.84

Notes:

1. ND is non-detect. Detection limit provided in parentheses.
2. "—" denotes insufficient sample volume for analysis or loss of sample.
3. TSS is total suspended solids.
4. DOC is dissolved organic carbon.

Table 9.9 Analytical results of mercury sampling at Genesee River. Samples collected and analyzed by Syracuse University from River St, Rochester, NY (43.251970, -77.609651).

Sample Date	THg ($ng\ L^{-1}$)	THg_D ($ng\ L^{-1}$)	MeHg ($ng\ L^{-1}$)	$MeHg_D$ ($ng\ L^{-1}$)	TSS ($mg\ L^{-1}$)	DOC ($mg\ L^{-1}$)
6/17/2009	2.44	0.80	0.12	0.12	14.72	3.33
6/30/2009	4.30	0.81	0.13	0.15	78.38	3.53
7/22/2009	1.79	1.80	0.12	0.12	29.40	3.30
8/11/2009	11.18	1.35	ND (0.02)	0.08	349.53	4.20
8/26/2009	2.74	1.00	ND (0.02)	ND (0.02)	34.31	4.26
9/9/2009	0.51	0.71	ND (0.02)	0.05	5.78	2.82
9/22/2009	0.59	0.32	0.05	0.21	8.27	2.71
10/7/2009	0.28	0.34	0.03	ND (0.02)	15.24	2.67
10/20/2009	0.77	0.54	ND (0.02)	0.14	28.36	4.14
11/12/2009	3.04	0.90	ND (0.02)	0.07	13.84	5.50
11/24/2009	0.78	0.32	—	ND (0.02)	7.35	2.71
12/8/2009	1.52	0.61	ND (0.02)	0.02	28.66	—
12/22/2009	0.94	0.55	—	ND (0.02)	14.50	—
1/12/2010	0.59	0.45	ND (0.02)	ND (0.02)	6.93	2.50
1/26/2010	14.02	0.60	ND (0.02)	0.02	333.40	4.30
2/8/2010	1.01	0.34	0.06	—	24.51	2.33
2/23/2010	0.59	0.27	ND (0.02)	ND (0.02)	16.25	2.70
3/9/2010	0.89	0.45	0.04	ND (0.02)	11.13	3.15
3/23/2010	4.43	1.05	0.14	0.03	ND (0.10)	7.81
4/1/2010	5.11	0.92	0.07	0.05	141.25	3.12
4/23/2010	0.84	0.27	0.07	0.06	13.69	3.21
5/11/2010	1.52	0.68	0.07	0.05	18.35	3.64
5/25/2010	0.98	0.41	0.13	0.03	13.67	4.11

Notes:

1. ND is non-detect. Detection limit provided in parentheses.
2. "—" denotes insufficient sample volume for analysis or loss of sample.
3. TSS is total suspended solids.
4. DOC is dissolved organic carbon.

Table 9.10 Analytical results of mercury sampling at Niagara River. Samples collected and analyzed by University of Toronto from dock at Fort George, Niagara-on-the-Lake, Ontario (43.252173, -79.058627).

Sample Date	THg (ng L^{-1})	THg_D (ng L^{-1})	MeHg (ng L^{-1})	$MeHg_D$ (ng L^{-1})	TSS (mg L^{-1})	DOC (mg L^{-1})
6/14/2008	0.68	0.63	0.13	0.02	—	—
6/28/2008	0.80	—	0.14	—	—	—
7/17/2008	0.85	—	0.23	—	—	—
8/15/2008	0.33	—	0.03	—	—	—
8/27/2008	1.14	—	ND (0.02)	—	—	—
9/9/2008	1.06	0.65	0.18	—	—	—
9/24/2008	0.88	—	0.21	—	—	—
10/7/2008	1.50	1.06	0.02	—	—	5.13
10/22/2008	0.96	0.78	—	—	47.53	—
11/6/2008	0.32	0.28	0.05	ND (0.02)	63.12	2.90
11/28/2008	0.63	0.45	ND (0.02)	0.02	64.28	3.24
12/14/2008	0.54	0.32	0.02	0.02	50.92	2.06
1/4/2009	2.63	2.16	—	—	81.73	2.84
1/13/2009	1.27	0.90	0.02	—	76.33	3.22
2/20/2009	1.10	0.88	1.26	0.10	72.55	3.25
3/16/2009	0.38	0.38	0.03	0.03	48.33	2.41
3/17/2009	0.21	0.12	0.03	ND (0.02)	106.33	1.85
4/3/2009	0.99	1.09	—	—	107.13	3.10
4/19/2009	0.87	0.62	—	—	83.25	3.01
4/27/2009	0.21	0.06	—	0.05	328.60	4.01
5/13/2009	0.49	0.11	—	—	316.20	3.16
5/26/2009	0.40	0.27	ND (0.02)	ND (0.02)	318.00	2.59
6/9/2009	0.43	0.36	—	ND (0.02)	158.70	3.52
6/21/2009	1.50	1.08	0.02	ND (0.02)	83.50	2.81
7/7/2009	1.33	0.76	—	—	82.35	2.37
7/22/2009	0.47	0.24	0.06	0.07	47.29	2.56
8/4/2009	0.84	0.62	0.09	0.07	—	2.58
8/24/2009	0.90	0.66	ND (0.02)	—	53.10	2.76
8/31/2009	1.32	0.75	0.04	0.03	127.62	2.49
9/24/2009	0.41	0.35	0.02	ND (0.02)	100.50	2.62
10/1/2009	1.21	0.21	0.05	0.03	275.00	2.81
10/15/2009	0.39	0.38	0.04	0.04	318.80	2.52
11/12/2009	0.27	0.13	0.02	ND (0.02)	68.17	2.56
12/17/2009	1.52	0.32	0.04	0.05	—	2.60

Notes:

1. ND is non-detect. Detection limit provided in parentheses.
2. "—" denotes insufficient sample volume for analysis or loss of sample.
3. TSS is total suspended solids.
4. DOC is dissolved organic carbon.

Table 9.11 Analytical results of mercury sampling at Twenty Mile Creek. Samples collected and analyzed by University of Toronto near Balls Falls Conservation Area, Jordan, Ontario (43.134643, -79.381825).

Sample Date	THg ($ng\ L^{-1}$)	THg_D ($ng\ L^{-1}$)	MeHg ($ng\ L^{-1}$)	$MeHg_D$ ($ng\ L^{-1}$)	TSS ($mg\ L^{-1}$)	DOC ($mg\ L^{-1}$)
6/14/2008	0.76	0.89	1.08	0.16	—	—
6/28/2008	2.54	—	0.38	—	—	—
7/17/2008	1.31	—	0.05	—	—	—
8/15/2008	3.21	—	0.07	—	—	—
8/27/2008	2.62	—	—	—	—	—
9/9/2008	1.52	—	0.04	—	—	—
9/24/2008	2.57	—	0.43	—	—	—
10/7/2008	1.73	—	0.04	—	—	—
10/22/2008	2.04	1.46	—	—	145.10	—
11/6/2008	0.93	1.01	0.02	0.03	295.80	11.40
11/28/2008	4.24	3.48	0.05	0.08	670.80	14.37
12/14/2008	3.04	2.88	—	0.02	260.80	10.14
1/4/2009	2.35	2.14	—	—	234.60	6.36
1/13/2009	—	—	—	—	—	—
2/20/2009	3.91	1.10	0.06	0.18	72.50	6.51
3/16/2009	3.89	3.00	0.02	0.02	155.90	10.81
3/17/2009	2.82	1.46	—	—	335.00	7.50
4/3/2009	7.48	3.72	—	—	359.40	10.78
4/19/2009	2.82	1.97	—	—	174.80	8.05
4/27/2009	5.02	1.88	—	0.10	353.60	14.41
5/13/2009	0.84	0.48	—	—	332.00	8.12
5/26/2009	0.66	0.44	ND (0.02)	ND (0.02)	310.00	7.26
6/9/2009	0.51	0.56	—	0.02	329.80	6.22
6/21/2009	1.59	1.37	0.09	0.07	162.70	8.69
7/7/2009	4.56	2.48	—	0.09	361.80	10.95
7/22/2009	0.83	0.55	0.09	0.18	168.30	9.16
8/4/2009	3.30	1.95	0.06	—	346.60	10.07
8/24/2009	3.67	2.15	0.12	0.11	402.50	9.43
8/31/2009	3.24	1.89	0.03	0.08	415.00	8.73
9/24/2009	0.84	0.46	—	0.02	264.83	5.98
10/1/2009	0.55	0.44	0.05	0.05	90.00	7.47
10/15/2009	0.67	0.38	0.07	0.06	319.40	9.25
11/12/2009	1.50	0.92	0.15	0.06	2249.33	9.45
12/17/2009	4.45	1.02	0.06	0.07	—	7.49

Notes:

1. ND is non-detect. Detection limit provided in parentheses.
2. "—" denotes insufficient sample volume for analysis or loss of sample.
3. TSS is total suspended solids.
4. DOC is dissolved organic carbon.

Table 9.12 Analytical results of mercury sampling at Credit River. Samples collected and analyzed by University of Toronto from Credit Memorial Park, Mississauga, Ontario (43.551223, -79.58784).

Sample Date	THg (ng L^{-1})	THg_D (ng L^{-1})	MeHg (ng L^{-1})	$MeHg_D$ (ng L^{-1})	TSS (mg L^{-1})	DOC (mg L^{-1})
6/14/2008	2.22	1.60	0.53	0.45	—	—
6/28/2008	2.45	—	0.07	—	—	—
7/17/2008	1.74	—	0.03	—	—	—
8/9/2008	1.98	—	ND (0.02)	—	—	—
8/13/2008	2.01	—	0.04	—	—	—
8/27/2008	1.78	—	ND (0.02)	—	—	—
9/9/2008	2.89	—	0.49	—	—	—
9/25/2008	2.28	—	0.32	—	—	—
10/7/2008	1.36	—	—	—	—	—
11/7/2008	0.65	0.41	—	0.06	66.20	5.96
11/28/2008	—	—	—	—	—	—
12/14/2008	—	—	—	—	—	—
1/9/2009	0.33	0.32	—	—	58.28	2.94
1/13/2009	—	—	—	—	—	—
2/20/2009	1.42	0.81	—	0.12	55.04	6.71
3/16/2009	0.46	0.39	ND (0.02)	0.03	48.07	4.39
3/17/2009	0.61	0.50	—	—	47.00	4.39
3/27/2009	2.00	1.59	—	—	162.10	4.93
4/3/2009	1.51	0.95	—	—	338.20	3.81
4/19/2009	1.03	0.78	—	—	180.50	4.30
4/21/2009	1.66	1.10	—	—	115.33	4.50
4/27/2009	1.01	0.32	ND (0.02)	0.04	169.30	5.92
5/13/2009	0.56	0.24	—	—	322.80	6.81
5/26/2009	1.72	0.39	ND (0.02)	0.02	330.00	4.00
6/9/2009	1.12	0.55	—	0.03	337.00	5.46
6/21/2009	1.74	1.22	0.09	0.06	333.80	4.76
7/8/2009	2.11	0.99	0.06	0.05	339.60	3.50
7/21/2009	0.68	0.30	0.08	0.14	255.08	3.84
8/5/2009	2.16	1.09	—	0.03	321.00	5.23
8/25/2009	1.93	0.86	0.05	0.04	270.00	4.43
9/1/2009	1.85	1.04	0.02	0.05	197.78	4.40
9/24/2009	4.80	0.45	0.02	0.04	504.89	3.65
10/1/2009	0.67	0.44	0.11	0.06	145.22	5.59
10/15/2009	1.52	0.28	0.17	0.06	338.00	4.51
11/12/2009	0.77	0.29	—	0.08	338.00	3.83
12/17/2009	0.43	0.24	ND (0.02)	0.04	—	3.61

Notes:

1. ND is non-detect. Detection limit provided in parentheses.
2. "—" denotes insufficient sample volume for analysis or loss of sample.
3. TSS is total suspended solids.
4. DOC is dissolved organic carbon.

Table 9.13 Analytical results of mercury sampling at Humber River. Samples collected and analyzed by University of Toronto from Humber Bay Park, Etobicoke, Ontario (43.620419, -79.479563).

Sample Date	THg (ng L^{-1})	THg_D (ng L^{-1})	MeHg (ng L^{-1})	$MeHg_D$ (ng L^{-1})	TSS (mg L^{-1})	DOC (mg L^{-1})
6/14/2008	2.28	—	0.12	—	—	—
7/2/2008	3.28	—	ND (0.02)	—	—	—
7/17/2008	2.01	—	0.04	—	—	—
8/13/2008	2.17	—	0.02	—	—	—
8/27/2008	2.41	—	0.03	—	—	—
9/9/2008	3.75	—	ND (0.02)	—	—	—
9/25/2008	2.47	—	0.13	—	—	—
10/7/2008	1.79	1.77	—	—	—	7.04
11/7/2008	0.60	0.50	—	—	65.84	4.85
11/28/2008	—	—	—	—	—	—
12/14/2008	—	—	—	—	—	—
1/9/2009	—	—	—	—	—	—
1/13/2009	—	—	—	—	—	—
2/20/2009	—	—	—	—	—	—
3/16/2009	1.13	0.60	ND (0.02)	0.03	151.70	4.45
3/17/2009	1.90	0.60	—	—	222.10	5.82
3/27/2009	2.92	2.04	—	0.03	325.20	5.72
4/3/2009	2.41	1.11	—	—	305.20	6.10
4/19/2009	1.47	1.00	—	—	175.00	4.66
4/21/2009	1.54	1.14	—	—	224.67	5.98
4/27/2009	1.38	0.34	0.06	0.09	238.67	7.14
5/13/2009	0.83	0.26	0.03	0.15	330.20	6.52
5/26/2009	1.24	0.69	—	—	338.00	5.21
6/9/2009	2.12	0.86	ND (0.02)	0.05	350.40	6.70
6/21/2009	3.15	1.35	0.13	0.08	344.60	6.14
7/8/2009	2.19	0.87	0.04	0.06	340.20	5.71
7/21/2009	1.55	0.46	0.09	0.07	285.33	3.50
8/5/2009	2.40	1.10	0.09	ND (0.02)	369.00	7.54
8/25/2009	5.99	1.09	0.03	0.06	344.00	5.81
9/1/2009	2.02	0.88	ND (0.02)	0.06	276.67	5.98
9/24/2009	1.87	0.53	0.10	0.09	274.67	3.92
10/1/2009	0.98	0.34	0.17	0.03	276.67	5.38
10/15/2009	0.55	0.28	0.08	0.12	317.20	5.13
11/12/2009	0.66	ND (0.20)	0.05	0.03	328.00	4.70
12/17/2009	—	0.22	—	0.06	—	4.44

Notes:

1. ND is non-detect. Detection limit provided in parentheses.
2. "—" denotes insufficient sample volume for analysis or loss of sample.
3. TSS is total suspended solids.
4. DOC is dissolved organic carbon.

Table 9.14 Analytical results of mercury sampling at Ganaraska River. Samples collected and analyzed by University of Toronto from Walton Street Bridge, Port Hope, Ontario (43.951088, -78.29233).

Sample Date	THg ($ng\ L^{-1}$)	THg_D ($ng\ L^{-1}$)	MeHg ($ng\ L^{-1}$)	$MeHg_D$ ($ng\ L^{-1}$)	TSS ($mg\ L^{-1}$)	DOC ($mg\ L^{-1}$)
6/14/2008	0.89	—	0.12	—	—	—
7/2/2008	0.61	—	0.28	—	—	—
7/18/2008	0.63	—	—	—	—	—
8/18/2008	0.57	—	0.02	—	—	—
8/27/2008	0.89	—	ND (0.02)	—	—	—
9/9/2008	2.22	—	0.07	—	—	—
9/22/2008	1.74	—	0.08	—	—	—
10/7/2008	3.44	1.08	—	—	—	3.60
11/7/2008	0.34	0.29	—	—	64.60	3.07
11/28/2008	0.90	0.38	0.02	0.04	106.87	6.03
12/12/2008	0.72	0.49	ND (0.02)	ND (0.02)	59.64	4.03
12/30/2008	1.39	0.32	—	—	50.88	3.71
1/13/2009	0.43	0.40	0.05	0.03	84.12	2.97
2/17/2009	1.51	0.89	—	—	52.90	2.90
3/16/2009	0.44	0.20	0.04	0.03	63.56	3.22
3/17/2009	0.91	0.25	—	—	224.80	2.93
4/3/2009	5.33	1.06	—	—	371.80	4.06
4/19/2009	0.91	0.76	—	—	87.25	2.94
4/27/2009	0.33	ND (0.20)	0.07	0.08	164.60	4.08
5/13/2009	0.32	ND (0.20)	0.10	0.05	320.20	3.39
5/26/2009	0.43	0.33	—	—	314.00	2.62
6/9/2009	1.29	0.44	—	—	232.93	3.64
6/21/2009	1.51	1.19	0.08	0.06	112.20	4.43
7/8/2009	1.16	1.14	ND (0.02)	0.06	84.90	2.50
7/21/2009	0.42	0.35	0.12	—	149.27	2.52
8/5/2009	1.07	0.83	ND (0.02)	0.04	295.83	2.69
8/25/2009	1.16	0.90	ND (0.02)	—	57.89	3.05
9/1/2009	1.53	1.07	ND (0.02)	0.05	100.63	4.96
9/24/2009	0.75	0.58	0.09	0.08	148.58	3.42
10/1/2009	0.99	0.25	0.02	0.07	128.15	4.43
10/15/2009	0.63	0.24	—	—	320.80	2.97
11/12/2009	0.50	ND (0.20)	0.08	0.09	144.09	2.53
12/17/2009	0.40	ND (0.20)	0.05	0.03	—	3.15

Notes:

1. ND is non-detect. Detection limit provided in parentheses.
2. "—" denotes insufficient sample volume for analysis or loss of sample.
3. TSS is total suspended solids.
4. DOC is dissolved organic carbon.

Table 9.15 Analytical results of mercury sampling at Trent River. Samples collected and analyzed by University of Toronto from upstream of the Glen Miller Dam, Trenton, Ontario (44.131864, -77.593439).

Sample Date	THg ($ng\ L^{-1}$)	THg_D ($ng\ L^{-1}$)	MeHg ($ng\ L^{-1}$)	$MeHg_D$ ($ng\ L^{-1}$)	TSS ($mg\ L^{-1}$)	DOC ($mg\ L^{-1}$)
6/14/2008	0.65	—	0.46	—	—	—
7/2/2008	0.62	—	0.13	—	—	—
7/18/2008	0.58	—	—	—	—	—
8/18/2008	0.55	—	0.02	—	—	—
8/27/2008	0.95	—	0.04	—	—	—
9/9/2008	1.13	—	0.02	—	—	—
9/22/2008	2.64	—	ND (0.02)	—	—	—
10/7/2008	0.74	0.74	—	—	—	11.25
11/7/2008	0.45	0.53	—	—	63.28	5.42
11/28/2008	0.42	0.30	0.02	ND (0.02)	62.32	5.42
12/12/2008	1.95	1.16	—	—	47.48	5.11
12/30/2008	1.36	0.52	—	—	47.57	5.35
1/13/2009	0.98	0.62	—	0.22	85.88	5.12
2/17/2009	1.88	1.30	—	—	48.30	6.08
3/16/2009	0.49	0.36	0.07	0.04	59.44	6.21
3/17/2009	0.35	0.35	—	—	106.53	6.39
4/3/2009	1.52	0.94	—	—	96.53	6.03
4/19/2009	1.51	0.99	—	—	308.27	5.87
4/27/2009	0.55	0.23	0.06	0.03	170.30	6.09
5/13/2009	0.46	0.29	ND (0.02)	0.07	320.40	6.46
5/26/2009	0.53	0.44	—	—	318.00	6.18
6/9/2009	0.50	0.37	—	—	82.00	5.71
6/21/2009	1.21	1.08	—	0.06	81.25	6.59
7/8/2009	1.23	1.04	ND (0.02)	0.03	324.20	5.90
7/21/2009	0.34	0.20	0.16	0.08	58.54	5.85
8/5/2009	0.93	0.80	—	0.03	223.29	6.10
8/25/2009	1.10	0.80	—	0.03	185.88	5.92
9/1/2009	1.09	0.72	ND (0.02)	0.03	258.33	4.06
9/24/2009	0.44	0.21	0.10	0.04	41.71	5.75
10/1/2009	0.35	0.25	ND (0.02)	ND (0.02)	102.58	4.70
10/15/2009	0.32	0.22	—	—	320.80	5.38
11/12/2009	0.45	0.20	0.02	0.37	92.18	5.67
12/17/2009	0.45	ND (0.20)	0.13	0.13	—	6.00

Notes:

1. ND is non-detect. Detection limit provided in parentheses.
2. "—" denotes insufficient sample volume for analysis or loss of sample.
3. TSS is total suspended solids.
4. DOC is dissolved organic carbon.

10. Bibliography

Ababneh FA, Scott SL, Al-Reasi HA, Lean DRS (2006) Photochemical reduction and reoxidation of aqueous mercuric chloride in the presence of ferrioxalate and air. Science of The Total Environment 367:831–839. doi: 10.1016/j.scitotenv.2006.02.018

Achá D, Hintelmann H, Pabón CA (2012) Sulfate-reducing Bacteria and Mercury Methylation in the Water Column of the Lake 658 of the Experimental Lake Area. Geomicrobiology Journal 29:667–674. doi: 10.1080/01490451.2011.606289

Akbari H, Shea Rose L, Taha H (2003) Analyzing the land cover of an urban environment using high-resolution orthophotos. Landscape and Urban Planning 63:1–14. doi: 10.1016/S0169-2046(02)00165-2

Amyot M, McQueen DJ, Mierle G, Lean DRS (1994) Sunlight-Induced Formation of Dissolved Gaseous Mercury in Lake Waters. Environ Sci Technol 28:2366–2371. doi: 10.1021/es00062a022

Amyot M, Southworth G, Lindberg S., et al. (2004) Formation and evasion of dissolved gaseous mercury in large enclosures amended with 200HgCl2. Atmospheric Environment 38:4279–4289. doi: 10.1016/j.atmosenv.2004.05.002

Babiarz C, Hoffmann S, Wieben A, et al. (2012) Watershed and discharge influences on the phase distribution and tributary loading of total mercury and methylmercury into Lake Superior. Environmental Pollution 161:299–310. doi: 10.1016/j.envpol.2011.09.026

Babiarz CL, Benoit JM, Shafer MM, et al. (1998) Seasonal influences on partitioning and transport of total and methylmercury in rivers from contrasting watersheds. Biogeochemistry 41:237–257. doi: 10.1023/A:1005940630948

Back RC, Gorski PR, Cleckner LB, Hurley JP (2003) Mercury content and speciation in the plankton and benthos of Lake Superior. Science of The Total Environment 304:349–354. doi: 10.1016/S0048-9697(02)00580-6

Back RC, Hurley JP, Rolfhus KR (2002) Watershed influences on the transport, fate and bioavailability of mercury in Lake Superior: Field measurements and modelling approaches. Lakes & Reservoirs: Research & Management 7:201–206. doi: 10.1046/j.1440-1770.2002.00188.x

Balogh SJ, Huang Y, Offerman HJ, et al. (2003) Methylmercury in rivers draining cultivated watersheds. Science of The Total Environment 304:305–313. doi: 10.1016/S0048-9697(02)00577-6

Balogh SJ, Meyer ML, Johnson DK (1998) Transport of Mercury in Three Contrasting River Basins. Environ Sci Technol 32:456–462. doi: 10.1021/es970506q

Balogh SJ, Nollet YH, Offerman HJ (2005) A comparison of total mercury and methylmercury export from various Minnesota watersheds. Science of The Total Environment 340:261–270. doi: 10.1016/j.scitotenv.2004.08.013

Benoit JM, Gilmour CC, Mason RP (2001) The Influence of Sulfide on Solid-Phase Mercury Bioavailability for Methylation by Pure Cultures of Desulfobulbus propionicus (1pr3). Environ Sci Technol 35:127–132. doi: 10.1021/es001415n

Bloom N (1989) Determination of Picogram Levels of Methylmercury by Aqueous Phase Ethylation, Followed by Cryogenic Gas Chromatography with Cold Vapour Atomic Fluorescence Detection. Canadian Journal of Fisheries and Aquatic Sciences 46:1131–1140. doi: 10.1139/f89-147

Bookman R, Driscoll CT, Engstrom DR, Effler SW (2008) Local to regional emission sources affecting mercury fluxes to New York lakes. Atmospheric Environment 42:6088–6097. doi: 10.1016/j.atmosenv.2008.03.045

Bradley PM, Burns DA, Murray KR-, et al. (2011) Spatial and Seasonal Variability of Dissolved Methylmercury in Two Stream Basins in the Eastern United States. Environ Sci Technol 45:2048–2055. doi: 10.1021/es103923j

Bradley PM, Journey CA, Brigham ME, et al. (2013) Intra- and inter-basin mercury comparisons: Importance of basin scale and time-weighted methylmercury estimates. Environmental Pollution 172:42–52. doi: 10.1016/j.envpol.2012.08.008

Brigham ME, Wentz DA, Aiken GR, Krabbenhoft DP (2009) Mercury Cycling in Stream Ecosystems. 1. Water Column Chemistry and Transport. Environ Sci Technol 43:2720–2725. doi: 10.1021/es802694n

Bullock OR, Brehme KA (2002) Atmospheric mercury simulation using the CMAQ model: formulation description and analysis of wet deposition results. Atmospheric Environment 36:2135–2146. doi: 10.1016/S1352-2310(02)00220-0

Burns DA, Riva-Murray K, Bradley PM, et al. (2012) Landscape controls on total and methyl Hg in the upper Hudson River basin, New York, USA. J Geophys Res 117:G01034. doi: 10.1029/2011JG001812

Cai Y, Jaff R, Jones RD (1999) Interactions between dissolved organic carbon and mercury species in surface waters of the Florida Everglades. Applied Geochemistry 14:395–407. doi: 10.1016/S0883-2927(98)00053-5

Canale R, Owens E, Auer M, Effler S (1995) Validation of Water-Quality Model for Seneca River, N.Y. Journal of Water Resources Planning and Management 121:241–250. doi: 10.1061/(ASCE)0733-9496(1995)121:3(241)

Carpi A, Lindberg SE (1998) Application of a teflon^{TM} dynamic flux chamber for quantifying soil mercury flux: Tests and results over background soil. Atmospheric Environment 32:873–882. doi: 10.1016/S1352-2310(97)00133-7

Choi H-D, Holsen TM (2009a) Gaseous mercury fluxes from the forest floor of the Adirondacks. Environmental Pollution 157:592–600. doi: 10.1016/j.envpol.2008.08.020

Choi H-D, Holsen TM (2009b) Gaseous mercury emissions from unsterilized and sterilized soils: The effect of temperature and UV radiation. Environmental Pollution 157:1673–1678. doi: 10.1016/j.envpol.2008.12.014

Choi H-D, Sharac TJ, Holsen TM (2008) Mercury deposition in the Adirondacks: A comparison between precipitation and throughfall. Atmospheric Environment 42:1818–1827. doi: 10.1016/j.atmosenv.2007.11.036

Cobbett FD, Van Heyst BJ (2007) Measurements of GEM fluxes and atmospheric mercury concentrations (GEM, RGM and Hgp) from an agricultural field amended with biosolids in Southern Ont., Canada (October 2004–November 2004). Atmospheric Environment 41:2270–2282. doi: 10.1016/j.atmosenv.2006.11.011

Cobos DR, Baker JM, Nater EA (2002) Conditional sampling for measuring mercury vapor fluxes. Atmospheric Environment 36:4309–4321. doi: 10.1016/S1352-2310(02)00400-4

Costa M, Liss P (2000) Photoreduction and evolution of mercury from seawater. Science of The Total Environment 261:125–135. doi: 10.1016/S0048-9697(00)00631-8

Dalziel JA, Amirault BP, Yeats PA (1998) Inorganic chemical analysis of major rivers flowing into the Bay of Fundy, Scotian Shelf and Bras D'Or lakes. Department of Fisheries & Oceans, Maritimes Region, Science Branch, Bedford Institute of Oceanography, Dartmouth, Nova Scotia

Demers JD, Driscoll CT, Fahey TJ, Yavitt JB (2007) Mercury cycling in litter and soil in different forest types in the Adirondack region, New York, USA. Ecological Applications 17:1341–1351. doi: 10.1890/06-1697.1

Demers JD, Driscoll CT, Shanley JB (2010) Mercury mobilization and episodic stream acidification during snowmelt: Role of hydrologic flow paths, source areas, and supply of dissolved organic carbon. Water Resources Research 46:n/a–n/a. doi: 10.1029/2008WR007021

Denkenberger JS, Driscoll CT, Branfireun BA, et al. (2012) A synthesis of rates and controls on elemental mercury evasion in the Great Lakes Basin. Environmental Pollution 161:291–298. doi: 10.1016/j.envpol.2011.06.007

Denkenberger JS, O'Donnell DM, Driscoll CT, Effler SW (2007) Robotic Monitoring to Assess Impacts of Zebra Mussels and Assimilative Capacity for a River. Journal of Environmental Engineering 133:498–506. doi: 10.1061/(ASCE)0733-9372(2007)133:5(498)

Dennis I, Clair T, Driscoll C, et al. (2005) Distribution Patterns of Mercury in Lakes and Rivers of Northeastern North America. Ecotoxicology 14:113–123. doi: 10.1007/s10646-004-6263-0

DePinto JV, Kaur J, Larson WM, Atkinson JF (2004) LOTOX2 Model Documentation–In support of Development of Load Reduction Strategies and a TMDL for PCBs in Lake Ontario. Submitted to New England Interstate Water Pollution Control Commission, Boot Mills South, Lowell, MA

Dittman JA, Shanley JB, Driscoll CT, et al. (2010) Mercury dynamics in relation to dissolved organic carbon concentration and quality during high flow events in three northeastern U.S. streams. Water Resources Research. doi: 10.1029/2009WR008351

Dommergue A, Ferrari CP, Poissant L, et al. (2003) Diurnal Cycles of Gaseous Mercury within the Snowpack at Kuujjuarapik/Whapmagoostui, Québec, Canada. Environ Sci Technol 37:3289–3297. doi: 10.1021/es026242b

Dove A, Hill B, Klawunn P, et al. (2012) Spatial distribution and trends of total mercury in waters of the Great Lakes and connecting channels using an improved sampling technique. Environmental Pollution 161:328–334. doi: 10.1016/j.envpol.2011.06.004

Drevnick PE, Engstrom DR, Driscoll CT, et al. (2012) Spatial and temporal patterns of mercury accumulation in lacustrine sediments across the Laurentian Great Lakes region. Environmental Pollution 161:252–260. doi: 10.1016/j.envpol.2011.05.025

Driscoll CT, Abbott M, Bullock R, et al. (2007a) Airsheds and Watersheds. Ecosystem Responses to Mercury Contamination: Indicators of Change. CRC Press, Boca Raton, Florida, pp 13–46

Driscoll CT, Blette V, Yan C, et al. (1995) The role of dissolved organic carbon in the chemistry and bioavailability of mercury in remote Adirondack lakes. Water, Air, & Soil Pollution 80:499–508. doi: 10.1007/BF01189700

Driscoll CT, Chen CY, Hammerschmidt CR, et al. (2012) Nutrient supply and mercury dynamics in marine ecosystems: A conceptual model. Environmental Research 119:118–131. doi: 10.1016/j.envres.2012.05.002

Driscoll CT, Han Y-J, Chen CY, et al. (2007b) Mercury Contamination in Forest and Freshwater Ecosystems in the Northeastern United States. BioScience 57:17–28. doi: 10.1641/B570106

Driscoll CT, Holsapple J, Schofield CL, Ron Munson (1998) The Chemistry and Transport of Mercury in a Small Wetland in the Adirondack Region of New York, USA. Biogeochemistry 40:137–146.

Driscoll CT, Mason RP, Chan HM, et al. (2013) Mercury as a Global Pollutant: Sources, Pathways, and Effects. Environ Sci Technol 47:4967–4983. doi: 10.1021/es305071v

Driscoll CT, Yan C, Schofield CL, et al. (1994) The mercury cycle and fish in the Adirondack lakes. Environ Sci Technol 28:136A–143A. doi: 10.1021/es00052a003

Eaton AD, Clesceri LS, Greenberg AE, et al. (1998) Standard methods for the examination of water and wastewater, 20th ed. American Public Health Association, Washington, DC

Eckhardt BW, Moore TR (1990) Controls on Dissolved Organic Carbon Concentrations in Streams, Southern Québec. Can J Fish Aquat Sci 47:1537–1544. doi: 10.1139/f90-173

Eckley CS, Branfireun B (2008) Gaseous mercury emissions from urban surfaces: Controls and spatiotemporal trends. Applied Geochemistry 23:369–383. doi: 10.1016/j.apgeochem.2007.12.008

Eckley CS, Gustin M, Lin C-J, et al. (2010) The influence of dynamic chamber design and operating parameters on calculated surface-to-air mercury fluxes. Atmospheric Environment 44:194–203. doi: 10.1016/j.atmosenv.2009.10.013

Eckley CS, Gustin M, Miller MB, Marsik F (2011) Scaling Non-Point-Source Mercury Emissions from Two Active Industrial Gold Mines: Influential Variables and Annual Emission Estimates. Environ Sci Technol 45:392–399. doi: 10.1021/es101820q

Eckley CS, Hintelmann H (2006) Determination of mercury methylation potentials in the water column of lakes across Canada. Science of The Total Environment 368:111–125. doi: 10.1016/j.scitotenv.2005.09.042

Effler SW, Bloom NS (1990) Seasonal variability in the Mercury speciation of Onondaga Lake (New York). Water Air Soil Pollut 53:251–265. doi: 10.1007/BF00170741

Effler SW, Brooks CM, Whitehead K, et al. (1996) Impact of Zebra Mussel Invasion on River Water Quality. Water Environment Research 68:205–214.

Effler SW, Carter CF (1987) Spatial Variability in Selected Physical Characteristics and Processes in Cross Lake, New York. Water Resour Bull 23:243–249. doi: 10.1111/j.1752-1688.1987.tb00803.x

Effler SW, Effler AJP, Prestigiacomo AR, et al. (2011) Effects of intervening Cross Lake on the Seneca River, New York. River Systems 19:301–314. doi: 10.1127/1868-5749/2011/0046

Effler SW, Matthews DA, Brooks-Matthews CM, et al. (2004) Water quality impacts and indicators of metabolic activity of the zebra mussel invasion of the Seneca River. JAWRA Journal of the American Water Resources Association 40:737–754. doi: 10.1111/j.1752-1688.2004.tb04456.x

Effler SW, McCarthy JM, Simpson KW, et al. (1984) Chemical stratification in the Seneca/Oswego rivers (NY). Water Air Soil Pollut 21:335–350. doi: 10.1007/BF00163634

Effler SW, O'Donnell DM, Owen CJ (2002) America's Most Polluted Lake: Using Robotic Buoys to Monitor the Rehabilitation of Onondaga Lake. Journal of Urban Technology 9:21–44. doi: 10.1080/1063073022000016469

Effler SW, Prestigiacomo AR, Effler AJP, Driscoll C (2010) Water quality patterns in a river-lake system from multiple drivers (Three Rivers, New York State). River Systems 19:75–94. doi: 10.1127/1868-5749/2010/019-0075

Effler SW, Siegfried C (1998) Tributary Water Quality Feedback from the Spread of Zebra Mussels: Oswego River, New York. Journal of Great Lakes Research 24:453–463. doi: 10.1016/S0380-1330(98)70835-4

Engle MA, Gustin MS, Zhang H (2001) Quantifying natural source mercury emissions from the Ivanhoe Mining District, north-central Nevada, USA. Atmospheric Environment 35:3987–3997. doi: 10.1016/S1352-2310(01)00184-4

Engstrom DR, Balogh SJ, Swain EB (2007) History of Mercury Inputs to Minnesota Lakes: Influences of Watershed Disturbance and Localized Atmospheric Deposition. Limnology and Oceanography 52:2467–2483. doi: 10.4319/lo.2007.52.6.2467

Ericksen J, Gustin M (2004) Foliar exchange of mercury as a function of soil and air mercury concentrations. Science of The Total Environment 324:271–279. doi: 10.1016/j.scitotenv.2003.10.034

Ericksen JA, Gustin MS, Xin M, et al. (2006) Air–soil exchange of mercury from background soils in the United States. Science of The Total Environment 366:851–863. doi: 10.1016/j.scitotenv.2005.08.019

Ethier ALM, Atkinson JF, DePinto JV, Lean DRS (2012) Estimating mercury concentrations and fluxes in the water column and sediment of Lake Ontario with HERMES model. Environmental Pollution 161:335–342. doi: 10.1016/j.envpol.2011.06.002

Evers D, Savoy L, DeSorbo C, et al. (2008) Adverse effects from environmental mercury loads on breeding common loons. Ecotoxicology 17:69–81. doi: 10.1007/s10646-007-0168-7

Evers DC, Wiener JG, Driscoll CT, et al. (2011) Great Lakes Mercury Connections: The Extent and Effects of Mercury Pollution in the Great Lakes Region. 44 PP.

Ferrari CP, Gauchard P-A, Aspmo K, et al. (2005) Snow-to-air exchanges of mercury in an Arctic seasonal snow pack in Ny-Ålesund, Svalbard. Atmospheric Environment 39:7633–7645. doi: 10.1016/j.atmosenv.2005.06.058

Fitzgerald WF, Engstrom DR, Mason RP, Nater EA (1998) The Case for Atmospheric Mercury Contamination in Remote Areas. Environ Sci Technol 32:1–7. doi: 10.1021/es970284w

Fitzgerald WF, Mason R, Vandal G (1991) Atmospheric cycling and air-water exchange of mercury over mid-continental lacustrine regions. Water, Air, & Soil Pollution 56:745–767. doi: 10.1007/BF00342314

Fitzgerald WF, Mason RP (1997) Biogeochemical Cycling of Mercury in the Marine Environment. Metal Ions in Biological Systems. Marcel Dekker, Inc., New York, pp 53–111

French TD, Campbell LM, Jackson DA, et al. (2006) Long-Term Changes in Legacy Trace Organic Contaminants and Mercury in Lake Ontario Salmon in Relation to Source Controls, Trophodynamics, and Climatic Variability. Limnology and Oceanography 51:2794–2807. doi: 10.4319/lo.2006.51.6.2794

Gabriel MC, Williamson DG, Zhang H, et al. (2006) Diurnal and seasonal trends in total gaseous mercury flux from three urban ground surfaces. Atmospheric Environment 40:4269–4284. doi: 10.1016/j.atmosenv.2006.04.004

Gårdfeldt K, Feng X, Sommar J, Lindqvist O (2001) Total gaseous mercury exchange between air and water at river and sea surfaces in Swedish coastal regions. Atmospheric Environment 35:3027–3038. doi: 10.1016/S1352-2310(01)00106-6

Glaser D, Rhea JR, Opdyke DR, et al. (2009) Model of zebra mussel growth and water quality impacts in the Seneca River, New York. Lake and Reservoir Management 25:49–72. doi: 10.1080/07438140802714411

Government of Canada, United States Environmental Protection Agency (1995) The Great Lakes An Environmental Atlas and Resource Book, 3rd ed. The Great Lakes National Program Office, Chicago, IL

Great Lakes Environmental Research Laboratory (2006) Great Lakes Sensitivity to Climatic Forcing: Hydrological Models. In: Great Lakes Sensitivity to Climatic Forcing. http://www.glerl.noaa.gov/res/Programs/glscf/hydrology.html. Accessed 13 Feb 2014

Grigal DF (2002) Inputs and outputs of mercury from terrestrial watersheds: a review. Environmental Reviews 10:1–39. doi: 10.1139/a01-013

Gustin MS, Coolbaugh M, Engle M, et al. (2003) Atmospheric mercury emissions from mine wastes and surrounding geologically enriched terrains. Environmental Geology 43:339–351. doi: 10.1007/s00254-002-0630-z

Gustin MS, Lindberg S, Marsik F, et al. (1999) Nevada STORMS project: Measurement of mercury emissions from naturally enriched surfaces. Journal of Geophysical Research: Atmospheres 104:21831–21844. doi: 10.1029/1999JD900351

Gustin MS, Lindberg SE, Weisberg PJ (2008) An update on the natural sources and sinks of atmospheric mercury. Applied Geochemistry 23:482–493. doi: 10.1016/j.apgeochem.2007.12.010

Hartman JS, Weisberg PJ, Pillai R, et al. (2009) Application of a Rule-Based Model to Estimate Mercury Exchange for Three Background Biomes in the Continental United States. Environ Sci Technol 43:4989–4994. doi: 10.1021/es900075q

Hennigan RD (1990) America's dirtiest lake. Clearwaters 19:8–13.

Hogan LS, Marschall E, Folt C, Stein RA (2007) How Non-native Species in Lake Erie Influence Trophic Transfer of Mercury and Lead to Top Predators. Journal of Great Lakes Research 33:46–61. doi: 10.3394/0380-1330(2007)33[46:HNSILE]2.0.CO;2

Honeywell (2013) 2012 and 2013 Source Control Summary for the Onondaga Lake Bottom Subsite. Parsons, O'Brien & Gere, Syracuse, New York. http://www.dec.ny.gov/docs/regions_pdf/sourcecontrol.pdf

Horvat M, Liang L, Bloom NS (1993a) Comparison of distillation with other current isolation methods for the determination of methyl mercury compounds in low level environmental samples. Part 1, Sediments. Analytica chimica acta 281:135–152.

Horvat M, Liang L, Bloom NS (1993b) Comparison of distillation with other current isolation methods for the determination of methyl mercury compounds in low level environmental samples. Part 2, Water. Analytica chimica acta 282:153–168.

Howell ET, Chomicki KM, Kaltenecker G (2012) Patterns in water quality on Canadian shores of Lake Ontario: Correspondence with proximity to land and level of urbanization. Journal of Great Lakes Research 38, Supplement 4:32–46. doi: 10.1016/j.jglr.2011.12.005

Hurley JP, Benoit JM, Babiarz CL, et al. (1995) Influences of Watershed Characteristics on Mercury Levels in Wisconsin Rivers. Environ Sci Technol 29:1867–1875. doi: 10.1021/es00007a026

Hurley JP, Cowell SE, Shafer MM, Hughes PE (1998a) Partitioning and Transport of Total and Methyl Mercury in the Lower Fox River, Wisconsin. Environ Sci Technol 32:1424–1432. doi: 10.1021/es970685b

Hurley JP, Cowell SE, Shafer MM, Hughes PE (1998b) Tributary loading of mercury to Lake Michigan: Importance of seasonal events and phase partitioning. Science of The Total Environment 213:129–137. doi: 10.1016/S0048-9697(98)00084-9

Hurley JP, Krabbenhoft DP, Babiarz CL, Andren AW (1994) Cycling of Mercury across the Sediment-Water Interface in Seepage Lakes. Environmental Chemistry of Lakes and Reservoirs. American Chemical Society, pp 425–449

Hurley JP, Manolopoulos H, Babiarz CL, et al. (2003) Methyl mercury in Lake Superior: Offshore processes and bioaccumulation. Journal de Physique IV (Proceedings) 107:4. doi: 10.1051/jp4:20030385

Hurley JP, Shafer MM, Cowell SE, et al. (1996) Trace Metal Assessment of Lake Michigan Tributaries Using Low-Level Techniques. Environ Sci Technol 30:2093–2098. doi: 10.1021/es9509543

Jeremiason JD, Kanne LA, Lacoe TA, et al. (2009) A Comparison of Mercury Cycling in Lakes Michigan and Superior. Journal of Great Lakes Research 35:329–336. doi: 10.1016/j.jglr.2009.06.001

Kamman N, Burgess N, Driscoll C, et al. (2005a) Mercury in Freshwater Fish of Northeast North America – A Geographic Perspective Based on Fish Tissue Monitoring Databases. Ecotoxicology 14:163–180. doi: 10.1007/s10646-004-6267-9

Kamman N, Chalmers A, Clair T, et al. (2005b) Factors Influencing Mercury in Freshwater Surface Sediments of Northeastern North America. Ecotoxicology 14:101–111. doi: 10.1007/s10646-004-6262-1

Kaur J, DePinto JV, Atkinson JF, et al. (2012) Development of a spatially resolved linked hydrodynamic and exposure model (LOTOX2) for PCBs in Lake Ontario. Journal of Great Lakes Research 38:490–503. doi: 10.1016/j.jglr.2012.06.011

Kelso JRM, Frank R (1974) Organochlorine Residues, Mercury, Copper and Cadmium in Yellow Perch, White Bass and Smallmouth Bass, Long Point Bay, Lake Erie. Transactions of the American Fisheries Society 103:577–581. doi: 10.1577/1548-8659(1974)103<577:ORMCAC>2.0.CO;2

Kemp AL, Thomas RL (1976) Sediment Geochemistry: Cultural Impact on the Geochemistry of the Sediments of Lakes Ontario, Erie and Huron. Geoscience Canada 3:191–207.

Kerfoot WC, Harting S, Rossmann R, Robbins JA (1999) Anthropogenic Copper Inventories and Mercury Profiles from Lake Superior: Evidence for Mining Impacts. Journal of Great Lakes Research 25:663–682. doi: 10.1016/S0380-1330(99)70769-0

Kozie KD, Anderson RK (1991) Productivity, diet, and environmental contaminants in bald eagles nesting near the Wisconsin shoreline of Lake Superior. Arch Environ Contam Toxicol 20:41–48. doi: 10.1007/BF01065326

Kuiken T, Zhang H, Gustin M, Lindberg S (2008) Mercury emission from terrestrial background surfaces in the eastern USA. Part I: Air/surface exchange of mercury within a southeastern deciduous forest (Tennessee) over one year. Applied Geochemistry 23:345–355. doi: 10.1016/j.apgeochem.2007.12.006

Lai S-O, Holsen TM, Han Y-J, et al. (2007) Estimation of mercury loadings to Lake Ontario: Results from the Lake Ontario atmospheric deposition study (LOADS). Atmospheric Environment 41:8205–8218. doi: 10.1016/j.atmosenv.2007.06.035

Lalonde JD, Poulain AJ, Amyot M (2002) The Role of Mercury Redox Reactions in Snow on Snow-to-Air Mercury Transfer. Environ Sci Technol 36:174–178. doi: 10.1021/es010786g

Landis MS, Keeler GJ (2002) Atmospheric Mercury Deposition to Lake Michigan during the Lake Michigan Mass Balance Study. Environ Sci Technol 36:4518–4524. doi: 10.1021/es011217b

Lawson NM, Mason RP (2001) Concentration of Mercury, Methylmercury, Cadmium, Lead, Arsenic, and Selenium in the Rain and Stream Water of Two Contrasting Watersheds in

Western Maryland. Water Research 35:4039–4052. doi: 10.1016/S0043-1354(01)00140-3

Lawson NM, Mason RP, Laporte J-M (2001) The fate and transport of mercury, methylmercury, and other trace metals in Chesapeake Bay tributaries. Water Research 35:501–515. doi: 10.1016/S0043-1354(00)00267-0

Liang L, Bloom NS, Horvat M (1994) Simultaneous determination of mercury speciation in biological materials by GC/CVAFS after ethylation and room-temperature precollection. Clinical Chemistry 40:602 –607.

Lindberg SE, Meyers TP (2001) Development of an automated micrometeorological method for measuring the emission of mercury vapor from wetland vegetation. Wetlands Ecology and Management 9:333–347. doi: 10.1023/A:1011804516643

Lindberg SE, Vette AF, Miles C, Schaedlich F (2000a) Mercury speciation in natural waters: Measurement of dissolved gaseous mercury with a field analyzer. Biogeochemistry 48:237–259. doi: 10.1023/A:1006228612872

Lindberg SE, Vette AF, Miles C, Schaedlich F (2000b) Mercury speciation in natural waters: Measurement of dissolved gaseous mercury with a field analyzer. Biogeochemistry 48:237–259. doi: 10.1023/A:1006228612872

Lindberg SE, Zhang H, Gustin M, et al. (1999) Increases in mercury emissions from desert soils in response to rainfall and irrigation. Journal of Geophysical Research: Atmospheres 104:21879–21888. doi: 10.1029/1999JD900202

Liss PS, Slater PG (1974) Flux of Gases across the Air-Sea Interface. Nature 247:181–184. doi: 10.1038/247181a0

Van Loon L, Mader E, Scott SL (2000) Reduction of the Aqueous Mercuric Ion by Sulfite: UV Spectrum of HgSO3 and Its Intramolecular Redox Reaction. J Phys Chem A 104:1621–1626. doi: 10.1021/jp994268s

Lyons WB, Fitzgibbon TO, Welch KA, Carey AE (2006) Mercury geochemistry of the Scioto River, Ohio: Impact of agriculture and urbanization. Applied Geochemistry 21:1880–1888. doi: 10.1016/j.apgeochem.2006.08.005

Mahaffey KR (1999) Methylmercury: a new look at the risks. Public Health Rep 114:396–413. http://www.ncbi.nlm.nih.gov/pmc/articles/PMC1308510/

Mahaffey KR (2004) Update on recent epidemiologic mercury studies. Presentation at 2004 National Fish Forum. San Diego, CA. EPA-823-R-05-006. http://water.epa.gov/scitech/swguidance/fishshellfish/techguidance/2004_index.cfm

Makarewicz JC, Lewis TW, Boyer GL, Edwards WJ (2012a) The influence of streams on nearshore water chemistry, Lake Ontario. Journal of Great Lakes Research 38, Supplement 4:62–71. doi: 10.1016/j.jglr.2012.02.010

Makarewicz JC, Lewis TW, Pennuto CM, et al. (2012b) Physical and chemical characteristics of the nearshore zone of Lake Ontario. Journal of Great Lakes Research 38, Supplement 4:21–31. doi: 10.1016/j.jglr.2011.11.013

Mason RP, Sullivan KA (1997) Mercury in Lake Michigan. Environ Sci Technol 31:942–947. doi: 10.1021/es960656l

Mason RP, Sullivan KA (1998) Mercury and methylmercury transport through an urban watershed. Water Research 32:321–330. doi: 10.1016/S0043-1354(97)00285-6

Meybeck M (1982) Carbon, nitrogen, and phosphorus transport by world rivers. Am J Sci 282:401–450. doi: 10.2475/ajs.282.4.401

Miller E, Vanarsdale A, Keeler G, et al. (2005) Estimation and Mapping of Wet and Dry Mercury Deposition Across Northeastern North America. Ecotoxicology 14:53–70. doi: 10.1007/s10646-004-6259-9

Mulholland PJ, Kuenzler EJ (1979) Organic Carbon Export from Upland and Forested Wetland Watersheds. Limnology and Oceanography 24:960–966. doi: 10.2307/2835336

Munthe J, McElroy WJ (1992) Some aqueous reactions of potential importance in the atmospheric chemistry of mercury. Atmospheric Environment Part A General Topics 26:553–557. doi: 10.1016/0960-1686(92)90168-K

Munthe J, Xiao Z, Lindqvist O (1991) The aqueous reduction of divalent mercury by sulfite. Water, Air, & Soil Pollution 56:621–630. doi: 10.1007/BF00342304

Nacht DM, Gustin MS (2004) Mercury Emissions from Background and Altered Geologic Units Throughout Nevada. Water, Air, & Soil Pollution 151:179–193. doi: 10.1023/B:WATE.0000009907.49577.a8

Nater EA, Grigal DF (1992) Regional trends in mercury distribution across the Great Lakes states, north central USA. Nature 358:139–141. doi: 10.1038/358139a0

Natural Resources Canada/Canadian Centre for Remote Sensing, United States Geological Survey, Insituto Nacional de Estadística y Geografía, et al. (2010) 2005 North American Land Cover at 250 m spatial resolution. North American Commission for Environmental Cooperation (CEC). http://www.cec.org/Page.asp?PageID=924&ContentID=2819

NESCAUM (2005) Inventory of anthropogenic mercury emissions in the northeast. Report from Northeast States for Coordinated Air Use Management. 40 pp. http://www.nescaum.org/documents/inventory-of-anthropogenic-mercury-emissions-in-the-northeast/

New York State Department of Environmental Conservation (2000) New York State Large Scale Hydrography Surface Water Areas by Sub-basin (ARC Export : 2000). http://cugir.mannlib.cornell.edu/datatheme.jsp?id=110

Nriagu JO (1994) Mechanistic steps in the photoreduction of mercury in natural waters. Science of The Total Environment 154:1–8. doi: 10.1016/0048-9697(94)90608-4

O'Donnell DM (2001) OurLake. www.ourlake.org. Accessed 21 Feb 2014

O'Driscoll NJ, Beauchamp S, Siciliano SD, et al. (2003a) Continuous Analysis of Dissolved Gaseous Mercury (DGM) and Mercury Flux in Two Freshwater Lakes in Kejimkujik Park, Nova Scotia: Evaluating Mercury Flux Models with Quantitative Data. Environ Sci Technol 37:2226–2235. doi: 10.1021/es025944y

O'Driscoll NJ, Siciliano SD, Lean DRS (2003b) Continuous analysis of dissolved gaseous mercury in freshwater lakes. Science of The Total Environment 304:285–294. doi: 10.1016/S0048-9697(02)00575-2

O'Driscoll, Poissant, Canário, et al. (2007) Continuous Analysis of Dissolved Gaseous Mercury and Mercury Volatilization in the Upper St. Lawrence River: Exploring Temporal Relationships and UV Attenuation. Environ Sci Technol 41:5342–5348. doi: 10.1021/es070147r

Oliver BG (1984) Distribution and pathways of some chlorinated benzenes in the Niagara River and Lake Ontario. Water Pollution Research Journal of Canada 19:47–58.

Oliver BG, Charlton MN, Durham RW (1989) Distribution, redistribution, and geochronology of polychlorinated biphenyl congeners and other chlorinated hydrocarbons in Lake Ontario sediments. Environ Sci Technol 23:200–208. doi: 10.1021/es00179a011

Ontario Ministry of Natural Resources (2011) National Hydro Network. Government of Canada, Natural Resources Canada, Earth Sciences Sector, Mapping Information Branch, Centre for Topographic Information - Sherbrooke. http://www.geobase.ca

Owens EM, Effler SW (1996) Modeling the Impacts of a Proposed Hypolimnetic Wastewater Discharge on Stratification and Mixing in Onondaga Lake. Lake and Reservoir Management 12:195–206. doi: 10.1080/07438149609354008

Paraquetti HHM, Ayres GA, de Almeida MD, et al. (2004) Mercury distribution, speciation and flux in the Sepetiba Bay tributaries, SE Brazil. Water Research 38:1439–1448. doi: 10.1016/j.watres.2003.11.039

Peckenham JM, Kahl JS, Mower B (2003) Background Mercury Concentrations in River Water in Maine, U.S.A. Environmental Monitoring and Assessment 89:129–152. doi: 10.1023/A:1026077824228

Peterjohn WT, Correll DL (1984) Nutrient Dynamics in an Agricultural Watershed: Observations on the Role of A Riparian Forest. Ecology 65:1466–1475. doi: 10.2307/1939127

Pirrone N, Allegrini I, Keeler GJ, et al. (1998) Historical atmospheric mercury emissions and depositions in North America compared to mercury accumulations in sedimentary records. Atmospheric Environment 32:929 – 940. doi: 10.1016/S1352-2310(97)00353-1

Pirrone N, Cinnirella S, Feng X, et al. (2010) Global mercury emissions to the atmosphere from anthropogenic and natural sources. Atmos Chem Phys 10:5951–5964. doi: 10.5194/acp-10-5951-2010

Pirrone N, Glinsorn G, Keeler GJ (1995) Ambient levels and dry deposition fluxes of mercury to Lakes Huron, Erie and St. Clair. Water Air Soil Pollut 80:179–188. doi: 10.1007/BF01189666

Poissant L, Pilote M, Constant P, et al. (2004) Mercury gas exchanges over selected bare soil and flooded sites in the bay St. François wetlands (Québec, Canada). Atmospheric Environment 38:4205–4214. doi: 10.1016/j.atmosenv.2004.03.068

Quémerais B, Cossa D, Rondeau B, et al. (1998) Mercury distribution in relation to iron and manganese in the waters of the St. Lawrence river. Science of The Total Environment 213:193–201. doi: 10.1016/S0048-9697(98)00092-8

Quémerais B, Cossa D, Rondeau B, et al. (1999) Sources and Fluxes of Mercury in the St. Lawrence River. Environ Sci Technol 33:840–849. doi: 10.1021/es980400a

Qureshi A, MacLeod M, Scheringer M, Hungerbühler K (2009) Mercury cycling and species mass balances in four North American lakes. Environmental Pollution 157:452–462. doi: 10.1016/j.envpol.2008.09.023

Rasmussen PE (1994) Current Methods of Estimating Atmospheric Mercury Fluxes in Remote Areas. Environ Sci Technol 28:2233–2241. doi: 10.1021/es00062a006

Ravichandran M (2004) Interactions between mercury and dissolved organic matter—a review. Chemosphere 55:319–331. doi: 10.1016/j.chemosphere.2003.11.011

Riscassi A, Hokanson K, Scanlon T (2011) Streamwater Particulate Mercury and Suspended Sediment Dynamics in a Forested Headwater Catchment. Water, Air, & Soil Pollution 220:23–36. doi: 10.1007/s11270-010-0731-3

Risch MR, DeWild JF, Krabbenhoft DP, et al. (2012a) Litterfall mercury dry deposition in the eastern USA. Environmental Pollution 161:284–290. doi: 10.1016/j.envpol.2011.06.005

Risch MR, Gay DA, Fowler KK, et al. (2012b) Spatial patterns and temporal trends in mercury concentrations, precipitation depths, and mercury wet deposition in the North American Great Lakes region, 2002–2008. Environmental Pollution 161:261–271. doi: 10.1016/j.envpol.2011.05.030

Rolfhus KR, Fitzgerald WF (2001) The evasion and spatial/temporal distribution of mercury species in Long Island Sound, CT-NY. Geochimica et Cosmochimica Acta 65:407–418. doi: 10.1016/S0016-7037(00)00519-6

Rolfhus KR, Sakamoto HE, Cleckner LB, et al. (2003) Distribution and Fluxes of Total and Methylmercury in Lake Superior. Environ Sci Technol 37:865–872. doi: 10.1021/es026065e

Rossmann R (1999) Horizontal and Vertical Distributions of Mercury in 1983 Lake Superior Sediments with Estimates of Storage and Mass Flux. Journal of Great Lakes Research 25:683–696. doi: 10.1016/S0380-1330(99)70770-7

Sandheinrich MB, Wiener JG (2011) Methylmercury in Freshwater Fish: Recent Advances in Assessing Toxicity of Environmentally Relevant Exposures. W.N. Beyer and J.P. Meador (ed). Environmental Contaminants in Biota: Interpreting Tissue Concentrations. 2nd Ed. Taylor and Francis Publishers. Boca Raton, Florida

Sanemasa I (1975) The solubility of elemental mercury vapor in water. Bulletin of the chemical society of Japan 48:1795–1798.

Schindel HL, Wagner LA, Haimeher P (1977) Time of travel studies and dye dispersion studies of selected central New York streams and lakes in the Oswego Basin, New York, 1967-1975. New York State Department of Environmental Conservation and the US Geological Survey. Albany, New York

Schmeltz D, Evers D, Driscoll C, et al. (2011) MercNet: a national monitoring network to assess responses to changing mercury emissions in the United States. Ecotoxicology 20:1713–1725. doi: 10.1007/s10646-011-0756-4

Schroeder W, Lindqvist O, Munthe J, Xiao Z (1992) Volatilization of mercury from lake surfaces. Science of The Total Environment 125:47–66. doi: 10.1016/0048-9697(92)90382-3

Schroeder WH, Beauchamp S, Edwards G, et al. (2005) Gaseous mercury emissions from natural sources in Canadian landscapes. Journal of Geophysical Research: Atmospheres 110:n/a–n/a. doi: 10.1029/2004JD005699

Schuster PF, Shanley JB, Marvin-DiPasquale M, et al. (2008) Mercury and Organic Carbon Dynamics During Runoff Episodes from a Northeastern USA Watershed. Water, Air, & Soil Pollution 187:89–108. doi: 10.1007/s11270-007-9500-3

Seigneur C, Lohman K, Vijayaraghavan K, Shia R-L (2003) Contributions of global and regional sources to mercury deposition in New York State. Environmental Pollution 123:365–373. doi: 10.1016/S0269-7491(03)00027-7

Sellers P, Kelly CA, Rudd JWM, MacHutchon AR (1996) Photodegradation of methylmercury in lakes. Nature 380:694–697. doi: 10.1038/380694a0

Selvendiran P, Driscoll CT, Bushey JT, Montesdeoca MR (2008a) Wetland influence on mercury fate and transport in a temperate forested watershed. Environmental Pollution 154:46–55. doi: 10.1016/j.envpol.2007.12.005

Selvendiran P, Driscoll CT, Montesdeoca MR, et al. (2009) Mercury dynamics and transport in two Adirondack Lakes. Limnology and Oceanography 54:413–427. doi: 10.4319/lo.2009.54.2.0413

Selvendiran P, Driscoll CT, Montesdeoca MR, Bushey JT (2008b) Inputs, storage, and transport of total and methyl mercury in two temperate forest wetlands. J Geophys Res 113:15 PP. doi: 200810.1029/2008JG000739

Shanley J, Kamman N, Clair T, Chalmers A (2005) Physical Controls on Total and Methylmercury Concentrations in Streams and Lakes of the Northeastern USA. Ecotoxicology 14:125–134. doi: 10.1007/s10646-004-6264-z

Shanley JB, Alisa Mast M, Campbell DH, et al. (2008) Comparison of total mercury and methylmercury cycling at five sites using the small watershed approach. Environmental Pollution 154:143–154. doi: 10.1016/j.envpol.2007.12.031

Smith-Downey NV, Sunderland EM, Jacob DJ (2010) Anthropogenic impacts on global storage and emissions of mercury from terrestrial soils: Insights from a new global model. J Geophys Res 115:G03008. doi: 10.1029/2009JG001124

St. Louis VL, Rudd JWM, Kelly CA, et al. (1996) Production and Loss of Methylmercury and Loss of Total Mercury from Boreal Forest Catchments Containing Different Types of Wetlands†. Environ Sci Technol 30:2719–2729. doi: 10.1021/es950856h

St. Louis VL, Rudd JWM, Kelly CA, et al. (2001) Importance of the Forest Canopy to Fluxes of Methyl Mercury and Total Mercury to Boreal Ecosystems. Environ Sci Technol 35:3089–3098. doi: 10.1021/es001924p

Stamenkovic J, Gustin MS, Arnone III JA, et al. (2008) Atmospheric mercury exchange with a tallgrass prairie ecosystem housed in mesocosms. Science of The Total Environment 406:227–238. doi: 10.1016/j.scitotenv.2008.07.047

Sullivan KA, Mason RP (1998) The concentration and distribution of mercury in Lake Michigan. Science of The Total Environment 213:213–228. doi: 10.1016/S0048-9697(98)00094-1

Systat Software, Inc. (2008) SigmaPlot, v. 11.0. http://www.sigmaplot.com/

Thomas RL (1973) The Distribution of Mercury in the Surficial Sediments of Lake Huron. Can J Earth Sci 10:194–204. doi: 10.1139/e73-021

Thomas RL, Jaquet J-M (1976) Mercury in the Surficial Sediments of Lake Erie. J Fish Res Bd Can 33:404–412. doi: 10.1139/f76-062

Thomas RL, Kemp ALW, Lewis CFM (1972) Distribution, composition and characteristics of the surficial sediments of Lake Ontario. Journal of Sedimentary Research 42:66–84. doi: 10.1306/74D72491-2B21-11D7-8648000102C1865D

Tossell JA (1998) Theoretical Study of the Photodecomposition of Methyl Hg Complexes. J Phys Chem A 102:3587–3591. doi: 10.1021/jp980244u

USEPA (2005) 2004 National Listing of Fish Advisories. http://water.epa.gov/scitech/swguidance/fishshellfish/fishadvisories/archive/2004_index.cfm. Accessed 29 Mar 2012

USEPA (1996) Method 1669: Sampling ambient water for trace metals at EPA water criteria levels. US Environmental Protection Agency, Office of Science and Technology, Environmental and Analysis Division (4303), 401 M Street SW, Washington, DC 20460. http://www.epa.gov/caddis/pdf/Metals_Sampling_EPA_method_1669.pdf

USEPA (2002) Method 1631: Mercury in water by oxidation, purge and trap, and cold vapor atomic fluorescence spectrometer. US Environmental Protection Agency, Office of Science and Technology, Environmental and Analysis Division (4303), 401 M Street SW, Washington, DC 20460. http://water.epa.gov/scitech/methods/cwa/metals/mercury/upload/2007_07_10_methods_method_mercury_1631.pdf

Vandal GM, Mason RP, Fitzgerald WF (1991) Cycling of volatile mercury in temperate lakes. Water, Air, and Soil Pollution 56:791–803. doi: 10.1007/BF00342317

Vette AF, Landis MS, Keeler GJ (2002) Deposition and Emission of Gaseous Mercury to and from Lake Michigan during the Lake Michigan Mass Balance Study (July, 1994−October, 1995). Environ Sci Technol 36:4525–4532. doi: 10.1021/es0112184

Walker WW (1987) Empirical Methods for Predicting Eutrophication in Impoundments. Report 4. Phase III. Applications Manual. U.S. Army Engineer Waterways Experiment Station, Vicksburg, Mississippi. http://stinet.dtic.mil/oai/oai?&verb=getRecord&metadataPrefix=html&identifier=ADA188261

Wang Q, Kim D, Dionysiou DD, et al. (2004) Sources and remediation for mercury contamination in aquatic systems—a literature review. Environmental Pollution 131:323–336. doi: 10.1016/j.envpol.2004.01.010

Warner KA, Bonzongo J-CJ, Roden EE, et al. (2005) Effect of watershed parameters on mercury distribution in different environmental compartments in the Mobile Alabama River Basin, USA. Science of The Total Environment 347:187–207. doi: 10.1016/j.scitotenv.2004.12.011

Weseloh DV, Teeple SM, Gilbertson M (1983) Double-crested Cormorants of the Great Lakes: egg-laying parameters, reproductive failure, and contaminant residues in eggs, Lake Huron 1972–1973. Can J Zool 61:427–436. doi: 10.1139/z83-057

Westenbroek SM (2010) Concentrations and estimated loads of nutrients, mercury, and polychlorinated biphenyls in selected tributaries to Lake Michigan, 2005–6. Scientific Investigations Report 2010-5029. U.S. Geological Survey. 73 pp. http://pubs.usgs.gov/sir/2010/5029/pdf/sir2010-5029_web.pdf

Wollenberg JL, Peters SC (2009) Mercury emission from a temperate lake during autumn turnover. Science of The Total Environment 407:2909–2918. doi: 10.1016/j.scitotenv.2008.12.017

Xiao ZF, Munthe J, Schroeder WH, Lindqvist O (1991) Vertical fluxes of volatile mercury over forest soil and lake surfaces in Sweden. Tellus B 43:267–279. doi: 10.1034/j.1600-0889.1990.t01-1-00009.x-i1

Xiao ZF, Strömberg D, Lindqvist O (1995) Influence of humic substances on photolysis of divalent mercury in aqueous solution. Water, Air, & Soil Pollution 80:789–798. doi: 10.1007/BF01189730

Zhang H, Lindberg SE (2001) Sunlight and Iron(III)-Induced Photochemical Production of Dissolved Gaseous Mercury in Freshwater. Environ Sci Technol 35:928–935. doi: 10.1021/es001521p

Zhang H, Lindberg SE, Marsik FJ, Keeler GJ (2001) Mercury Air/Surface Exchange Kinetics of Background Soils of the Tahquamenon River Watershed in the Michigan Upper Peninsula. Water, Air, & Soil Pollution 126:151–169. doi: 10.1023/A:1005227802306

11. Vita

Joseph S. Denkenberger
jsdenken@syr.edu
151 Link Hall, Civil and Environmental Engineering Department
Syracuse University, Syracuse, New York 13244

EDUCATION

Department of Civil and Environmental Engineering, Syracuse University
Ph.D. Civil Engineering, May 2014
Ph.D. Dissertation: *Mercury Transport and Fluxes in the Lake Ontario Basin*

M.S. Environmental Engineering Science, December 2005
M.S. Thesis: *Assessment of Water Quality in Central New York through Near-Real-Time Robotic Monitoring*

Le Moyne College, Syracuse, NY
B.S. Chemistry, *summa cum laude*, May 2000

WORK EXPERIENCE

Anchor QEA, Liverpool, NY
Engineer – April 2014 to present
- Support remedial investigations and feasibility studies at hazardous waste sites
- Conduct environmental remediation oversight
- Perform model analysis of engineered cap design
- Analyze data in support of site characterization and investigation

ARCADIS, Syracuse, NY
Project Environmental Engineer – February 2006 to June 2009; November 2012 to April 2014
- Support remedial investigations and feasibility studies at hazardous waste sites
- Coordinate activities with subcontractors and conduct environmental remediation oversight
- Perform field work focusing on ecological risk assessments and contaminant delineation
- Provide technical reviews of regulatory documents
- Analyze data in support of site characterization and investigation

Syracuse University, Department of Civil and Environmental Engineering
Graduate Research Assistant – August 2003 to August 2005; July 2009 to present
- Environmental research and engineering analysis on various freshwater ecosystems
- Focus on measures of water quality and the fate and transport of mercury
- Coordinate and conduct environmental field work in support of research activities

New York State Department of Environmental Conservation, Avon, NY
Environmental Program Specialist Trainee I – December 2005 to February 2006
- Assisted in evaluation of environmental compliance at Kodak Park
- Conducted oversight of soil and water sample collection

Upstate Freshwater Institute, Syracuse, NY
Research Scientist and Field Technician – April 2004 to September 2005
- Performed analysis and synthesis of water quality data for scientific review
- Performed laboratory analysis of freshwater samples
- Installed and maintained Remote Underwater Sampling Station monitoring buoys
- Managed and performed field sampling and monitoring in surface waters of central New York region

Syracuse University, Department of Civil and Environmental Engineering
Laboratory Assistant III – June 2000 to August 2003
- Assisted in laboratory Standard Operating Procedures and Quality Control program development
- Performed various water quality chemical analyses
- Assisted in hiring and training laboratory assistants, undergraduate and graduate students
- Managed and performed various environmental sampling procedures

Bristol-Myers Squibb Company, Process Development, Syracuse, NY
Laboratory Technician – May 1999 to August 1999
- Performed organic synthesis reactions
- Analyzed reaction products and impurities through TLC, NMR, and HPLC

Bristol-Myers Squibb Company, Histology Department, Syracuse, NY
Laboratory Aid – May 1997 to August 1997, February 1998 to August 1998
- Performed laboratory maintenance as required through Quality Assurance program

ENVIRONMENTAL FIELD EXPERIENCE
- Deployment and maintenance of dissolved gaseous mercury monitoring equipment
- Oversight of sediment cap installation activities
- Oversight of soil and sediment sample collection activities
- Collection of groundwater, lotic, lentic, soil solution, and soil samples
- Installation and maintenance of piezometers and throughfall collectors
- Installation and maintenance of Remote Underwater Sampling Stations
- Installation and maintenance of Hydrolab probe packages

AWARDS AND INTERESTS
- Li Graduate Fellowship, 2011-2012
- Syracuse University Graduate Fellowship, 2010-2011
- Avid outdoorsmen

PUBLICATIONS

J.S. Denkenberger, C.T. Driscoll, B.A. Branfireun, C.S. Eckley, M. Cohen, and P. Selvendiran. 2012. A synthesis of rates and controls on elemental mercury evasion in the Great Lakes Basin. Environmental Pollution. Vol. 161:291-298. doi:10.1016/j.envpol.2011.06.007.

J.S. Denkenberger, D.M. O'Donnell, C.T. Driscoll, and S.W. Effler. 2007. Robotic monitoring to assess impacts of zebra mussels and assimilative capacity for a river. ASCE Journal of Environmental Engineering. Vol. 133(5):498-506. doi: 10.1061/(ASCE)0733-9372(2007)133:5(498).

J.S. Denkenberger, C.T. Driscoll, S.W. Effler, D.M. O'Donnell, and D.A. Matthews. 2007. Comparisons of an urban lake targeted for rehabilitation and a reference lake based on robotic monitoring. Lake and Reservoir Management. Vol. 23:11-26. doi: 10.1080/07438140709353906.

J.S. Denkenberger, C.T. Driscoll, B. Branfireun, A. Warnock, and E. Mason. Watershed influences on mercury in tributaries to Lake Ontario. *Under Review.*

J.S. Denkenberger, C.T. Driscoll, B. Branfireun, A. Warnock, and E. Mason. A fluvial mercury budget for Lake Ontario. *Under Review.*

PROFESSIONAL PRESENTATIONS

J.S. Denkenberger, C.T. Driscoll, and B.A. Branfireun. 2011. An Analysis of Lake Ontario's Mercury Budget: Is it Balanced? 10th International Conference on Mercury as a Global Pollutant. July 2011 (oral presentation).

J.S. Denkenberger, C.T. Driscoll, B.A. Branfireun, C.S. Eckley, M. Cohen, and P. Selvendiran. A Synthesis of Rates and Controls on Elemental Mercury Evasion in the Great Lakes Basin. 10th International Conference on Mercury as a Global Pollutant. July 2011 (oral presentation given by C.T. Driscoll).

J.S. Denkenberger, C.T. Driscoll, M. Montesdeoca, and K. Arend. 2010. Mercury Transport and Contamination in the Lake Ontario Basin. CARTI Program Review. Syracuse, NY. April 2010 (oral presentation).

J.S. Denkenberger, C.T. Driscoll, S.W. Effler, D.M. O'Donnell, and D.A. Matthews. Comparison of an urban lake targeted for rehabilitation and a reference lake based on robotic monitoring. 7th Annual Onondaga Lake Scientific Forum. Liverpool, NY. November 2005 (oral presentation given by C.T. Driscoll).

J.S. Denkenberger, C.T. Driscoll, S.W. Effler, D.M. O'Donnell, and D.A. Matthews. Comparison of an urban lake targeted for rehabilitation and a reference lake based on robotic monitoring. EPA Review Board. Syracuse, NY. October 2005 (oral presentation given by C.T. Driscoll).

J.S. Denkenberger, C.T. Driscoll, D.M. O'Donnell, and S.W. Effler. Insights from the robotic water quality monitoring network. II. Seneca River, impacts of zebra mussel metabolism.

Sixth Annual Onondaga Lake Scientific Forum. Liverpool, NY. November 2004 (oral presentation).

J.S. Denkenberger, C.T. Driscoll, D.M. O'Donnell, and S.W. Effler. Insights from the robotic water quality monitoring network. II. Seneca River, impacts of zebra mussel metabolism. EPA Review Board. Syracuse, NY. October 2004 (oral presentation).

J.S. Denkenberger, C.T. Driscoll, M. Montesdeoca, E.F. Mason, Jr., and S.W. Effler. 2009. Quicksilver fluxes in the Three Rivers and Lake Ontario Systems. 11th Annual Onondaga Lake Scientific Forum. Liverpool, NY. November 2009 (poster presentation).